Aus der Klinik für Innere Medizin II der Medizinischen Fakultät
der Universität des Saarlandes

Systemische Auswirkungen chronisch cholestatischer Lebererkrankungen im ABCB4-defizienten Mausmodell

Kumulative Dissertation zur Erlangung des akademischen Grades einer Doktorin der Naturwissenschaften (Dr. rer. nat.) der Medizinischen Fakultät der
UNIVERSITÄT DES SAARLANDES
2014

vorgelegt von: Diplom-Biologin Katrin Hochrath
geboren am: 30.01.1979 in Bonn

Erstgutachter: Universitätsprofessorin Dr. rer. physiol. Carola Meier
Zweitgutachter: Universitätsprofessor Dr. med. Frank Lammert

Für Anna und Günther

EIDESSTATTLICHE ERKLÄRUNG

Hiermit erkläre ich, Katrin Hochrath, dass ich die vorliegende Arbeit - mit Ausnahme der aufgeführten Quellen und Hilfsmittel - selbstständig und ohne unzulässige Hilfe Dritter durchgeführt habe. Die aus anderen Quellen direkt oder indirekt übernommen Daten und Konzepte sind mit einer Quellenangabe gekennzeichnet.

Die Inhalte der vorliegenden kumulativen Dissertation wurden bereits in Teilen in internationalen Fachzeitschriften (peer-reviewed Journalen) unter den folgenden Titeln veröffentlicht:

- „The hepatic phosphatidylcholine tranporter ABCB4 as modulator of glucose homeostasis.“ *FASEB J 2012; 26:5081-5091*
- „Modeling hepatic osteodystrophy in *Abcb4* deficient mice.“ *BONE 2013; 55:501-511*
- „Vitamin D modulates biliary fibrosis in *Abcb4* deficient mice.“ *Hepatology International 2014; 1-10*

Arbeiten, die von Co-Autoren durchgeführt wurden, verwendetes Material und Daten, die andere Personen oder Institutionen bereitgestellt haben, sind gekennzeichnet.

INHALTSVERZEICHNIS

NOMENKLATUR & ABKÜRZUNGSVERZEICHNIS

NOMENKLATUR

Für die Unterscheidung zwischen Protein und Gen mit humanem oder murinem Ursprung gilt bei der vorliegenden Arbeit, in Anlehnung an die Vorgaben des „Human Genome Organisation Gene Nomenclature Committee“:
Großbuchstaben bezeichnen die Proteine von Mensch und Maus (z.B. ABCB4).
Gen-Namen sind kursiv geschrieben. Großbuchstaben kennzeichnen die humanen Gene (z.B. *ABCB4*), während für die Gene der Maus nur der erste Buchstabe groß geschrieben wird (z.B. *Abcb4*).

ABKÜRZUNGSVERZEICHNIS

ABC	adenosine 5'-triphosphate (ATP) – binding cassette
ABCB11	ATP-binding cassette transporter, sub-family B, member 11
ABCB4	ATP-binding cassette transporter, sub-family B, member 4
Abcb4$^{-/-}$	ATP-binding cassette transporter, sub-family B, member 4 knockout mouse
ABCG5/8	ATP-binding cassette transporter, subfamily G, member 5 and 8
Actb	β-actin
AIC	Akaikes information criteria
ALT	alanine aminotransferase
ANCOVA	analysis of covariance
ANOVA	analysis of variance
AP	alkaline phosphatase
αSMA	α-smooth muscle actin
AUC	area under the curve
Bglap	bone γ-carboxyglutamate protein (osteocalcin)
BMC	bone mineral content
BMD	bone mineral density

BMI	body mass index
BS	bile salts
BV	bone volume
BV/TV	bone volume fraction (bone volume/total volume)
c.	codon (nucleotide number)
CK19	cytokeratin 19
Col1α2	collagen type I, α 2
Conn.D	connective density
Cps1	carbonylphophate synthetase
Cramp	cathelicidin (murine)
ct	cycle threshold
Ctsb	cathepsin B
Cyp27a1	cytochrome P450, family 27, subfamily A, polypeptide 1
Cyp27b1	cytochrome P450, family 27, subfamily B, polypeptide 1
Cyp2j2	cytochrome P450, family 2, subfamily J, polypeptide 2
Cyp2r1	cytochrome P450, family 2, subfamily R, polypeptide 1
Cyp3a4	cytochrome P450, family 3, subfamily A, polypeptide 4
Cyp7a1	cytochrome P450, family 7, subfamily A, polypeptide 1
Cyp7b1	cytochrome P450, family 7, subfamily B, polypeptide 1
Cyp8b1	cytochrome P450, family 8, subfamily B, polypeptide 1
Dcn	decorin
DLPC	dilauroyl-phosphatidylcholine
dNTP	di-nucleotide triphosphate
DUPC	diundecanoyl-phosphatidylcholine
DXA	Dual-energy x-ray absorptiometry
ESI	electrospray ionization
Fasn	fatty acid synthase
Foxo1	forkhead box O1
FTICR	fourier transform ion cyclotron resonance
G6pc	glucose-6-phophatase, catalytic subunit

Gc	groupe specific component (also known as: groupe specific globulin or vitamin D binding protein)
Gck	glucokinase, hexokinase IV
GEO	gene expression omnibus, (http://www.ncbi.nlm.nih.gov/geo/)
GMC	German Mouse Clinic
Gnmt	glycine N-methyltransferase
GO	gene ontology
H&E	hematoxylin and eosin
HA	hydroxyapatite
Hc	hemolytic complement (complement factor 5, *C5*)
HOD	hepatic osteodystrophy
HSC	hepatic stellate cells
Hyp	hydroxyproline
IGF-1	insulin-like growth factor-1
IPA	ingenuity pathway analysis (http://www.ingenuity.com/)
IpGTT	intraperitoneal glucose tolerance test
IU	International Unit
LCA	lithocholic acid
Lcn2	lipocalin-2
LDH	lactate dehydrogenase
LRH-1	liver receptor homolog-1
MALDI	matrix-assisted laser desorption/ionization
µCT	micro-computed tomography
MIDAS	modular fourier transform ion cyclotron resonance mass spectrometry data acquisition system
MMP	matrix metalloproteinase
MSI	mass spectrometry imaging
NHMFL	national high magnetic field laboratory
Nr0b2	nuclear receptor subfamily 0, group B, member 2 (small heterodimer partner, SHP)

Nr1h4	nuclear receptor subfamily 1, group H, member 4 (farnesoid X receptor, FXR)
Nr5a2	nuclear receptor subfamily 5, group A member 2, (liver receptor homolog 1, LRH-1)
OPG	osteoprotegerin
PC	phosphatidylcholine
Pck1	phosphoenolpyruvate carboxykinase
PCR	polymerase chain reaction
Pctp$^{-/-}$	phosphatidylcholine transfer protein knockout mouse
PFIC	progressive familial intrahepatic cholestasis
Ppar-γ	peroxisome proliferative activated receptor γ
Pparγc1a	peroxisome proliferative activated receptor γ, co-activator 1 alpha
pQCT	peripheral quantitative computed tomography
qPCR	quantitative real-time polymerase chain reaction
RANKL	receptor activator of nuclear factor κB ligand
ROS	reactive oxygen spezies
RQ	relative quotient = $2^{-\Delta\Delta ct}$
RT-PCR	reverse transcription polymerase chain reaction
RXR	retinoid X receptor
SCD	stearoyl-CoA desaturase
SE	standard error of the mean
SHIRPA	SmithKline Beecham, Harwell, Imperial College, Royal Hospital, phenotype assessment
SMAD3	SMAD family member 3 (alias: mothers against decapentaplegic homolog 3
SNP	single nucleotide polymorphism
Spp1	secreted phosphoprotein-1 (osteopontin)
Srebf1	sterol regulatory element binding transcription factor-1
Tb.	trabecular
Tb.S	trabecular separation
Tb.Th	trabecular thickness

TGF-β	transforming growth factor-β
Tnfrsf11b	tumor necrosis factor receptor superfamily, member 11b (osteoprotegerin, OPG)
Vdr	vitamin D receptor
VDRE	vitamin D response element

VORBEMERKUNG ZUM AUFBAU DER ARBEIT

Die vorliegende Arbeit beginnt mit einer allgemeinen Einleitung über die Leberfibrose als gemeinsame Endstrecke chronischer Lebererkrankungen. Es werden die Cholestase als Ausgangspunkt für chronisch cholestatische Lebererkrankungen und das untersuchte Mausmodell erläutert. Die molekularen Mechanismen, mit den für diese Arbeit relevanten Mediatoren der Leberfibrogenese, werden ebenfalls vorgestellt. Es folgt ein Abschnitt über die Vorarbeiten, die Grundlage für weitere Analysen und die hier vorgestellten Publikationen waren. Die einzelnen Veröffentlichungen mit je einer deutschen Zusammenfassung befinden sich in den Kapiteln 2-4. Kapitel 2 beinhaltet die Studien zu den Auswirkungen des *Abcb4* und *ABCB4* -Defekts auf die Glukose-homöostase in Maus und Mensch. In Kapitel 3 wird die Eignung der ABCB4-defizienten Maus als Modell für die hepatische Osteodystrophie beschrieben. Die Darstellung des modulierenden Effekts von Vitamin D auf die Fibrogenese im *Abcb4*-Knockout Mausmodell folgt in Kapitel 4. Eine übergreifende Diskussion ist in Kapitel 5 zu finden.

KAPITEL 1:

ALLGEMEINE EINLEITUNG

ZIEL DER ARBEIT

ALLGEMEINE EINLEITUNG

Als zentrales Stoffwechselorgan hat die Leber sehr vielfältige Aufgaben. Sie ist zugleich Syntheseort (z.B. Cholesterin, Gallensäuren, Hormone), Entgiftungsorgan (z.B. Steroide, Bilirubin, Alkohol, Pharmaka) und Speicherort (z.B. Vitamine A, Glykogen, Eisen). Um diese zahlreichen Aufgaben erfüllen zu können, ist die Leber architektonisch entsprechend komplex aufgebaut und strukturiert (Abbildung 1).

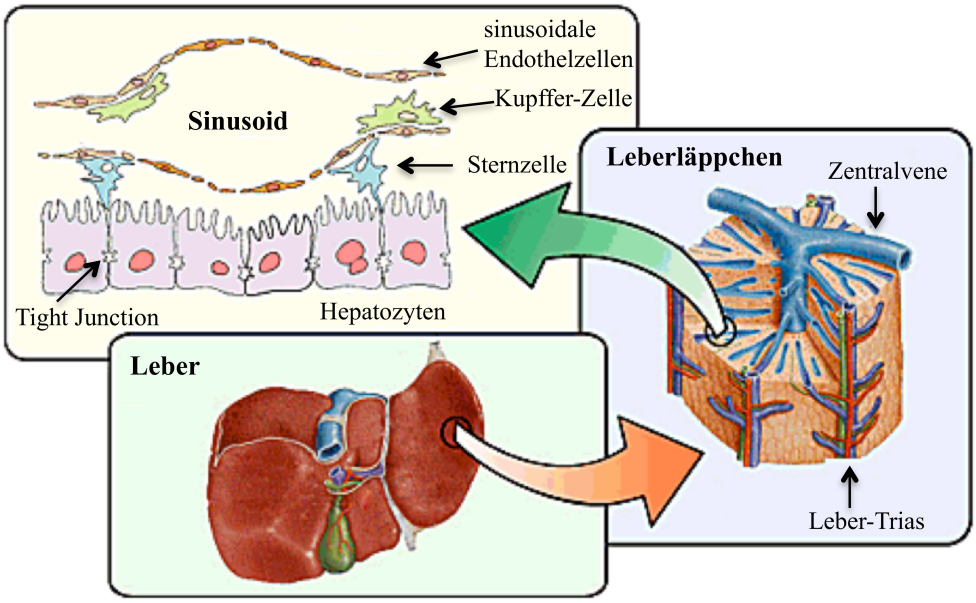

Abbildung 1: Aufbau der Leber. Als Grundeinheit das sechseckige Leberläppchen mit der Zentralvene und dem Leber-Trias bestehend aus Vene (blau), Arterie (rot) und Gallengang (grün). Die Sinusoide mit den gefensterten Endothelzellen, Kupffer-Zellen und hepatischen Sternzellen. Quelle: www.akaike-lab.bio.titech.ac.jp

Die anatomische Grundeinheit bilden die sechseckigen Leberläppchen. Diese beinhalten in Zellbalken organisierte Hepatozyten, die radiär um die Zentralvene angeordnet sind. Zwischen den benachbarten Läppchen liegt das Portalfeld mit der Leber-Trias, bestehend aus *Arteria* und *Vena interlobularis* und dem Gallengang (*Ductus interlobularis*). Die Blutflussrichtung erfolgt vom Portalfeld zur Zentralvene und bewirkt eine an Substrat- und Sauerstoffangebot angepasste Zonierung. Eine doppelte Blutversorgung der Leber über die *Arteria*

hepatica propria und Pfortader gewährleistet die Zufuhr des Sauerstoffs und der resorbierten Nährstoffe für die Stoffwechselvorgänge. Beide Gefäße teilen sich weiter auf, bis sie letztlich ein feines Netz an Leberkapillaren zwischen den Leberbalken bilden, die sogenannten Sinusoide. Das einschichtige, gefensterte Epithel der Sinusoide erlaubt den ungehinderten Substrataustausch des Blutes mit den Hepatozyten über den Dissé-Raum (Raum zwischen Hepatozyten und Sinusoid) und stellt somit den intrahepatischen Stoffaustausch sicher (Braet and Wisse 2002, Wallace *et al.* 2008).

Die komplexe Leberstruktur wird sowohl von den parenchymalen Hepatozyten als auch von nicht-parenchymalen Zellen gewährleistet. Die Hepatozyten nehmen mit 80% den größten Volumenanteil des Organs ein. Sie sind der Syntheseort der Gallensäuren. Gleichzeitig sind sie auch für die Ausbildung der Gallenkanälchen verantwortlich, die sich durch die apikale Verknüpfung von zusammenliegenden Zellmembranen mittels Zellhaft-Kontakten (Tight Junctions) ergibt. Zu den nicht-parenchymalen Zellen gehören die sinusoidalen Endothelzellen, die Kupffer-Zellen als spezifische Lebermakrophagen, biliäre Epithelzellen und die im Dissé-Raum lokalisierten Vitamin A-speichernden hepatischen Sternzellen.

Chronische und akute Entzündungen in der Leber können zu Änderungen der anatomischen Struktur und damit zu Funktionsstörungen führen, die sich auf den gesamten Organismus auswirken. Die Auslöser des Entzündungsreizes sind dabei sehr vielseitig und umfassen virale Infektionen (Hepatitis-Viren A, B, C, D), chemische Substanzen (Alkohol, Medikamente) sowie metabolische, autoimmune oder cholestatische Erkrankungen. Leberfibrose, die Vernarbung der Leber, resultiert aus einem exzessiven Wundheilungsprozess als Antwort auf den chronisch bestehenden Entzündungsreiz, unabhängig von dessen Ursprung. Es handelt sich dabei um einen dynamischen und reversiblen Prozess, der den Auf- und Umbau extrazellulärer Matrixkomponenten, insbesondere von Kollagen, beinhaltet. Bleibt der Entzündungsreiz bestehen, kommt es durch die vermehrte Einlagerung von Kollagen zu einer Umwandlung der Leberzellstruktur, einem gestörten intrahepatischen Stoffaustausch und irreparablen Veränderungen der

Leberarchitektur. Einschränkungen der metabolischen Funktion bis hin zum kompletten Funktionsverlust des Organs gehen mit dem fortschreitenden Umbau einher (Bataller and Brenner 2005). Das Endstadium der Fibrose stellt die Zirrhose dar, sie gilt im Gegensatz zur Fibrose in fortgeschrittenen Fällen als irreversibel. Für viele Patienten ist dann eine Lebertransplantation lebensnotwendig (Fowler 2013). Das Voranschreiten der Fibrosierung, die Fibrogenese, wird dabei durch verschiedene Umwelteinflüsse, genetische Determinanten und intestinale Faktoren beeinflusst, deren Identifizierung und Charakterisierung Gegenstand der aktuellen Forschung ist.

Cholestatische Lebererkrankungen

Cholestatische Lebererkrankungen repräsentieren eine wichtige heterogene Gruppe von Lebererkrankungen, die zur Fibrose oder Zirrhose führen können. Für sie charakteristisch ist eine Störung des Gallenflusses im Bereich der Hepatozyten, der Gallenkanälchen oder der Gallengänge inner- und/oder außerhalb der Leber.

Im gesunden Organismus besteht die Gallenflüssigkeit neben Wasser (82%) aus Gallensalzen, Phospholipiden, Cholesterin, Bilirubin und anorganischen Elektrolyten. Die Synthese erfolgt überwiegend in den Hepatozyten, die anschließend die Einzelkomponenten (z.B. Gallensalze, Phospholipide, Cholesterin) aktiv mittels verschiedener Transporter in die Gallenkapillaren sezernieren (Abbildung 2). Komponenten wie Wasser und Elektrolyte folgen aufgrund des osmotischen Gradienten. Von den Gallenkapillaren fließt die Galle über die Gallengänge zur Speicherung in die Gallenblase oder für die Resorption von Nahrungsfetten in den Dünndarm. Mit der Galle erfolgt auf diesem Weg auch die Entgiftung und Ausscheidung endogener (z.B. Bilirubin, Steroidhormone) und exogener (z.B. Medikamente, Schwermetalle) Substanzen.

Ein Gallenstau, die sogenannte Cholestase, entsteht durch Behinderungen des Gallenflusses als Resultat von mechanischen Blockaden (z.B. durch Gallensteine) oder Schädigungen der Transportmechanismen in den Hepatozyten.

Infolge der Cholestase können die polaren Gallensalze die Membranen der Leberzellen und des umliegenden Gewebes schädigen. Häufige Begleiterscheinung einer chronischen Cholestase sind daher Entzündungen der Gallengänge (Cholangitis), die sich über die Portalfelder der Leber ausbreiten und in einer biliären Fibrose und der Zirrhose münden können (Martin 1993, Angulo and Lindor 1999). Weiterhin sind mit der Cholestase Veränderungen im Zytoskelett der Hepatozyten und der funktionalen Membranintegrität assoziiert (Trauner *et al.* 1998). Hier sind vor allem Schädigungen der Tight Junctions nachweisbar. Diese führen zu einer erhöhten Permeabilität und ermöglichen Bilirubin und den anderen Gallensubstanzen den Übertritt in das sinnusoidale Blut. Mit der gestörten hepatozellulären Integrität und einer vermehrten Apoptose von Hepatozyten werden gleichzeitig Enzyme freigesetzt, deren Anstieg im Blut messbar ist. Zu diesen gehören als Indikatoren eines Leberparenchymschadens die Transaminasen Alanin-Aminotransferase (ALT) und Aspartat-Aminotransferase (AST), sowie die Alkalische Phosphatase (AP) als Indikator einer Schädigung des Gallengangepithels. Weitere Auswirkungen der Cholestase finden sich im Darm in Form einer verminderten Resorption von Fettsäuren und fettlöslichen Vitaminen.

Für viele der cholestatischen Erkrankungen gilt, dass der genaue pathologische Mechanismus nur unvollständig charakterisiert ist. Vermutet wird, dass Initiierung und Fortschreiten einer Cholestase durch beides, genetische Determinanten und Umwelteinflüsse, bedingt sind.

Das Mausmodell der biliären Fibrose

Entsprechend den vielfältigen Ursachen einer Leberfibrose stehen für die Forschung verschiedene Tiermodelle zur Verfügung. Als etabliertes Modell für chronisch cholestatische Lebererkrankungen und die biliäre Fibrose gilt die *Abcb4*- (ATP-binding cassette transporter, subfamily B, member 4) defiziente Maus (Smit *et al.* 1993).

Das *Abcb4*-Gen kodiert das gleichnamige Transporterprotein (ABCB4), welches ausschließlich in der Leber exprimiert wird. Der Transporter, eine

Floppase, ist in der kanalikulären Membran der Hepatozyten lokalisiert, wo er Phosphatidylcholin (Lecithin) über die Membran in das Lumen der Gallenkanälchen transloziert (Smith *et al.* 1994, Ruetz and Gros 1994). Dort bildet das Phosphatidylcholin, zusammen mit Cholesterin und Gallensalzen, gemischte Mizellen und schützt so die Zellmembranen der umliegenden Gallengänge vor den toxischen Effekten der polaren Gallensalze (Abbildung 2). Defekte des *Abcb4*-Gens und der daraus resultierende Verlust des Proteins führen bei der Maus ebenso wie bei Menschen zu einer phosphatidylcholinarmen Zusammensetzung der Gallenflüssigkeit bei gleichbleibendem Gehalt an Gallensalzen (Smit *et al.* 1993, Davit-Spraul *et al.* 2009). Es kommt zu einer Schädigung des biliären Epithels und der Hepatozyten. Die Folge ist eine chronische gallensäureinduzierte Entzündung der Gallengänge, die progressive zwiebelartige (sklerosierende) Fibrosierung der Gallengänge und letztlich eine biliäre Fibrose, vergleichbar mit der primären sklerosierenden Cholangitis (PSC) bei Patienten (Lammert *et al.* 2004, Fickert *et al.* 2004).

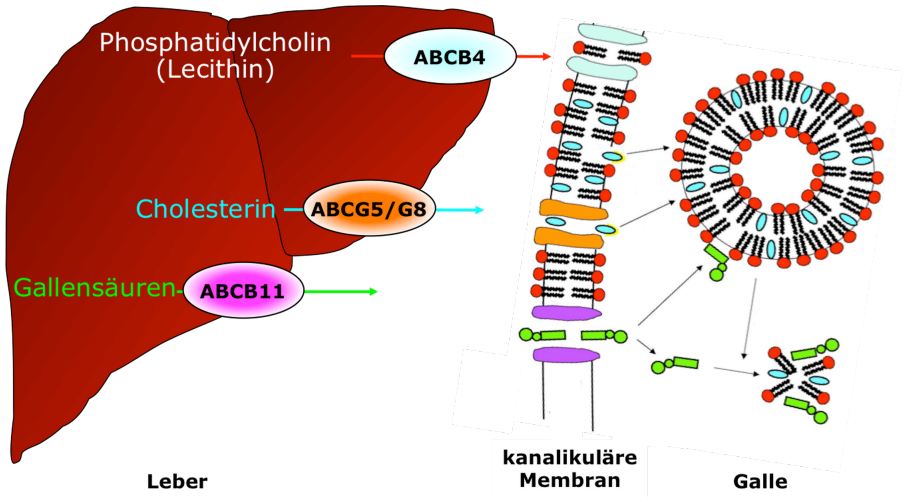

Abbildung 2: Darstellung der hepatischen ABC-Transporter die den aktiven Transfer der Gallenkomponenten Phosphatidylcholin, Cholesterin und Gallensäuren von der Leber in die Galle gewährleisten. In der Galle formatieren sich Gallensalze (Grün), Cholesterin (Türkis) und Phosphatidylcholin (Rot) zu gemischte Mizellen. Der funktionale Defekt oder der Verlust des ABCB4-Transporters führt im murinen und humanen Organismus zu einer phosphatidylcholinarmen Gallenflüssigkeit. Modifiziert nach Small *Proc Natl Acad Sci* 2003 (Small 2003).

Defekte des humanen *ABCB4*-Gens liegen auch der progressiven familiären intrahepatischen Cholestase Typ 3 (PFIC3) zugrunde, die häufig bereits im Kindesalter zur Leberzirrhose führt (Davit-Spraul *et al.* 2009 und 2010). Des Weiteren sind *ABCB4*-Varianten mit einem erhöhten Risiko einer Schwangerschafts-Cholestase (Müllenbach *et al.* 2003, Wasmuth *et al.* 2007) und der Bildung von Gallensteinen bei jungen Erwachsenen (Low phospholipid-associated cholelithiasis-Syndrom) assoziiert (Rosmorduc *et al.* 2001 und 2003, Poupon *et al.* 2013).

Seit die *Abcb4*$^{-/-}$-Maus im Jahr 1993 von Smit und Borst generiert wurde (Smit *et al*. 1993), sind zahlreiche Analysen zu hepatischen Phänotypen der Tiere publiziert worden (Borst and Schinkel 1996, Lammert *et al*. 2004, Fickert *et al*. 2006, Baghdasaryan *et al*. 2008, 2010 und 2011, Moustafa *et al*. 2012). Die Wechselwirkungen mit dem extrahepatischen Organsystem und die systemischen Auswirkungen des *Abcb4*-Defekts sind allerdings bisher nur unzureichend untersucht und verstanden.

Mechanismen und Mediatoren der Fibrogenese

Trotz der unterschiedlichen Ursachen, die eine hepatische Fibrose auslösen können, verläuft die Fibrogenese weitgehend uniform, wobei es zu vielschichtigen Wechselwirkungen der verschiedenen Zellpopulationen der Leber kommt. Im Zentrum der Fibrogenese stehen die profibrogenen hepatischen Myofibroblasten. Die charakteristisch sternförmigen und kontraktilen Zellen besitzen ein ausgeprägtes Zytoskelett aus glattmuskulärem α-Aktin (α-smouth muscle actin, αSMA) und sind Produzenten von extrazellulären Matrixmolekülen, die kollagene (Kollagen I-V) und nicht-kollagene (z.B. Proteoglykane, Glykoproteine) Proteine umfassen. Sie sind in aktivierter Form ausschließlich in der entzündeten Leber zu finden. Ihre Herkunft ist derzeit noch unklar und variiert vermutlich in Abhängigkeit von der Ätiologie der Lebererkrankung (Iwaisako *et al.* 2012). Aktuell gelten als Hauptquelle für Myofibroblasten bei cholestatischen Leber-

erkrankungen vor allem hepatische Sternzellen (hepatic stellate cells, HSC) (Mederacke *et al.* 2013).

Die Differenzierung hepatischer Sternzellen zum profibrogenen hepatischen Myofibroblasten wird über parakrine Signalmoleküle initiiert. Hepatozyten und biliäre Zellen, geschädigt durch hepatotoxische Agenzien (z.B. Gallensäuren, Alkohol, Viren), setzen reaktive Sauerstoffspezie (reactive oxygen species, ROS) frei und rekrutieren inflammatorische Zellen (verschiedene T-Lymphozyten). Zusätzlich aktiviert die Apoptose der Hepatozyten Kupffer-Zellen, die ihrerseits ROS, Wachstumsfaktoren und verschiedene Zytokine, wie das profibrogene TGF-β (transforming growth factor β), freisetzen (Abbildung 3). HSC werden in diesem Rahmen durch die Synthese von αSMA kontraktil. Sie verändern das Proliferations- und Migrationsverhalten, verlieren ihre Vitamin A-Speicher und sezernieren vermehrt Kollagen und inflammatorische Zytokine (Bataller and Brenner 2005). Die daraus resultierenden Veränderungen der extrazellulären Matrix führen über einen positiv verstärkenden Feedback-Mechanismus zur Progression der Fibrosierung. Matrix abbauende Proteasen (matrix metallo-proteinases, MMPs) werden über die Bindung an spezifische Inhibitoren (tissue inhibitor of matrix metalloproteinases, TIMPs) gehemmt. Gleichzeitig wirken einzelne TIMPs anti-apoptotisch auf die aktivierten Myofibroblasten (Murphy *et al.* 2002). Sie reduzieren damit den Kollagenabbau und erhöhen zusätzlich die Anzahl an aktivierten Myofibroblasten. Klingt der Entzündungsreiz ab, regeneriert das Gewebe, die Apoptose aktivierter Myofibroblasten bzw. ihre Rückkehr in den inaktiven Zustand wird eingeleitet (Kisseleva *et al.* 2012, Troeger *et al.* 2012). Eine Zunahme der MMP-Aktivität und die Suppression von TIMPs bewirkt den Abbau der extrazellulären Matrix und Kollagen (Bataller and Brenner 2005).

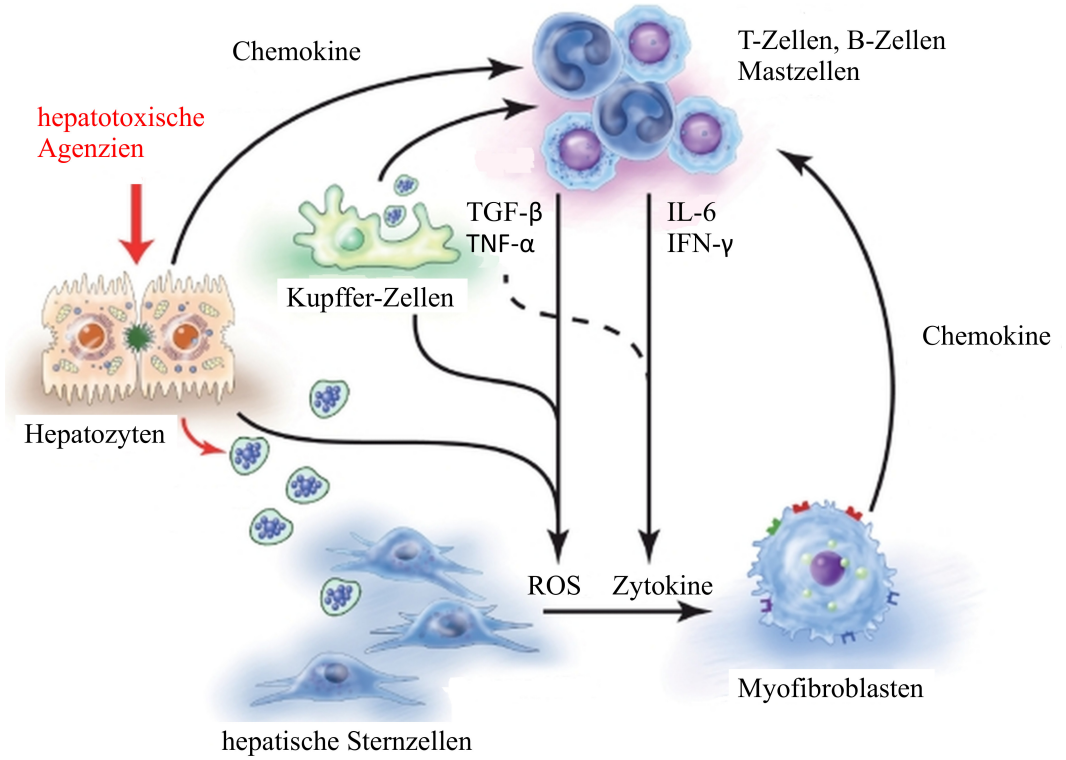

Abbildung 3: Entzündungskaskade der Leberfibrose. Geschädigte Hepatozyten setzen reaktive Sauerstoffspezie (ROS) und Chemokine frei. Über die Aktivierung von Kupffer-Zellen kommt es zur vermehrten Freisetzung von ROS, Wachstumsfaktoren und Zytokinen die eine trans-differenzierung hepatischer Sternzellen in Myofibroblasten initiieren. Myofibroblasten ihrerseits stimulieren die Rekrutierung inflammatorischer Zellen. Nach Cohen-Naftaly & Friedman *Therap Adv Gastroenterol* 2011 (Cohen-Naftaly and Friedman 2011).

ZIEL DER ARBEIT

Hauptziel der Arbeit war die Analyse und Charakterisierung systemischer Auswirkungen des *Abcb4*-Defekts, um die zu Grunde liegenden molekularen Mechanismen chronisch cholestatischer Lebererkrankungen besser zu verstehen und potenzielle Einflussgrößen der Fibrogenese und Interaktionen mit anderen Organen identifizieren zu können.

Aus dieser Zielsetzung wurden die folgenden Unterziele abgeleitet:

1) Identifizierung der systemischen Auswirkungen des *Abcb4*-Defekts im Mausmodell als Ausgangsbasis für die weitere Charakterisierung einzelner extrahepatischer Manifestationen.

2) Charakterisierung des Glukosestoffwechsels im *Abcb4*$^{-/-}$-Mausmodell und Analyse der Assoziation von *ABCB4*-Varianten mit den Glukose-Konzentrationen bei Patienten.

3) Charakterisierung des Knochenphänotypen als extrahepatische Manifestation in der *Abcb4*$^{-/-}$-Maus.

4) Untersuchung der Effekte von Vitamin D auf die Knochenmorphologie und die biliäre Fibrose im *Abcb4*$^{-/-}$-Mausmodell.

ABCB4-defiziente Mäuse: Eine systematische Phänotypisierung

Mit dem Ziel, die systemischen Auswirkungen des *Abcb4*-Defekts zu identifizieren, wurden umfangreiche Analysen des gesamten Phänotyps der ABCB4-defizienten Mäuse vorgenommen. Über die Zusammenarbeit mit der „German Mouse Clinic“ (www.mouseclinic.de) konnten standardisierte Tests in insgesamt 80 *Abcb4*$^{-/-}$-Mäusen und Kontrolltieren für die folgenden Bereiche durchgeführt werden: Morphologie, Verhalten, Neurologie, Augen, Energie-Stoffwechsel, Klinische Chemie, Immunologie, Lipid- und Steroid-Metabolismus, kardiovaskuläre Parameter, Lungenfunktion und Pathologie (Gailus-Durner *et al.* 2005), (Tabelle 1).

Über die Analysen aus den Bereichen Klinische Chemie und Pathologie der *Abcb4*$^{-/-}$-Mäuse im Vergleich zu Kontrolltieren konnten zu erwartende, klassische pathologische Parameter einer Cholestase dargestellt werden. Dazu gehören als Indikator für die Leberzellschädigung der signifikante Anstieg verschiedener Leberenzyme (ALT, AST, AP, LDH) im Blut, morphologische Veränderungen der Leber mit typischen Kennzeichen einer sklerosierenden Cholangits und eine milde bis ausgeprägte Fibrose bei allen ABCB4-defizienten Mäusen. Unterschiede zwischen *Abcb4*$^{-/-}$ und Wildtyp -Mäusen konnten aber auch in einer Vielzahl weiterer Phänotypen demonstriert werden. So weisen *Abcb4*$^{-/-}$-Tiere signifikant geringere Blut-Glukose-Konzentrationen auf. Mittels quantitativer Massen-spektrometrie von insgesamt 164 Plasma-Metaboliten konnten verschiedene Phosphatidylcholin-Spezies identifiziert werden, die in ABCB4-defizienten Mäusen reduziert sind. Unterschiede fanden sich auch in der Knochenmasse des Gesamtskeletts und in der Konzentration des Steroidhormons Dehydroepiandro-steron im Blut. Die immunologische Phänotypisierung wies zudem Unterschiede in den zirkulierenden Leukozyten-Populationen von *Abcb4*$^{-/-}$- und Kontrollmäusen nach. Phänotypische Analysen zum Energie-Stoffwechsel und kardiovaskulären Parametern ergaben dagegen keine Genotyp-spezifischen Unterschiede.

Tabelle 1: Übersicht der Untersuchungen, die im Rahmen der systematischen Phänotypisierung von *Abcb4*$^{-/-}$-Mäusen und Kontrolltieren durchgeführt wurden. Je Analysebereich wurden 40 *Abcb4*$^{-/-}$-Mäuse und Wildtyp-Kontrolltiere analysiert (Geschlechterverhältnis 1:1), soweit dies nicht anders gekennzeichnet ist.

	Analysebereich	**Methode**
Morphologie	Gesamter Körper, Knorpel und Gesamtskelett	Dokumentation Körpergröße, Gewicht, Fellbeschaffenheit, etc.; Knochendichtemessung (DEXA)
Verhalten	Lokomotorische Eigenschaften, Angstverhalten, Sensomotorik	Open Field-Test, Prä-Pulsinhibition
Neurologie	Zerebrale Funktion, Gleichgewicht, Bewegungskoordination, Haltekraft	SHIRPA Protokoll, Rotationsrad
Augen	Funktion und Morphologie von Retina, Linse, Kornea; Axiale Augenlänge	Funduskopie, Laser Interferenz Biometrie, Spaltlampen-Mikroskopie, Histologie
Energie-stoffwechsel	Körpergewicht, Temperatur, Aktivität, Sauerstoffkonsum, Kohlenstoffdioxidproduktion, Respirationsrate	indirekte Kalometrie
Klinische Chemie	klinisch chemische und hämatologische Parameter, Elektrolyte, Glukosetoleranz	Blutautoanalyser, Intraperitonealer Glukosetoleranz Test
Immunologie	Verteilung der Lymphozyten Population, Immunglobuline	Durchflusszytometrie, Multiplex Array
Steroid Stoffwechsel	Dehydroepiandrosteron, Testosteron	Enzym-linked Immunosorbent Assay
Kardiologie	Funktionale Herzparameter, Blutdruck, Atriales natriuretisches Peptid	Elektrokardiogramm, Echokardiographie, Enzym-linked Immunosorbent Assay
Lunge	Lungenfunktion	Ganzkörper Plethysmografie
Metabolomics	Quantifizierung von Lipiden, Lipidderivaten, Glukose, Aminosäuren (164 Metabolite)	Elektrospray-Ionisations-Tandem-Massenspektrometrie
Genetik	Leber RNA Expressionsprofil*	DNA-Chip
Pathologie	Haut, Auge, Cerebrum, Cerebellum, Herz, Lunge, Trachea, Zähne, Speicheldrüse, Ösophagus, Magen, Darm, zervikale Lymphknoten, Thymus, Nebenschilddrüse, Pankreas, Milz, Niere, Nebenniere, Harnblase, Geschlechtsorgane	Makro- und Mikroskopie, Histologie

*Für diese Analysen wurde das Lebergewebe von je acht männlichen *Abcb4*$^{-/-}$- und Wildtyp-Mäusen verwendet. DEXA: dual-energy X-ray absorptiometry; SHIRPA: SmithKline Beecham, Harwell, Imperial College, Royal Hospital, phenotype assessment

Eine ausführliche Darstellung der Ergebnisse aus allen Analysebereichen der Phänotypisierung ist veröffentlicht unter

http://146.107.35.38/phenomap/jsp/annotation/public/phenomap.jsf .

KAPITEL 2:

ABCB4 ALS MODULATOR DER GLUKOSEHOMÖOSTASE

ABCB4 ALS MODULATOR DER GLUKOSEHOMÖOSTASE

Phosphatidylcholine, die mittels des ABCB4-Transporters von der Leber in die Galle transportiert werden, unterscheiden sich in der Zusammensetzung ihrer Fettsäuren. Der Hauptanteil an Phosphatidylcholin in der gesunden Galle der Maus besteht aus einer Kombination von gesättigten und ungesättigten Fettsäuren, mit einer Kettenlänge von 16 bis 20 Kohlenstoffatomen (Lammert *et al.* 2004). Interessanterweise konnte von anderen Arbeitsgruppen gezeigt werden, dass spezifische Phosphatidylcholine mit kürzeren Fettsäureseitenketten, wie Diundecanoyl-Phosphatidylcholin (DUPC) und Dilauroyl-Phosphatidylcholin (DLPC), an LRH-1 (liver receptor homolog-1) binden (Forman 2005, Lee *et al.* 2011). LRH-1 ist ein nukleärer Rezeptor, der erstmals in der Leber entdeckt wurde und als Transkriptionsfaktor Gene der Cholesterin- und Lipid-Absorption und des Gallensäurestoffwechsels reguliert (Ortlund *et al.* 2005). Die Aktivierung von LRH-1 durch seinen Liganden DLPC verbessert zudem die Insulin-Sensitivität von Mäusen mit diabetischer Stoffwechsellage (Lee *et al.* 2011).

Zusätzlich haben humane Studien gezeigt, dass die Region, in der das *ABCB4*-Gen lokalisiert ist (7q21.1), mit Insulinresistenz und Diabetes assoziiert ist (Prochazka *et al.* 1995, Mochizuki *et al.* 1998, Iyengar *et al.* 2007). In diesem Kontext und auf Basis der Daten, die bereits aus der systematischen Phänotypisierung der ABCB4-defizienten Mäuse vorlagen, wurden detaillierte Analysen zum Glukosestoffwechsel in der Maus und weitere Assoziationsstudien bei Patienten durchgeführt.

Als Maß für die Geschwindigkeit, mit der Glukose aus dem Blutplasma abtransportiert wird, wurden intraperitoneale Glukose-Toleranz-Tests bei *Abcb4*$^{-/-}$-Mäusen und Kontrolltieren durchgeführt, die über Nacht keinen Zugang zu Futter hatten. Die hepatische Expression verschiedener Gene, die Schlüsselenzyme des Glukose- und Gallensäurestoffwechsels kodieren, sowie von LRH-1 wurde vor und nach Glukose-Applikation ermittelt. Für die Identifizierung spezifischer Phosphatidylcholine in der Leber konnte als bildgebendes Verfahren die Matrix-

unterstützte Laser-Desorption/Ionisation (MALDI) mit Fouriertransformation-Ionenzyklotron-Resonanz (FTICR) -Massenspektrometrie eingesetzt werden.

Für die humane Studie standen zwei unabhängige europäische Kohorten mit insgesamt 682 Individuen zur Verfügung. In beiden Kohorten wurden vier häufige pro-cholestatische Varianten des *ABCB4*-Gens typisiert. Anschließend wurden die Nüchtern-Glukose-Konzentrationen im Serum mit den Genotypen korreliert.

Im Rahmen dieser Studie konnten wir zeigen, dass sich die systemischen Glukosespiegel zwischen *Abcb4*$^{-/-}$-Mäusen und Kontrolltieren unterscheiden und dass ABCB4-defiziente Tiere eine veränderte Glukosetoleranz aufweisen. Des Weiteren wird das Gen, welches den antidiabetischen Rezeptor LRH-1 kodiert, in der Leber von *Abcb4*$^{-/-}$-Mäusen stärker exprimiert. Erstmals wurden die spezifischen Phosphatidylcholin-Liganden des LRH-1-Rezeptors (DUPC und DLPC) in der Mausleber nachgewiesen.

In den humanen Kohorten konnte zudem gezeigt werden, dass der *ABCB4*-Genotyp c.711A>T mit den Serum-Glukose-Konzentrationen assoziiert ist. Ein zentrales Ergebnis dieser Studie ist, dass der ABCB4-Transporter sowohl im murinen Organismus als auch beim Menschen die Glukosehomöostase moduliert. Zudem weisen die Daten auf die potenzielle Rolle von Phosphatidylcholin bei der Regulation des Glukosestoffwechsels hin. Im Rahmen von zukünftigen anti-diabetischen Therapien mit LRH-1-Agonisten (Hohenester and Beuers 2011) könnte daher eine Genotypisierung von *ABCB4*-Varianten für die Stratifizierung der Patienten hilfreich sein.

Die hier dargestellte Studie wurde mit freundlicher Unterstützung der Arbeitsgruppe von Prof. Dr. Dietrich Volmer (Institut für Bioanalytische Chemie, Universität des Saarlandes), welche die Identifizierung der Phosphatidylcholine mittels MALDI-FTICR übernommen hat, durchgeführt. Dr. Marcin Krawczyk (Klinik für Innere Medizin II, Universitätsklinikum des Saarlandes) war als gleichberechtigter Erstautor maßgeblich an der genetischen Assoziationsstudie und der Erstellung des Manuskripts beteiligt.

THE HEPATIC PHOSPHATIDYLCHOLINE TRANSPORTER ABCB4 AS MODULATOR OF GLUCOSE HOMEOSTASIS

Katrin Hochrath[1*], Marcin Krawczyk[1*], Reinhild Goebel[1], Miriam Langhirt[1], Birgit Rathkolb[2,3], Kateryna Micklich[2,3], Jan Rozman[3,4], Marion Horsch[3], Johannes Beckers[3,5], Martin Klingenspor[4], Helmut Fuchs[3], Valérie Gailus-Durner[3], Eckhard Wolf[2], Monica Acalovschi[6], Dietrich A. Volmer[7], Martin Hrabě de Angelis[3,5,8], Frank Lammert[1]

[1]Department of Medicine II, Saarland University Medical Center, Homburg, Germany; [2]Institute of Molecular Animal Breeding and Biotechnology, Ludwig-Maximilians-Universität München, Munich, Germany; [3]German Mouse Clinic, Institute of Experimental Genetics, Helmholtz Zentrum München, German Research Center for Environmental Health GmbH, Neuherberg, Germany; [4]Department of Molecular Nutritional Medicine, Else Kröner-Fresenius Center & Z I E L - Research Center for Nutrition and Food Science, and [5]Chair of Experimental Genetics, Technische Universität München, Freising-Weihenstephan, Germany; [6]Department of Medicine III, Iuliu Hatieganu University of Medicine and Pharmacy, Cluj-Napoca, Romania; [7]Institute of Bioanalytical Chemistry, Saarland University, Germany, [8]German Center for Diabetes Research (DZD), Neuherberg, Germany

[*]Contributed equally

FASEB Journal 2012; 26:5081-5091

ABSTRACT

Purpose: The hepatic phosphatidylcholine (PC) transporter ABCB4 flops PC from hepatocytes into bile, and its dysfunction causes chronic cholestasis and fibrosis. Since a nuclear receptor-dependent PC pathway has been identified to exert antidiabetic effects, we now analyzed the role of ABCB4 in glucose metabolism.

Procedures: We bred congenic *Abcb4* knockout (*Abcb4*$^{-/-}$) mice on the fibrosis-susceptible BALB/cJ background. Knockout mice and wild-type controls were phenotyped by measuring plasma glucose concentrations, intraperitoneal glucose tolerance tests, hepatic RNA expression profiles, and liver histology. In addition, four pro-cholestatic *ABCB4* gene variants were correlated with blood glucose levels in 682 individuals from two independent European cohorts.

Findings: Systemic glucose levels differ significantly between *Abcb4*$^{-/-}$ mice and wild-type controls, and knockout mice display improved glucose tolerance with significantly lower area-under-the-curve values upon intraperitoneal glucose challenge. Of note, hepatic expression of the anti-diabetic nuclear receptor 5A2 (*LRH-1*) is induced consistently in *Abcb4*$^{-/-}$ mice and its specific rare PC ligands are detected in liver by mass spectrometry imaging. In humans, serum glucose levels are associated significantly with the common *ABCB4* variant c.711A>T.

Conclusions: ABCB4 might play a critical role in glucose homeostasis in mice and men. We speculate that the effects could be mediated via *LRH-1*-dependent PC pathways.

INTRODUCTION

Bile is composed mainly of water, sterols, bile salts (BS), and phospholipids, in particular phosphatidylcholine (PC) [1]. These substances, apart from water, are transported from hepatocytes into bile by specific hepatobiliary ATP-binding cassette (ABC) proteins, namely ABCB4 (PC floppase), ABCB11 (BS export pump), and ABCG5/8 (sterol transporter) [2]. Once transferred into the lumen of bile ducts, sterols, BS and PC form mixed micelles to reduce the toxicity of bile acids and to establish physiological bile flow. Conversely, in case of dysfunction of the ABC proteins, bile composition is deranged and cholestatic disorders with liver dysfunction prevail [3]. Recently others and we identified *ABCB4* gene variants that increase the risk of cholestasis in pregnancy [4, 5] and showed that rare mutations in the hepatic PC transporter cause the so-called LPAC ('low phospholipid-associated cholelithiasis') syndrome, characterized by recurrent extra- and intrahepatic gallstones in young adults [6, 7]. In line with these results, mice lacking the ABCB4 transporter are characterized by the absence of PC in bile and increased bile toxicity [8, 9]. As a result, ABCB4 deficient animals spontaneously develop chronic cholangitis and secondary biliary fibrosis [10], resembling sclerosing cholangitis in humans [11].

PC flopped from hepatocytes into bile by ABCB4 is composed of a variety of fatty acids. As we reported previously [9], the major PC species in murine bile include C16:0/C18:2, C16:0/C18:1 and C16:0/C20:4 fatty acids. Lately PC with even shorter saturated fatty acid acyl side chains (i.e. diundecanoyl-PC (DUPC); C11:0/C11:0 and dilauroyl-PC (DLPC); C12:0/C12:0) have been recognized as endogenous ligands of the nuclear receptor liver receptor homologue-1 (LRH-1) [12, 13]. Nuclear receptors serve as transcriptional factors, and LRH-1 is expressed predominantly in liver, small intestine, preadipocytes and adrenal glands, where it is involved in metabolic pathways governing sterol transport, BS homeostasis, and steroidogenesis [14]. Interestingly, activation of LRH-1 by PC has been demonstrated to improve insulin sensitivity in diabetic mice [13]. Besides this, studies of phophatidylcholine transfer protein knockout (*Pctp*$^{-/-}$) mice

show a link of specific phosphatidylcholine species and the regulation of hepatic glucose metabolism [15, 16].

To date, *Abcb4* knockout (*Abcb4*$^{-/-}$) mice have been broadly investigated with respect to liver phenotypes [8-10, 17], but associations between dysfunction of the ABCB4 transporter and glucose metabolism or with other metabolic traits have not been elucidated. Of note, genetic studies in humans have linked the 7q21.1 locus, harboring the *ABCB4* gene, with an increased risk of diabetic nephropathy [18], whereas linkage and association between 7q21.1-21.3 loci and non-insulin dependent diabetes as well as insulin resistance were reported almost two decades ago [19, 20].

In our current study we have performed a systematic phenotyping [21] of *Abcb4*$^{-/-}$ mice and found a novel association between glucose levels and deficiency of the hepatic PC transporter. Subsequent expression analyses in *Abcb4*$^{-/-}$ animals allowed us to dissect metabolic pathways that contribute to lower glucose levels. In addition, we genotyped four common *ABCB4* polymorphisms in 682 adult individuals from two independent European cohorts and correlated serum glucose levels with the frequencies of pro-cholestatic variants.

METHODS

Animals

Generation of congenic BALB-Abcb4$^{-/-}$ mice

The BALB-*Abcb4*$^{-/-}$ mouse was generated by backcrossing the *Abcb4*^{tm1Bor} knockout from the fibrosis-resistant FVB/NJ strain (The Jackson Laboratory, Bar Harbor, ME, USA) into the fibrosis-susceptible BALB/cJ background for 10 generations [22, 23]. BALB/cJ control mice were obtained from Charles River Laboratories (Sulzfeld, Germany). Mice were housed in individually ventilated cages with a 12-hr light-dark cycle; temperature and humidity were regulated to 22 ± 1°C and 55 ± 5% respectively, with water and standard diet (Altromin 1314, Lage, Germany) provided *ad libitum*. All mice used for experiments were aged between 14 to 20 weeks.

Genotypes of mice were confirmed by polymerase chain reaction (PCR) of tail DNA using *neo* (5´- CTT GGG TGG AGA GGC TAT TC -3´; 5´-AGG TGA GAT GAC AGG AGA TC -3´) and *Abcb4* (5´-CAC TTG GAC CTG AGG CTG TG; TCA GGA CTC CGC TAT AAC GG -3´) specific primer pairs. The PCR reaction contained 10 × PCR buffer (Applied Biosystems, Darmstadt, Germany), 2 mM $MgCl_2$, 10 µM dNTPs, 10 µM primer, 1.25 U Taq DNA polymerase (Invitrogen, Darmstadt, Germany) and 20 -100 ng DNA in 25-µl reactions. PCR cycling conditions were 94°C/30 s, 55°C/60 s and 72°C/30 s for 35 cycles, and a final extension step of 10 min at 72°C.

Phenotypic characterisation of biliary fibrosis

Liver samples for histopathological evaluation were fixed in 4% neutral buffered formalin at 4°C for 24 hrs and embedded in paraffin. Paraffin sections (1 µm) were stained with hematoxylin-eosin (H&E), or Sirius red for the detection of collagen. Histomorphometric analysis of hepatic fibrosis was performed with semiautomatic microscopic image analysis (Leica application suite software,

Wetzlar, Germany). Relative collagenous areas were calculated from 10 microscopic fields (magnification 100 ×) randomly chosen on each liver section. In addition, we quantified collagen in liver by colorimetric measurement of the collagen specific amino acid hydroxyproline (Hyp), as described [22, 24].

Blood samples were obtained from isoflurane-anesthetized mice by puncturing the retro-orbital sinus with capillaries and collected in heparinized tubes. Plasma alanine aminotransferase and alkaline phosphatase activities as well as glucose concentrations were measured with an Olympus AU400 chemistry analyzer, using adapted reagents provided by Olympus (Hamburg, Germany).

Intraperitoneal glucose tolerance test (IpGTT)

After overnight food withdrawal (16 - 18 hrs), mice were weighed and intraperitoneally injected with 2 g glucose/kg body weight. Blood samples for glucose measurements (Accu-Chek Aviva, Roche Diagnostics, Mannheim, Germany) were collected from tail vein and analyzed before glucose injection as well as 15, 30, 60 and 120 min afterwards. For calculating the area-under-the-curves (AUC), the trapezoidal rule was used, and the area below the baseline glucose level was excluded.

Genome-wide hepatic expression profiling

For genome-wide expression analysis, liver tissue of four male *Abcb4*$^{-/-}$ and four BALB/cJ control mice was snap frozen in liquid nitrogen, and total RNA was isolated using RNeasy Midi kit (Qiagen, Hilden, Germany). The cDNA microarrays were generated, hybridized and analyzed as described [25, 26]. Two chip hybridizations were performed with total RNA for each individual mutant mouse against a reference RNA pool of the same organ. The normalization [27] and the selection of the significantly differentially expressed genes with reproducible up- or down-regulation [26, 28] includes 1.3% false positives in combination with mean fold change > 1.3 ×. Expression data were submitted to the Gene Expression Omnibus (GEO) database

(http://www.ncbi.nlm.nih.gov/geo/) (GSE26699), where also a full description of the microarray platform is available (GPL4937). Ingenuity Pathway analysis (IPA, www.ingenuity.com) was utilized to identify over-represented Gene Ontology (GO) terms in the categories molecular functions and canonical pathways among the differentially expressed genes.

Hepatic expression of genes involved in glucose homeostasis

To determine the hepatic expression of single genes involved in glucose metabolism, liver samples of mice allowed access to food overnight were harvested. For expression analysis during IpGTT, organs were collected from animals denied access to food overnight that were euthanized at baseline (t_0) and after 60 min (t_{60}). All samples were immediately snap-frozen in liquid nitrogen and stored at -80°C until analyzed. To minimize the effects of circadian rhythm, all mice were euthanized between 9 and 11 AM.

The steady-state hepatic mRNA expression levels of individual genes were determined by quantitative real-time PCR (TaqMan®, Applied Biosystems, California, USA), using 1 µg RNA for reverse transcription and 18S RNA as endogenous control, with one cycle at 95°C for 10 min, followed by 45 cycles at 95°C/30 s and 60°C/60 s. The expression level of each gene was calculated by the ΔΔct-method [29], in relation to counterpart wild-type controls and also normalized to wild-type animals. For expression analysis after IpGTT, ΔΔct was calculated relative to the dedicated genotype-specific controls at t_0 (e.g. $\Delta\Delta ct_{Lrh\text{-}1}$ = $\Delta ct_{Lrh\text{-}1}$ BALB-*Abcb4*$^{-/-}$ female at t_{60} - mean $\Delta ct_{Lrh\text{-}1}$ BALB-*Abcb4*$^{-/-}$ females at t_0). The RQ (relative quotient, $2^{-\Delta\Delta ct}$) of all data was normalized to values of BALB/cJ mice at t_0.

Primary hepatocytes

Hepatocytes of BALB/cJ and BALB-*Abcb4*$^{-/-}$ mice (n = 5 - 7 per genotype and treatment group) were isolated using collagenase perfusion two-step system as described before [30]. After purification, hepatocytes were cultured on collagen-

coated 6-well plates (300,000 cells/well) in Williams E medium supplemented with 10% fetal bovine serum and 100 nM dexamethasone for 4 hours. Subsequently, medium was changed for overnight serum starvation. Hepatocytes were incubated with 100 µM DLPC (Tocris, Bristol, United Kingdom) or ethanol only for 24 hours. Cells were washed twice with ice-cold phosphate-buffered saline and harvested. Total RNA was isolated with the Qiagen RNeasy Mini kit as described above. Relative RNA quantification by real-time PCR was performed for *Cyp7a1, Cyp7b1, Cyp8b1, Gck1, G6pc, Lrh-1, Nr0b2* and *Pck1* with TaqMan® assays as described above.

Identification of hepatic phospholipids

Mass spectrometry imaging (MSI) experiments for identification of phospholipid species including the LRH-1 ligands DUPC ($C_{30}H_{61}NO_8P$) and DLPC ($C_{32}H_{65}NO_8P$) in liver were performed on a Bruker solariX 12 Tesla matrix-assisted laser desorption/ionization (MALDI) Fourier transform ion cyclotron resonance (FTICR) instrument equipped with an Apollo II MALDI/ESI source and a Smart Beam II NdYAG 1 kHz high repetition rate laser (Bruker, Bremen, Germany). Liver samples were snap-frozen, sliced into 4 µm sections using a cryostat and placed onto microscopy glass slides. Homogenous MALDI matrix layers were deposited onto the tissue surface by means of a Bruker ImagePrep system using α-cyano-4-hydroxycinnamic acid solution at 7 mg/ml dissolved in 50% acetonitrile/water (v/v) + 0.2% trifluoracetic acid. The pixel size in imaging experiments was 75 µm. Positive ions were monitored in experiments in the *m/z* range of 150-1500. For elemental formula assignments, no atom constraints for C, H, N, O and P were set. All calculations were performed with the MIDAS molecular formula calculator (NHMFL, Florida, USA).

Patients

Recruitment of cohorts

We analyzed two independent, previously described cohorts (N = 682, 485 females, age 21 - 89 years) from Germany (N = 366) [31] and Romania (N = 316) [32, 33]. Table 1 summarizes the baseline clinical characteristics of both cohorts. The German cohort comprised unrelated individuals with gallstones (N = 183) and stone-free controls (N = 183). The Romanian cohort consisted of 235 sibs with gallstones from 100 families and 216 unrelated stone-free controls. In the analysis, all German individuals, all Romanian controls and one randomly selected sib from each Romanian family were included. Serum glucose levels from fasted blood samples were determined by standard clinical-chemical assays in the central laboratories at both university hospitals. None of the individuals was under glucose lowering therapy at inclusion. Informed consent was obtained from all patients, and the study was approved by the independent Ethics Committees of the University of Aachen and the University of Cluj-Napoca.

Table 1: Clinical characteristics of study cohorts

Characteristic	**Value**
Patients (N)	682
Romania	316
Germany	366
Gender (N)	
Females	485
Males	197
Serum glucose (mM)	
Median	5.36
Range	2.76 - 21.82
Body mass index (kg/m^2)	
Median	26
Range	14 - 49
Age (years)[a]	
Median	59
Range	21 - 89

[a]Date was calculated at the date of inclusion

Genotyping of ABCB4 polymorphisms

Genomic DNA was isolated from EDTA-anticoagulated blood according to the membrane-based QIAamp DNA extraction protocol (Qiagen, Hilden, Germany). The *ABCB4* single nucleotide polymorphisms (SNP) in exon 6 (c.504C>T, rs1202283), exon 8 (c.711A>T, rs2109505), exon 16 (c.1954A>G, rs2230028) and intron 26 (rs31653) were genotyped using solution-phase hybridization reactions with 5'-nuclease and fluorescence detection (TaqMan® SNP genotyping assays) in a 7500 FAST real-time PCR system (TaqMan®, Applied Biosystems, California, USA). The PCR reactions contained 20 - 40 ng DNA, 1 × TaqMan® genotyping master mix and 1 × TaqMan® SNP genotyping assay in 10 µl-reactions. Amplification conditions were 95°C for 10 min, followed by 40 cycles of 95°C/10 s, and 60°C/60 s. Genotyping success rates were > 99%.

Statistics

Statistical analysis was performed with SPSS 19 (IBM, Ehningen, Germany), unless stated otherwise. The Kolmogorov-Smirnov test was used to determine whether data had a normal distribution. Quantitative data were expressed as means ± SE or median and ranges, as appropriate. Means and medians were compared with Student's t-tests or Mann-Whitney U tests, respectively. Two-way ANOVA was applied to assess the influence of mice gender and *Abcb4* genotype on glucose levels during IpGTT. For all tests, p-values < 0.05 were regarded as significant.

The consistency of genotyping results with Hardy-Weinberg equilibrium was checked by exact test (http://ihg2.helmholtz-muenchen.de/cgi-bin/hw/hwa1.pl) [34]. The effects of genotype, age, gender and body mass index (BMI) on glucose levels were assessed by linear regression analyses. To characterize the influence of the above factors on glucose levels and to obtain the optimal linear model, a backward variable selection using Akaikes information criteria (AIC) was computed. The AIC optimal model includes genotype, age, and BMI.

RESULTS

Hepatic phenotype of *Abcb4*$^{-/-}$ mice

Increased serum activities of alkaline phosphatase (AP) and bilirubin levels demonstrate prominent cholestasis in BALB-*Abcb4*$^{-/-}$ mice lacking the hepatic PC transporter as compared to controls (Figure 1, panel A). Simultaneous increases of alanine aminotransferase (ALT) and lactate dehydrogenase (LDH) activities indicate mixed hepatocellular and cholestatic liver injury. Panel B of Figure 1 demonstrates that the hepatic collagen concentrations in *Abcb4*$^{-/-}$ mice as assessed by Hyp contents are markedly increased in comparison to controls (males 289 *vs*. 191 µg Hyp/g liver; females 343 *vs*. 213 µg Hyp/g liver). Panel C of Figure 1 shows representative liver sections of BALB-*Abcb4*$^{-/-}$ mice stained with Sirius red. We observed proliferation of bile ducts and prominent periportal collagen aggregation. Accordingly, panel D of Figure 1 shows that mean collagen areas are significantly ($p < 0.01$) enhanced in livers from *Abcb4*$^{-/-}$ mice of both genders as compared to wild-type animals (males 1.67 ± 0.22% *vs*. 0.36 ± 0.09%; females 2.01 ± 0.29% *vs*. 0.82 ± 0.13%).

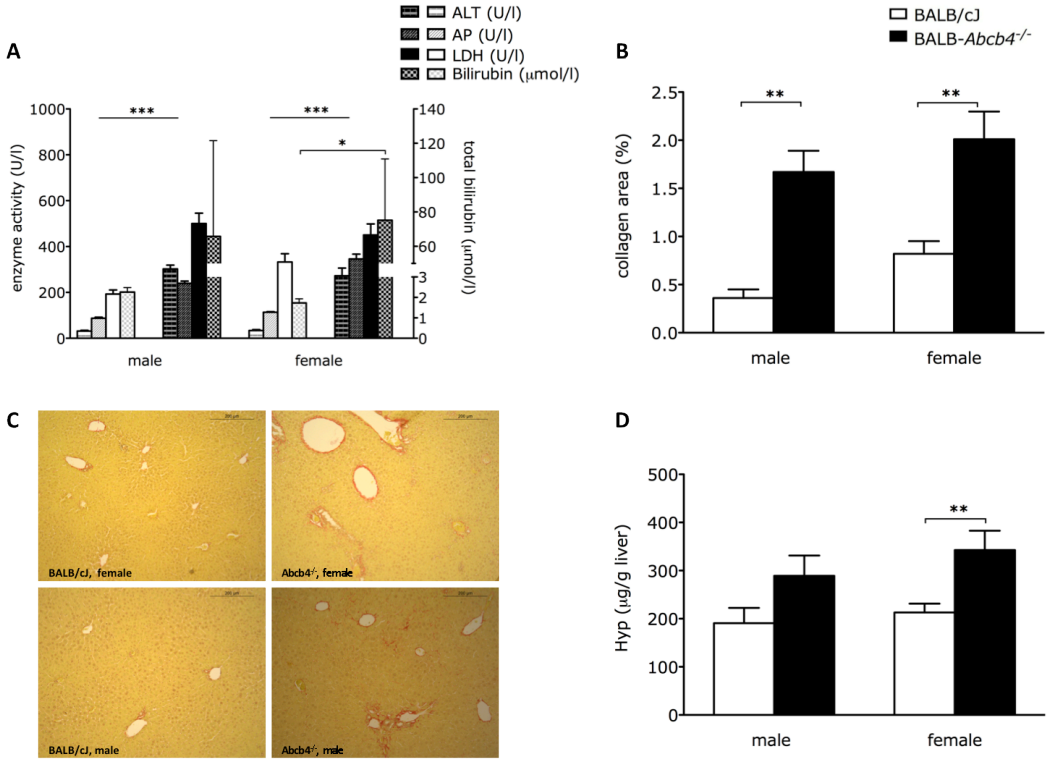

Figure 1: **(A)** Liver enzyme activities and bilirubin concentrations in plasma from male and female BALB-*Abcb4*$^{-/-}$ (dark bars) and BALB/cJ wild-type mice (light bars); N = 10 per gender and genotype. Abbreviations: ALT, alanine aminotransferase; AP alkaline phosphatase; LDH, lactate dehydrogenase.
(**B**) Hepatic hydroxyproline (Hyp) levels in *Abcb4*$^{-/-}$ (solid bars) and wild-type mice (open bars). N = 11 - 26 per gender and genotype.
(**C**) Representative liver sections from female (top panels) and male (bottom panels) *Abcb4*$^{-/-}$ mice (right panels) and wild-type controls (left panels). Sirius red stain.
(**D**) Hepatic collagen areas in *Abcb4*$^{-/-}$ and wild-type mice, measured in paraffin sections stained with Sirius red (*see* panel C) and calculated by semiautomatic microscopic image analysis. N = 5 - 7 per gender and genotype.
* $p < 0.05$** $p < 0.01$, *** $p < 0.001$.

Glucose tolerance in *Abcb4*$^{-/-}$ mice

Figure 2 (panel A) illustrates that *Abcb4* knockout mice allowed access to food overnight display significantly ($p < 0.001$) lower plasma glucose concentrations than corresponding wild-type controls (males 6.40 ± 0.29 *vs*. 9.05 ± 0.54 mmol/l; females 4.08 ± 0.52 *vs*. 6.90 ± 0.39 mmol/l). Of note, glucose concentrations in ABCB4 deficient mice after overnight food withdrawal are significantly

($p < 0.05$) higher as compared to wild-types (males 4.10 ± 0.11 *vs*. 3.40 ± 0.05 mmol/l; females 3.20 ± 0.12 *vs*. 2.90 ± 0.07 mmol/l; Figure 2, panel B).

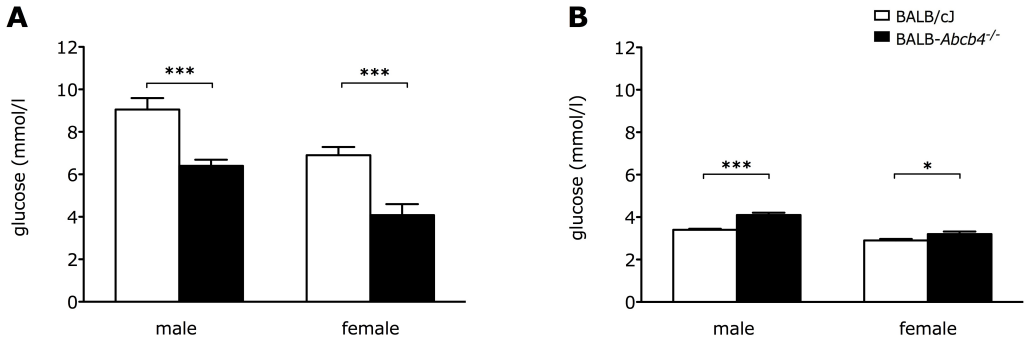

Figure 2: Plasma glucose levels in male and female BALB-*Abcb4*$^{-/-}$ mice (solid bars) and BALB/cJ wild-type controls (open bars) in mice allowed access to food overnight (**A**) and after overnight food withdrawal (**B**). N = 10 per gender and genotype. * $p < 0.05$,*** $p < 0.001$.

The graphic of the plasma glucose levels at different time points during IpGTT (Figure 3, panel A) shows that *Abcb4* knockout mice display significantly ($p < 0.001$) lower glucose peaks during IpGTT. Based on the glucose concentrations at different time points, we calculated AUC values (Figure 3, panel B), demonstrating that *Abcb4*$^{-/-}$ animals have significantly ($p < 0.01$) lower AUC between 30 and 120 min after glucose administration. Two-way ANOVA (Supplementary Table 1) indicated that each variable (i.e. *Abcb4* genotype, gender and time) affects glucose levels independently ($p < 0.001$). For comparison, we performed IpGTT in female *Abcb4*$^{-/-}$ mice on the FVB/NJ background, which also showed significantly ($p = 0.01$) lower AUC between 30 and 120 min after glucose exposure compared with FVB wild-type controls.

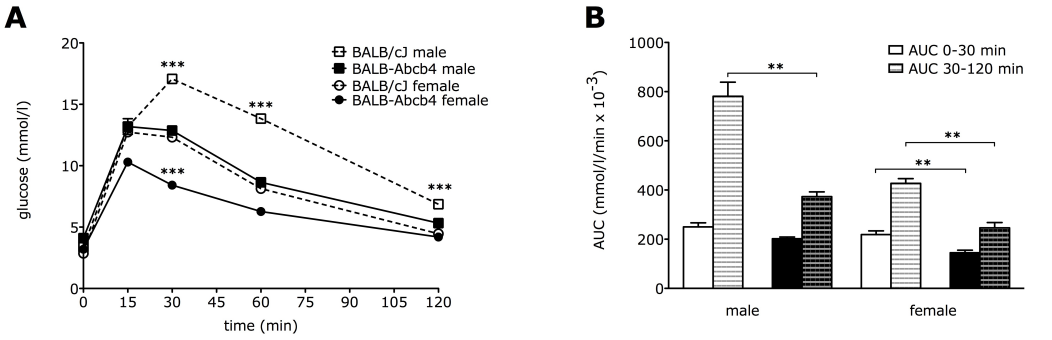

Figure 3: Intraperitoneal glucose tolerance test (IpGTT) in male and female BALB-*Abcb4*$^{-/-}$ mice (solid symbols) and BALB/cJ wild-type controls (open symbols).
(**A**) Plasma glucose levels before and 15, 30, 60 and 120 min after glucose challenge. Female mice are indicated by circles and male animals by squares.
(**B**) AUC during IpGTT for the time intervals 0 - 30 min (open and solid bars) and 30 -120 min (light and dark striped bars), as approximated using the trapezoidal rule excluding the area below the baseline glucose level (glucose at t0). ** $p < 0.01$. *** $p < 0.001$

Hepatic expression profiles in *Abcb4*$^{-/-}$ mice

Statistical analyses of the cDNA transcriptome profiles of liver identified a total of 85 genes differentially regulated between *Abcb4*$^{-/-}$ and wild-type mice (Supplementary figure 1). Among the dataset of regulated genes GO analysis (*see* Methods) revealed over-representation of several terms in the categories molecular functions and canonical pathways (Table 2). The expression profiling (Supplementary figure 1) highlighted genes that we and other have previously identified as modifiers of chronic liver inflammation and fibrosis, such as cathepsin B (*Ctsb*) [35], carbamoyl-phosphate synthetase 1 (*Cps1*) [36], complement factor 5 (*Hc*) [23], decorin (*Dcn*) [37], glycine N-methyltransferase (*Gnmt*) [38], and lipocalin 2 (*Lcn2*) [39]. Moreover, as shown in Table 2, we identified induced expression of 11 genes involved in carbohydrate metabolism.

Table 2: Go terms of the categories molecular function and canonical pathways overrepresented in *Abcb4*$^{-/-}$ mice compared with those in wild-type controls

GO term	
Molecular function	**Genes**
Amino Acid Metabolism	*Gnmt, Ass1, Oat, DdAh1, Csad, Tat, Slc6a7, Cps1*
Cancer	*Gstp1, Ass1, Gpx1, Clu, Psen2, Orm1, Csf2ra, Anxa5, Plin2, Lsr, Ly6e, Enpp2, Tmsb4x, Gstm1, Hpx, Dcn, Gstm3, Lcn2, Pold1, Fabp5, Eef1a1, Ctsb, Ubc, Tmem176b, Rap2a, Col3a1*
Carbohydrate metabolism	*Gnmt, Apoa4, Fabp5, Plin2, Anxa5, Gpx1, Lpl, Eef1a1, Ctsb, Enpp2, Cps1*
Cardiovascular disease	*Gstm1, Gstp1, Apoa4, Gpx1, Lcn2, Clu, Psen2, Ttpa, Nad*$^{+}$*, Dlg5, Csf2ra, Lsr, Anxa5, Cnst, Pros1, Ddah1, Lpl, Col3a1*
Cell death	*Gstm1, Gstp1, Nfic, Gsta1, Dcn, Lcn2, Gpx1, Clu, Psen2, Nad*$^{+}$*, G0s2, Csf2ra, Anxa5, Ctsp, Eef1a1, Tmsb4x*
Cell signaling	*Ass1, Ddah1, Eef1a1, Psen2, Cps1, Nad*$^{+}$
Drug metabolism	*Gstm1, Gstp1, Gnmt, Gsta1, Gstm3, Gpx1, Ctsb, Ly6e*
Gastrointestinal disease	*Dhx58, Gstm1, Gstp1, Hpx, Lcn2, Gpx1, Clu, Arnt2, Pold1, Dlg5, Csf2ra, Cnst, Ctsb, Enpp, Cps1, Col3a1*
Hepatic system disease	*Gstm1, Hpx, Gstp1, Fabp5, Csf2ra, Plin2, Lpl, Clu, Arnt2, Pold1, Col3a1*
Lipid metabolism	*Gstm1, Hpx, Gstp1, Apoa4, Gstm3, Gsta1, Gpx1, Clu, Ttpa, Fabp5, Lsr, Anxa5, Plin2, Lpl, Eef1a1, Enpp2, Cps1*
Neurological disease	*Gstp1, Itih3, Apoa4, Zep36l1, Clu, Psen2, Ttpa, Slc6a7, Arnt2, Orm1, Nad+, Ccf2ra, Pros1, Cnst, Anxa5, Lpl, Enpp2, Tmsb4x, Ubb, Gstm1, Hpx, Ush2a, Orm2, Arhgap10, Dcn, Lcn2, Fam49a, Dlg5, Ctsb, Eef1a1*
Vitamin and mineral metabolism	*Gnmt, Plin2, Gsta1, Lpl, Psen2, Ttpa*
Canonical pathway	**Genes**
Acute phase response signaling	*Hpx, Itih3, Orm2, Itih2, Orm1*
Aryl hydrocarbon receptor signaling	*Gstm1, Gstp1, Nfic, Gstm3, Gsta1*
Glutathione metabolism	*Gstm1, Gstp1, Gstm3, Gsta1, Gpx1*
LPS/IL-1 mediated inhibition of RXR function	*Gstm1, Gstp1, Fabp5, Gstm3, Gsta1*
Metabolism of xenobiotics by cytochrome P450	*Gstm1, Gstp1, Gstm3, Gsta1*
NRF2-mediated oxidative stress response	*Gstm1, Ubb, Gstp1, Gstm3, Gsta1*

Data of microarray experiments; genes were classified by IPA (see Methods).

Therefore we analyzed by real-time PCR hepatic expression of genes encoding key enzymes and transcription factors implicated in glucose homeostasis in mice allowed access to food overnight (Figure 4, panel A) and in mice denied access to food overnight before and during the first 60 min of IpGTT (Figure 4, panel B). Panel A of Figure 4 shows that steady-state mRNA levels of phosphoenolpyruvate carboxykinase (*Pck1*), glucokinase (*Gck*) and glucose-6-

phosphatase (*G6pc*) are all markedly induced in *Abcb4*$^{-/-}$ in comparison to wild-type mice. Of note, the expression of the PC-activated nuclear receptor *Lrh-1* (*Nr5a2*), the *bona fide* PC receptor [13], shows a 5-fold increase in *Abcb4* deficient ice as compared to controls. In primary hepatocytes (which however do not express the PC transporter ABCB4 properly at a canalicular domain), we also observed highest *Lrh-1* mRNA levels in *Abcb4* deficient cells treated with DLPC (*see* Methods). However, we did not detect major expression differences for the gene set tested *in vivo* (Figure 4) under our experimental conditions (data not shown).

We did also not detect any expression difference for the transcription factor *Srebf1*, which activates the expression of genes dedicated to sterol, triglyceride and PC synthesis [40] and is repressed by PC [13], between *Abcb4*$^{-/-}$ and wild-type mice *in vivo*. In contrast, the expression of the coactivator 1 alpha of PPAR-γ (*Ppargc1a*) and the transcription factor *Foxo1*, both involved in the regulation of gluconeogenesis [41], is induced.

Figure 4B compares the gene expression changes during glucose challenge (IpGTT). After overnight food withdrawal (t_0), only the expression of *Gck* is appreciably enhanced in *Abcb4*$^{-/-}$ in comparison to wild-type mice. Sixty minutes after glucose administration (t_{60}), the expression levels of all measured genes, with exception of *Gck,* increase. In particular, the genes encoding PCK1, G6PC and LRH-1 are markedly induced in ABCB4 deficient in comparison to control mice.

To provide evidence for LRH-1 activation in *Abcb4*$^{-/-}$ mice, we measured hepatic gene expression of LRH-1 target genes (in particular *Cyp8b1*), the *Lrh-1* co-repressor *Nr0b2* (a.k.a. small heterodimer partner, *Shp*) and the bile salt farnesoid X receptor *Nr1h4* (alias *Fxr)* in mice challenged with glucose. As presented in panel C of Figure 4, *Abcb4*$^{-/-}$ mice demonstrate significantly ($p < 0.05$) increased expression of *Cyp8b1* and *Cyp7b1* compared with basal levels and with those in wild-type animals. In contrast, expression levels of *Cyp7a1* and *Nr1h4* did not differ between *Abcb4*$^{-/-}$ and wild-type mice in this setting.

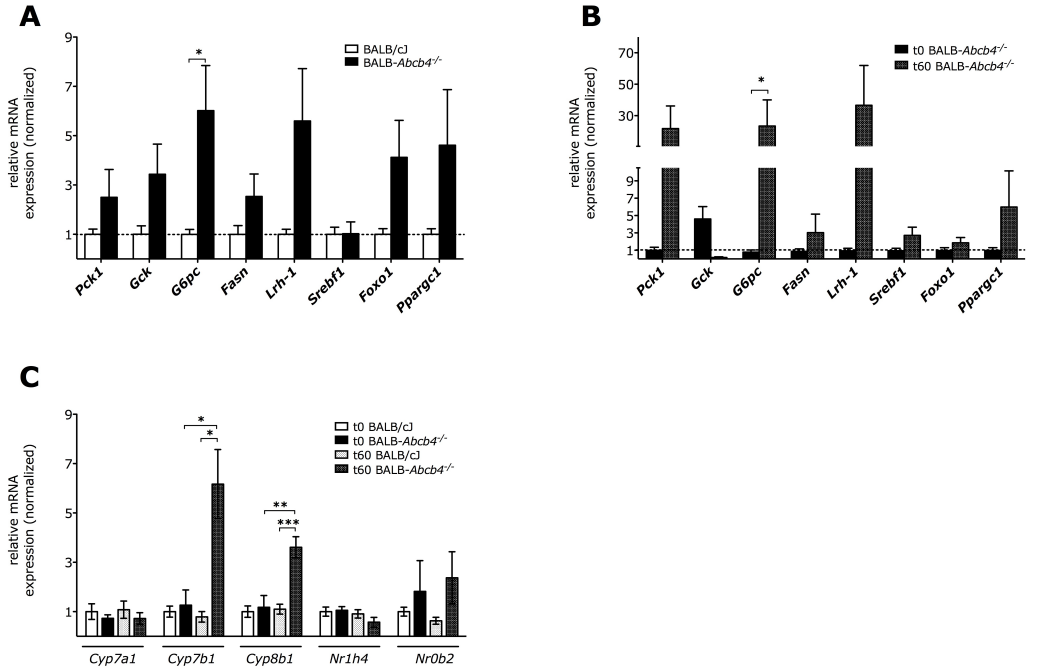

Figure 4: Relative mRNA expression levels of genes involved in glucose homeostasis in BALB-*Abcb4*$^{-/-}$ and BALB/cJ wild-type mice.
(**A**) *Abcb4*$^{-/-}$ mice (solid bars) and wild-type mice (open bars) allowed access to food overnight. All expression levels are normalized to controls. Black dotted line marks the expression levels in controls at t_0. N = 5 -12 per genotype.
(B) Expression in *Abcb4*$^{-/-}$ mice relative to wild-type mice during IpGTT at baseline (t_0; solid bars) and after 60 min (t_{60}; hashed bars). All expression levels are normalized to those of corresponding controls at t_0. Black dotted line marks the expression levels in controls at t_0. N = 3 - 10 per time point and genotype.
(**C**) Hepatic expression levels of LRH-1 target genes and genes involved in bile salt homeostasis in BALB/cJ and BALB-*Abcb4*$^{-/-}$ mice during IpGTT. N = 5 - 9 per time point and genotype. * $p < 0.05$, ** $p < 0.01$, *** $p < 0.001$.
Gene symbols: *Cyp7a1*, cytochrome P450 family 7, subfamily A, polypeptide 1; *Cyp7b1*, cytochrome P450 family 7, subfamily B, polypeptide 1; *Cyp8b1*, cytochrome P450, family 8, subfamily B, polypeptide 1; *Fasn*, fatty acid synthase; *Foxo1*, forkhead box O1; *G6pc*, glucose-6-phosphatase, catalytic subunit; *Gck*, glucokinase; *Lrh-1*, liver receptor homolog 1; *Nr0b2*, nuclear receptor subfamily 0, group B, member 2; *Nr1h4*, nuclear receptor subfamily 1, group H, member 4; *Pck1*, phosphoenolpyruvate carboxykinase 1; *Pparγc1α*, peroxisome proliferate activated receptor gamma coactivator 1 alpha; *Srebf1*, sterol regulatory element binding transcription factor 1.

Mass spectrometry imaging experiments identify LRH-1 agonists in *Abcb4*$^{-/-}$ liver

Imaging of liver sections using ultra high resolution, accurate mass MALDI-MSI proved the presence of the phospholipids DUPC (C11:0/C11:0) and DLPC (C12:0/C12:0) in murine liver. In these imaging experiments (Figure 5), we were able to identify distinct distribution patterns of these two natural ligands. Importantly, the experimental mass uncertainties for the measured *m/z* ratios of the lipid species on the tissue slice were ≤ 0.27 ppm as compared to calculated, exact *m/z* ratios, with no alternative formula proposals within ± 2 ppm centered on the measured [M+H] ions, thus providing adequate confidence for positive identification of the two lipid species. These *bona fide* LRH-1 agonists were not previously detected in liver.

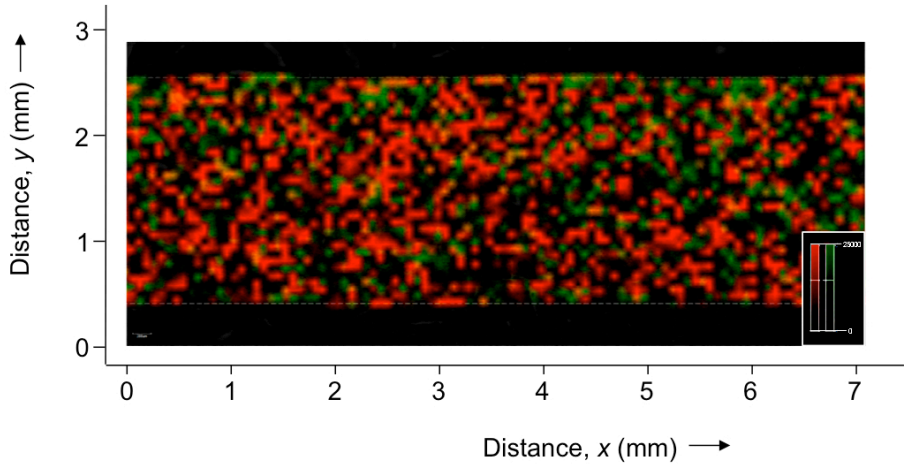

Figure 5: MALDI-MSI analysis of mouse liver section using high resolution, accurate mass FTICR-MS. Composite image illustrating spatial distribution of dilauroyl-PC (DLPC, C12:0/C12:0; red) and diundecanoyl-PC (DUPC, C11:0/C11:0; green). Orange color indicates overlapping areas of DUPC and DLPC. The intensity scale of the heatmap corresponds to color contrast units (25,000 arbitrary units for maximum brightness (red/green); it is not calibrated for concentration units. Extracted $[M+H]^+$ species: DUPC, *m/z* 594.4129, DLPC, *m/z* 622.4442; extraction window: *m/z* ± 2 mDa; matrix: CHCA; pixel (laser) size: 75 µm.

Serum glucose levels in humans are associated with a common *ABCB4* variant

We genotyped four common *ABCB4* variants that were previously shown by us and other groups to be associated with hepatic phenotypes [4, 5]. Consistency with Hardy-Weinberg equilibrium confirmed robust genotyping (all $p > 0.05$), and the genotyping results were in line with the frequencies reported in the *Entrez* SNP database and previous publications [4, 5].

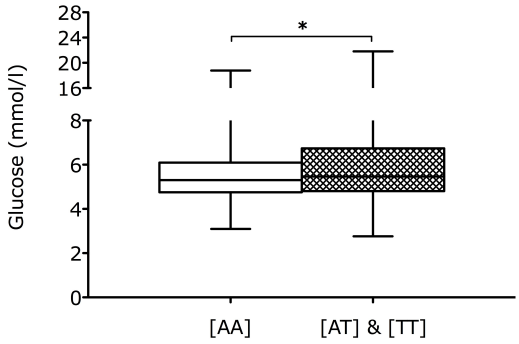

Figure 6: Median and range of serum glucose levels in patients with different genotypes of *ABCB4* variant c.711A>T.
Glucose concentrations in carriers of the genotype [AA] are significantly lower as compared to carriers of genotypes [AT] and [TT]. * $p < 0.05$.

Figure 6 illustrates that carriers of specific *ABCB4* c.711 variants display significantly ($p < 0.05$) different serum glucose levels. The genotypes [AA], [AT] and [TT] variants were carried by 478, 184 and 20 individuals, respectively. The homozygous carriers of the procholestatic genotype [AA] present with significantly lower median glucose levels (5.33 mmol/l, range 3.09 - 18.78 mmol/l) as compared to carriers of variants [AT] and [TT] (5.47 mmol/l, range 2.76 - 21.82 mmol/l). As shown in Table 3, the linear model after backward variable selection demonstrated that both the *ABCB4* variant and age independently affect serum glucose levels.

Table 3: Linear model for serum glucose levels after backward variable selection using the Akaikes information criteria

Coefficients	Estimate	P-value
ABCB4 [AA] ←→ [AT] [TT]	0.484 ± 0.199	0.015
Age (years)	0.024 ± 0.005	< 0.001
BMI (kg/m^2)	0.264 ± 0.018	0.144

DISCUSSION

To date, genetic polymorphisms in the *ABCB4* locus in humans and deficiency of the PC transporter in *Abcb4*$^{-/-}$ mice have been associated solely with cholestatic disease. This study is first to underscore an association between the ABCB4 transporter and serum glucose levels both in mice and humans. Our results show that individuals carrying an *ABCB4* pro-cholestatic risk variant have decreased glucose levels in general, and mice lacking the ABCB4 protein present with lower glucose levels in the fed state as compared to wild-type controls.

In our previous studies we observed marked differences in fibrosis susceptibility in inbred mouse strains, with BALB/cJ inbred mice being most susceptible, whereas FVB/NJ mice were more fibrosis-resistant [22]. By introgressing the *Abcb4* knockout from the resistant FVB/NJ strain into the fibrosis-susceptible BALB/cJ background, we created a unique congenic *Abcb4* mouse model with a more severe liver phenotype. Although we observed similar alterations of glucose homeostasis in both knockout lines, all subsequent experiments were performed in BALB-*Abcb4*$^{-/-}$ mice, which showed more pronounced alterations than the FVB-*Abcb4*$^{-/-}$ line. *Abcb4*$^{-/-}$ mice demonstrate an abnormal hepatic expression of genes involved in glycolysis and gluconeogenesis. This simultaneous induction of both pathways is noteworthy and is indicative for pathological processes resulting decreased serum glucose levels. The expression levels of regulators of insulin-dependent glucose metabolism (e.g. *Foxo1* and *Srebf1*) [42, 43] differ only slightly between *Abcb4*$^{-/-}$ mice and controls after glucose challenge, hence lower glucose levels do not seem to be related to insulin effects. Since hepatic expression profiles after food withdrawal do not differ between knockout and wild-type mice (except for *Gck*), ABCB4 deficiency appears to confer an improvement of glucose homeostasis that becomes apparent in the setting of increased systemic glucose levels. Our findings are supported by recent findings placing *Abcb4* in an expression network of murine genes associated with AUC of glucose in IpGTT, with *Abcb4* showing a positive

association with glucose intolerance [44].

Since ABCB4 represents the single PC export pump of liver, one of the possible explanations of our results relates glucose levels to distorted hepatic PC metabolism. Based on reports that PC acts as ligand for LRH-1 [45], it can be suspected that this nuclear receptor represents a critical regulator of glucose metabolism in ABCB4 deficient mice. Indeed, we found an increased expression of the *Lrh-1* gene in *Abcb4*$^{-/-}$ mice, which might be related to altered dynamics of hepatic PC metabolism. As shown recently [13], the activation of LRH-1 by specific PC species leads to decreased serum glucose levels in diabetic mice. In fact although the overall composition of major hepatic phospholipids has been reported to be stable in *Abcb4*$^{-/-}$ mice [46], we were able to demonstrate the presence of the *bona fide* LRH-1 ligands DUPC and DLPC in murine liver by MALDI-MSI. In search for LRH-1 target proteins that directly regulate glucose homeostasis, a recent article reported that mice with conditional deletion of *Lrh-1* in liver show reduced transcriptional activation of *Gck* by LRH-1, resulting in reduced glycolysis and glycogen synthesis in response to glucose exposure [47]. These findings are in line with our view of LRH-1 as regulator of postprandial glucose homeostasis. Expression analyses during IpGTT in our study clearly demonstrated an induction of LRH-1 targets, particularly *Cyp8b1*, in livers from *Abcb4*$^{-/-}$ mice after acute glucose challenge as compared to control, whereas *Cyp7a1* expression remained constantly low, in line with independent regulation of the rate-limiting step of bile salt synthesis in the setting of high systemic bile salt levels of cholestatic *Abcb4*$^{-/-}$ mice [48].

In humans, the composition of hepatic PC in carriers of *ABCB4* variants would be difficult to predict, but based on our findings in the mouse model a shift toward molecular species that activate LRH-1 and induce the expression of genes that modify glucose metabolism might be expected. On the other hand, given the complexity of glucose homeostasis one cannot exclude other, non-LRH-1-mediated regulatory pathways that contribute to lower serum glucose levels in *Abcb4*$^{-/-}$ mice. Since *Abcb4*$^{-/-}$ mice display intrahepatic cholestasis and increased serum bile salt concentrations [10], bile salt-dependent modulation of glucose

homeostasis via the membrane receptor TGR5 could play a role [49, 50], and in fact our systematic phenotypic characterization of metabolic rates (O_2 consumption) points to increased energy expenditure in *Abcb4*$^{-/-}$ mice (data not shown), albeit additional functional studies are needed. Furthermore in our translational study, none of the patients carrying *ABCB4* variants presented with cholestasis, indicating that the observed effects on glucose homeostasis are not related primarily to altered bile salt signaling.

The *ABCB4* c.711A allele that associates with lower serum glucose levels in our cohorts, is estimated to be carried by more than 80% of Europeans. The effect on glucose levels is underscored by the analysis that included non-genetic variables, demonstrating that the differences between carriers of distinct *ABCB4* genotypes remain significant even after inclusion of additional factors in the model (Table 3). This finding supports the potential role of variant *ABCB4* in glucose homeostasis. According to our previous study [5], the presence of the common c.711A allele increases the risk of cholestasis in pregnancy. In the patients from our current study we do not possess data on the frequency of obstetric cholestasis, but in general individuals carrying the risk allele c.711A do not display any specific hepatic phenotype, unless additional triggers induce liver disease. Data on associations of this *ABCB4* polymorphism with other disease traits are limited. In the previous analysis [51], we demonstrated that gallstone carriers of the common allele present with lower total serum cholesterol levels as compared to gallstone-free controls; moreover, the same variant affects HDL cholesterol levels but not serum triglycerides. Apart from intrahepatic cholestasis of pregnancy, dysfunction of the hepatic PC transporter ABCB4 has been reported to underlie other cholestatic disorders, namely progressive familial intrahepatic cholestasis type 3 [52], transient neonatal cholestasis [53], drug-induced cholestasis [54], and low-phospholipid associated cholelithiasis [3, 6, 7]. Nevertheless these phenotypes are confined solely to the liver, and metabolic traits in carriers of the c.711A risk variants are most likely not associated with hepatic dysfunction.

In conclusion, this study shows that genetic variation in *ABCB4* substantially influences glucose metabolism. Moreover, our results further underscore the role of phospholipids in the regulation of glucose metabolism. In this respect, *Abcb4*$^{-/-}$ mice represent an experimental framework to further study effects of disturbed PC homeostasis on glycemia. As future anti-diabetic therapies with LRH-1 agonists may be envisioned [55], we advocate that genotyping of the *ABCB4* polymorphisms should be included in the initial work up of the patients.

REFERENCES

1. Carey, M. C., and Lamont, J. T. (1992) Cholesterol gallstone formation. 1. Physical-chemistry of bile and biliary lipid secretion. *Prog Liver Dis* 10, 139-163
2. Oude Elferink, R. P., Paulusma, C. C., and Groen, A. K. (2006) Hepatocanalicular transport defects: pathophysiologic mechanisms of rare diseases. *Gastroenterology* 130, 908-925
3. Krawczyk, M., Wang, D. Q., Portincasa, P., and Lammert, F. (2011) Dissecting the genetic heterogeneity of gallbladder stone formation. *Semin Liver Dis* 31, 157-172
4. Müllenbach, R., Linton, K. J., Wiltshire, S., Weerasekera, N., Chambers, J., Elias, E., Higgins, C. F., Johnston, D. G., McCarthy, M. I., and Williamson, C. (2003) ABCB4 gene sequence variation in women with intrahepatic cholestasis of pregnancy. *J Med Genet* 40, e70
5. Wasmuth, H. E., Glantz, A., Keppeler, H., Simon, E., Bartz, C., Rath, W., Mattsson, L. A., Marschall, H. U., and Lammert, F. (2007) Intrahepatic cholestasis of pregnancy: the severe form is associated with common variants of the hepatobiliary phospholipid transporter ABCB4 gene. *Gut* 56, 265-270
6. Rosmorduc, O., Hermelin, B., and Poupon, R. (2001) MDR3 gene defect in adults with symptomatic intrahepatic and gallbladder cholesterol cholelithiasis. *Gastroenterology* 120, 1459-1467
7. Rosmorduc, O., Hermelin, B., Boelle, P. Y., Parc, R., Taboury, J., and Poupon, R. (2003) *ABCB4* gene mutation-associated cholelithiasis in adults. *Gastroenterology* 125, 452-459
8. Smit, J. J., Schinkel, A. H., Oude Elferink, R. P., Groen, A. K., Wagenaar, E., van Deemter, L., Mol, C. A., Ottenhoff, R., van der Lugt, N. M., van Roon, M. A. (1993) Homozygous disruption of the murine mdr2 P-glycoprotein gene leads to a complete absence of phospholipid from bile and to liver disease. *Cell* 75, 451-462
9. Lammert, F., Wang, D. Q., Hillebrandt, S., Geier, A., Fickert, P., Trauner, M., Matern, S., Paigen, B., and Carey, M. C. (2004) Spontaneous cholecysto- and hepatolithiasis in Mdr2-/- mice: a model for low phospholipid-associated cholelithiasis. *Hepatology* 39, 117-128
10. Fickert, P., Fuchsbichler, A., Wagner, M., Zollner, G., Kaser, A., Tilg, H., Krause, R., Lammert, F., Langner, C., Zatloukal, K., Marschall, H. U., Denk, H., and Trauner, M. (2004) Regurgitation of bile acids from leaky bile ducts causes sclerosing cholangitis in Mdr2 (Abcb4) knockout mice. Gastroenterology 127, 261-274
11. Vacca, M., Krawczyk, M., Petruzzelli, M., Sasso, R. C., van Erpecum, K. J., Palasciano, G., van Berge-Henegouwen, G. P., Moschetta, A., and Portincasa, P. (2007) Current treatments of primary sclerosing cholangitis. Curr Med Chem 14, 2081-2094
12. Forman, B. M. (2005) Are those phospholipids in your pocket? Cell Metab 1, 153-155
13. Lee, J. M., Lee, Y. K., Mamrosh, J. L., Busby, S. A., Griffin, P. R., Pathak, M. C., Ortlund, E. A., and Moore, D. D. (2011) A nuclear-receptor-dependent phosphatidylcholine pathway with antidiabetic effects. Nature 474, 506-510
14. Fayard, E., Auwerx, J., and Schoonjans, K. (2004) LRH-1: an orphan nuclear receptor involved in development, metabolism and steroidogenesis. Trends Cell Biol 14, 250-260
15. Roderick, S. L., Chan, W. W., Agate, D. S., Olsen, L. R., Vetting, M. W., Rajashankar, K. R., and Cohen, D. E. (2002) Structure of human phosphatidylcholine transfer protein in complex with its ligand. Nat Struct Biol 9, 507-511
16. Shishova, E. Y., Stoll, J. M., Ersoy, B. A., Shrestha, S., Scapa, E. F., Li, Y., Niepel, M. W., Su, Y., Jelicks, L. A., Stahl, G. L., Glicksman, M. A., Gutierrez-Juarez, R., Cuny, G. D., and Cohen, D. E. (2011) Genetic ablation or chemical inhibition of phosphatidylcholine transfer protein attenuates diet-induced hepatic glucose production. Hepatology 54, 664-674
17. Popov, Y., Patsenker, E., Fickert, P., Trauner, M., and Schuppan, D. (2005) *Mdr2* (*Abcb4*)-/- mice spontaneously develop severe biliary fibrosis via massive dysregulation of pro- and antifibrogenic genes. J Hepatol 43, 1045-1054

18. Iyengar, S. K., Abboud, H. E., Goddard, K. A., Saad, M. F., Adler, S. G., Arar, N. H., Bowden, D. W., Duggirala, R., Elston, R. C., Hanson, R. L., Ipp, E., Kao, W. H., Kimmel, P. L., Klag, M. J., Knowler, W. C., Meoni, L. A., Nelson, R. G., Nicholas, S. B., Pahl, M. V., Parekh, R. S., Quade, S. R., Rich, S. S., Rotter, J. I., Scavini, M., Schelling, J. R., Sedor, J. R., Sehgal, A. R., Shah, V. O., Smith, M. W., Taylor, K. D., Winkler, C. A., Zager, P. G., and Freedman, B. I. (2007) Genome-wide scans for diabetic nephropathy and albuminuria in multiethnic populations: the family investigation of nephropathy and diabetes (FIND). Diabetes 56, 1577-1585
19. Prochazka, M., Mochizuki, H., Baier, L. J., Cohen, P. T., and Bogardus, C. (1995) Molecular and linkage analysis of type-1 protein phosphatase catalytic beta-subunit gene: lack of evidence for its major role in insulin resistance in Pima Indians. Diabetologia 38, 461-466
20. Mochizuki, H., Scherer, S. W., Xi, T., Nickle, D. C., Majer, M., Huizenga, J. J., Tsui, L. C., and Prochazka, M. (1998) Human PON2 gene at 7q21.3: cloning, multiple mRNA forms, and missense polymorphisms in the coding sequence. Gene 213, 149-157
21. Gailus-Durner, V., Fuchs, H., Becker, L., Bolle, I., Brielmeier, M., Calzada-Wack, J., Elvert, R., Ehrhardt, N., Dalke, C., Franz, T. J., Grundner-Culemann, E., Hammelbacher, S., Hölter, S. M., Hölzlwimmer, G., Horsch, M., Javaheri, A., Kalaydjiev, S. V., Klempt, M., Kling, E., Kunder, S., Lengger, C., Lisse, T., Mijalski, T., Naton, B., Pedersen, V., Prehn, C., Przemeck, G., Racz, I., Reinhard, C., Reitmeir, P., Schneider, I., Schrewe, A., Steinkamp, R., Zybill, C., Adamski, J., Beckers, J., Behrendt, H., Favor, J., Graw, J., Heldmaier, G., Höfler, H., Ivandic, B., Katus, H., Kirchhof, P., Klingenspor, M., Klopstock, T., Lengeling, A., Muller, W., Ohl, F., Ollert, M., Quintanilla-Martinez, L., Schmidt, J., Schulz, H., Wolf, E., Wurst, W., Zimmer, A., Busch, D. H., and Hrabě de Angelis, M. (2005) Introducing the German Mouse Clinic: open access platform for standardized phenotyping. Nat Methods 2, 403-404
22. Hillebrandt, S., Goos, C., Matern, S., and Lammert, F. (2002) Genome-wide analysis of hepatic fibrosis in inbred mice identifies the susceptibility locus *Hfib1* on chromosome 15. Gastroenterology 123, 2041-2051
23. Hillebrandt, S., Wasmuth, H. E., Weiskirchen, R., Hellerbrand, C., Keppeler, H., Werth, A., Schirin-Sokhan, R., Wilkens, G., Geier, A., Lorenzen, J., Kohl, J., Gressner, A. M., Matern, S., and Lammert, F. (2005) Complement factor 5 is a quantitative trait gene that modifies liver fibrogenesis in mice and humans. Nat Genet 37, 835-843
24. Jamall, I.S., Finelli V.N., Que Hee S.S. (1981) A simple method to determine nanogram levels of 4-hdydroxyproline in biological tissues. Anal Biochem 112, 70-75
25. Hegde, P., Qi, R., Abernathy, K., Gay, C., Dharap, S., Gaspard, R., Hughes, J. E., Snesrud, E., Lee, N., and Quackenbush, J. (2000) A concise guide to cDNA microarray analysis. Biotechniques 29, 548-550, 552-544, 556 passim
26. Horsch, M., Schädler, S., Gailus-Durner, V., Fuchs, H., Meyer, H., Hrabě de Angelis, M., and Beckers, J. (2008) Systematic gene expression profiling of mouse model series reveals coexpressed genes. Proteomics 8, 1248-1256
27. Quackenbush, J. (2002) Microarray data normalization and transformation. Nat Genet 32 Suppl, 496-501
28. Tusher, V. G., Tibshirani, R., and Chu, G. (2001) Significance analysis of microarrays applied to the ionizing radiation response. Proc Natl Acad Sci U S A 98, 5116-5121
29. Livak, K. J., and Schmittgen, T. D. (2001) Analysis of relative gene expression data using real-time quantitative PCR and the $2^{-\Delta\Delta CT}$ Method. Methods 25, 402-408
30. Dooley, S., Hamzavi, J., Ciuclan, L., Godoy, P., Ilkavets, I., Ehnert, S., Ueberham, E., Gebhardt, R., Kanzler, S., Geier, A., Breitkopf, K., Weng, H., and Mertens, P. R. (2008) Hepatocyte-specific Smad7 expression attenuates TGF-beta-mediated fibrogenesis and protects against liver damage. Gastroenterology 135, 642-659
31. Kovacs, P., Kress, R., Rocha, J., Kurtz, U., Miquel, J. F., Nervi, F., Méndez-Sánchez, N., Uribe, M., Bock, H. H., Schirin-Sokhan, R., Stumvoll, M., Mössner, J., Lammert, F., and Wittenburg, H. (2008) Variation of the gene encoding the nuclear bile salt receptor FXR and gallstone susceptibility in mice and humans. J Hepatol 48, 116-124

32. Grünhage, F., Acalovschi, M., Tirziu, S., Walier, M., Wienker, T. F., Ciocan, A., Mosteanu, O., Sauerbruch, T., and Lammert, F. (2007) Increased gallstone risk in humans conferred by common variant of hepatic ATP-binding cassette transporter for cholesterol. Hepatology 46, 793-801
33. Krawczyk, M., Rusticeanu, M., Grünhage, F., Mahler, M., Portincasa, P., Acalovschi, M., and Lammert, F. (2010) Analysis of the common vasoactive intestinal peptide receptor 1 polymorphism in gallstone patients. J Gastrointestin Liver Dis 19, 273-277
34. Krawczyk, M., Grünhage, F., Mahler, M., Tirziu, S., Acalovschi, M., and Lammert, F. (2011) The common adiponutrin variant p.I148M does not confer gallstone risk but affects fasting glucose and triglyceride levels. J Physiol Pharmacol 62, 369-375
35. Moles, A., Tarrats, N., Fernandez-Checa, J. C., and Mari, M. (2011) Cathepsin B overexpression due to acid sphingomyelinase ablation promotes liver fibrosis in Niemann Pick disease. J Biol Chem 287, 1178-88
36. Perez-Carreon, J. I., Martinez-Perez, L., Loredo, M. L., Yanez-Maldonado, L., Velasco-Loyden, G., Vidrio-Gomez, S., Ramirez-Salcedo, J., Hernandez-Luis, F., Velazquez-Martinez, I., Suarez-Cuenca, J. A., Hernandez-Munoz, R., and de Sanchez, V. C. (2010) An adenosine derivative compound, IFC305, reverses fibrosis and alters gene expression in a pre-established CCl(4)-induced rat cirrhosis. Int J Biochem Cell Biol 42, 287-296
37. Baghy, K., Dezso, K., Laszlo, V., Fullar, A., Peterfia, B., Paku, S., Nagy, P., Schaff, Z., Iozzo, R. V., and Kovalszky, I. (2011) Ablation of the decorin gene enhances experimental hepatic fibrosis and impairs hepatic healing in mice. Lab Invest 91, 439-451
38. Varela-Rey, M., Martinez-Lopez, N., Fernandez-Ramos, D., Embade, N., Calvisi, D. F., Woodhoo, A., Rodriguez, J., Fraga, M. F., Julve, J., Rodriguez-Millan, E., Frades, I., Torres, L., Luka, Z., Wagner, C., Esteller, M., Lu, S. C., Martinez-Chantar, M. L., and Mato, J. M. (2010) Fatty liver and fibrosis in glycine N-methyltransferase knockout mice is prevented by nicotinamide. Hepatology 52, 105-114
39. Borkham-Kamphorst, E., Drews, F., and Weiskirchen, R. (2011) Induction of lipocalin-2 expression in acute and chronic experimental liver injury moderated by pro-inflammatory cytokines interleukin-1beta through nuclear factor-kappaB activation. Liver Int 31, 656-665
40. Horton, J. D., Goldstein, J. L., and Brown, M. S. (2002) SREBPs: activators of the complete program of cholesterol and fatty acid synthesis in the liver. J Clin Invest 109, 1125-1131
41. Müllenbach, R., Weber, N. S., and Lammert, F. (2011) Nuclear receptor variants in liver disease. J Lipids 2012, ID934707
42. Biddinger, S. B., Haas, J. T., Yu, B. B., Bezy, O., Jing, E., Zhang, W., Unterman, T. G., Carey, M. C., and Kahn, C. R. (2008) Hepatic insulin resistance directly promotes formation of cholesterol gallstones. Nat Med 14, 778-782
43. Scapa, E. F., Pocai, A., Wu, M. K., Gutierrez-Juarez, R., Glenz, L., Kanno, K., Li, H., Biddinger, S., Jelicks, L. A., Rossetti, L., and Cohen, D. E. (2008) Regulation of energy substrate utilization and hepatic insulin sensitivity by phosphatidylcholine transfer protein/StarD2. FASEB J 22, 2579-2590
44. Wopereis, S., Radonjic, M., Rubingh, C., van Erk, M., Smilde, A., van Duyvenvoorde, W., Cnubben, N., Kooistra, T., van Ommen, B., and Kleemann, R. (2012) Identification of prognostic and diagnostic biomarkers of glucose intolerance in ApoE3Leiden mice. Physiol Genomics 44, 293-304
45. Ortlund, E. A., Lee, Y., Solomon, I. H., Hager, J. M., Safi, R., Choi, Y., Guan, Z., Tripathy, A., Raetz, C. R., McDonnell, D. P., Moore, D. D., and Redinbo, M. R. (2005) Modulation of human nuclear receptor LRH-1 activity by phospholipids and SHP. Nat Struct Mol Biol 12, 357-363
46. Baghdasaryan, A., Fickert, P., Fuchsbichler, A., Silbert, D., Gumhold, J., Horl, G., Langner, C., Moustafa, T., Halilbasic, E., Claudel, T., and Trauner, M. (2008) Role of hepatic phospholipids in development of liver injury in Mdr2 (Abcb4) knockout mice. Liver Int 28, 948-958

47. Oosterveer, M. H., Mataki, C., Yamamoto, H., Harach, T., Moullan, N., van Dijk, T. H., Ayuso, E., Bosch, F., Postic, C., Groen, A. K., Auwerx, J., and Schoonjans, K. (2012) LRH-1-dependent glucose sensing determines intermediary metabolism in liver. J Clin Invest 122, 2817-2826
48. Lee, Y. K., Schmidt, D. R., Cummins, C. L., Choi, M., Peng, L., Zhang, Y., Goodwin, B., Hammer, R. E., Mangelsdorf, D. J., and Kliewer, S. A. (2008) Liver receptor homolog-1 regulates bile acid homeostasis but is not essential for feedback regulation of bile acid synthesis. Mol Endocrinol 22, 1345-1356
49. Keitel V. Bile acids as extrahepatic and interorgan signaling molecules. In: Häussinger D, Keitel V, Kubitz R (eds.). Hepatobiliary transport in health and disease. De Gruyter, Berlin 2012:117-129
50. Watanabe, M., Houten, S. M., Mataki, C., Christoffolete, M. A., Kim, B. W., Sato, H., Messaddeq, N., Harney, J. W., Ezaki, O., Kodama, T., Schoonjans, K., Bianco, A. C., and Auwerx, J. (2006) Bile acids induce energy expenditure by promoting intracellular thyroid hormone activation. Nature 439, 484-489
51. Acalovschi, M., Tirziu, S., Chiorean, E., Krawczyk, M., Grünhage, F., and Lammert, F. (2009) Common variants of ABCB4 and ABCB11 and plasma lipid levels: a study in sib pairs with gallstones, and controls. Lipids 44, 521-526
52. de Vree, J. M., Jacquemin, E., Sturm, E., Cresteil, D., Bosma, P. J., Aten, J., Deleuze, J. F., Desrochers, M., Burdelski, M., Bernard, O., Oude Elferink, R. P., and Hadchouel, M. (1998) Mutations in the MDR3 gene cause progressive familial intrahepatic cholestasis. Proc Natl Acad Sci U S A 95, 282-287
53. Jung, C., Driancourt, C., Baussan, C., Zater, M., Hadchouel, M., Meunier-Rotival, M., Guiochon-Mantel, A., and Jacquemin, E. (2007) Prenatal molecular diagnosis of inherited cholestatic diseases. J Pediatr Gastroenterol Nutr 44, 453-458
54. Lang, C., Meier, Y., Stieger, B., Beuers, U., Lang, T., Kerb, R., Kullak-Ublick, G. A., Meier, P. J., and Pauli-Magnus, C. (2007) Mutations and polymorphisms in the bile salt export pump and the multidrug resistance protein 3 associated with drug-induced liver injury. Pharmacogenet Genomics 17, 47-60
55. Hohenester, S., and Beuers, U. (2011) Phosphatidylcholines as regulators of glucose and lipid homeostasis: Promises and potential risks. Hepatology 54, 2266-2268

KAPITEL 3:

DIE ABCB4-DEFIZIENTE MAUS ALS MODELL DER HEPATISCHEN OSTEODYSTROPHIE

DIE ABCB4-DEFIZIENTE MAUS ALS MODELL DER HEPATISCHEN OSTEODYSTROPHIE

Das Knochengewebe unterliegt einem permanenten Umbauprozess. Im gesunden Organismus handelt es sich dabei um ein ausgeglichenes Verhältnis von Knochenaufbau und Knochenresorption. Auf zellulärer Ebene wird diese Balance über Osteoblasten und Osteoklasten umgesetzt und durch molekulare Mechanismen (Zytokine, Hormone, Wachstumsfaktoren) reguliert.

Bei Patienten mit chronischen Lebererkrankungen ist dieses Gleichgewicht beeinträchtigt. Die hepatische Osteodystrophie bezeichnet metabolische Veränderungen des Knochens, die eine häufige Begleiterscheinung bei diesen Patienten sind (Nakchbandi and van der Merwe 2009). Charakteristisch sind eine verminderte Knochenneubildung und eine verstärkte Knochenresorption, sowie eine reduzierte Knochenmasse und Änderungen in der Knochenstruktur (Nakchbandi and van der Merwe 2009). Insbesondere Patienten mit cholestatischen Lebererkrankungen weisen in bis zu 60% der Fälle eine verringerte Knochenmasse auf, die mit einem erhöhten Frakturrisiko einhergeht (Pusl and Beuers 2005). Knochenbrüche wiederum beeinträchtigen die Lebensqualität und erhöhen sowohl Morbidität als auch Sterblichkeit der Patienten mit chronischen Lebererkrankungen (Navasa *et al.* 1996, Luxon 2011).

Für präventive Maßnahmen und die Entwicklung einer adäquaten Behandlungsstrategie sind detaillierte Kenntnisse der Krankheitsmechanismen der hepatischen Osteodystrophie unabdingbar. Bis heute sind eine Vielzahl von Faktoren bekannt, die im direkten oder indirekten Zusammenhang mit der hepatischen Osteodystrophie stehen, der pathobiologische Mechanismus ist jedoch nur unzureichend verstanden. Ziel dieser Studie war es daher, die Eignung der *Abcb4*$^{-/-}$-Maus als Forschungsmodell für die hepatische Osteodystrophie bei chronisch cholestatischen Lebererkrankungen zu prüfen.

Unter diesem Aspekt wurden in *Abcb4*-defizienten Mäusen detaillierte Analysen von Knochen-Morphologie, -Architektur und -Stoffwechsel durchgeführt und in einem zweiten Schritt der Einfluss von Vitamin D auf die

Knochenqualität untersucht. Anhand der folgenden Abbildung 4 sind einige der Parameter erläutert die im Rahmen Knochenanalysen bestimmt wurden.

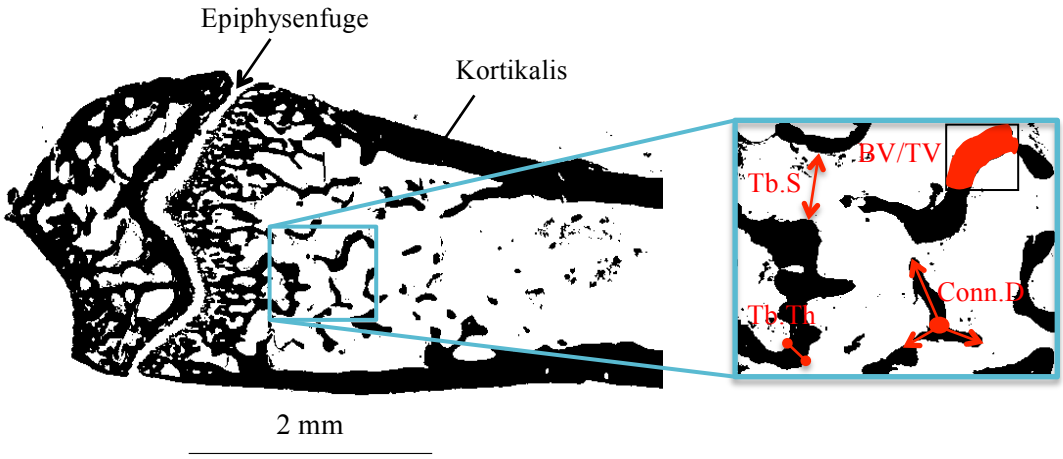

Abbildung 4: Morphologie des Femur der Maus mit einzelnen für die Knochenanalyse relevanten Parametern. Links, die kompakte Kortikalis, rechts ein Ausschnitt des Trabekelnetzwerks mit den Parametern Trabekeldicke (Tb.Th), Trabekelabstand (Tb.S), Konnektivität (Conn.D) und Knochenvolumenanteil (BV/TV).
(Die Abbildung basiert auf einem histologischen Schnittbild nach von-Kossa Färbung, Femur BALB/cJ. Mit freundlicher Genehmigung von Dr. Yvonne Lau)

Die Ergebnisse der morphologischen und architektonischen Untersuchungen spiegeln wider, dass in *Abcb4*$^{-/-}$-Mäusen mit fortgeschrittener Fibrose eine Beeinträchtigung der Knochenqualität vorliegt. So weisen die Knochen von *Abcb4*$^{-/-}$-Mäusen einen verminderten Mineralstoffgehalt und eine Abnahme der Trabekelanzahl sowie einen erhöhten Abstand zwischen den einzelnen Trabekeln und eine verminderte Konnektivität. Zusätzlich findet sich eine geringere Dichte in den kortikalen Bestandteilen der Knochen von ABCB4-defizienten Weibchen. Da sowohl die Mineralisierung als auch die trabekuläre und kortikale Architektur die Stärke des Knochen bestimmen (Wehrli 2007), ist eine Minderung der Knochenstabilität anzunehmen. Im Einklang mit den fast 50% niedrigeren Vitamin D-Konzentrationen in *Abcb4*$^{-/-}$-Mäusen kommt es bei diesen Tieren auch zu Änderungen der Calcium- und Phosphat-Konzentrationen. Das Expressionsprofil von Genen in Leber und Knochen, die regulatorische Proteine des Vitamin D- und Knochenstoffwechsels kodieren, unterscheidet sich ebenfalls in Knockout-

und Wildtyp-Mäusen. Zusätzlich finden sich im Serum von *Abcb4*$^{-/-}$-Mäusen mit einer fortgeschrittenen Fibrose erhöhte Konzentrationen des Receptor Activator Nuklear Factor - κB Liganden (RANKL). Dieser Schlüsselregulator des Knochenstoffwechsels wird von Osteoblasten sezerniert und vermittelt über die Aktivierung von Osteoklasten die Knochenresorption. Insgesamt veranschaulichen die Daten, dass in ABCB4-defizienten Mäusen eine deutliche Beeinträchtigung der Struktur und damit der Qualität sowie ein alterierter Metabolismus der Knochen vorliegt. Über die Intervention mit Vitamin D konnte zwar eine Beeinflussung der Knochenphänotyps erzielt werden, jedoch ermöglicht die Vitamin D-Supplementation keine Sicherstellung der Mineralstoffdichte im Femur der *Abcb4*$^{-/-}$-Mäuse.

Die Analysen dieser Studie zeigen erstmals, dass die *Abcb4*$^{-/-}$-Maus, als präklinisches Modell für chronisch cholestatische Erkrankungen, auch einen pathologischen Knochenphänotyp entwickelt und ein experimentelles Modell für die hepatische Osteodystrophie darstellt. Die Tiere bieten damit die Möglichkeit, die Pathomechanismen metabolischer Knochenerkrankungen, wie sie bei cholestatischen Patienten auftreten, näher zu untersuchen. Weiterhin lässt die Studie vermuten, dass der Vitamin D-Stoffwechsel in der hepatischen Osteodystrophie eine zentrale Rolle spielt, dass aber auch weitere Faktoren die Knochenmorphologie mitbeeinflussen.

Diese Studie erfolgte in Zusammenarbeit mit Mitarbeitern der Universität Tübingen und dem Zentrum für Regenerative Therapien der Charité in Berlin. Die Datenerhebung der trabekulären Struktur mittels Mikro-Computer Tomographie, die Histologie des Femurs und die Bestimmung der Expression von Genen des Vitamin D- und Knochenstoffwechsels wurden dort durchgeführt. Die quantitative Computertomographie für die detaillierten Analysen der Knochenbestandteile hat Dr. Cheryl Ackert-Bicknell (Jackson Laboratory in Bar Habor, Main) vorgenommen. Frau Ackert-Bicknell stand auch beratend für die Interpretation der Daten zur Verfügung.

MODELING HEPATIC OSTEODYSTROPHY IN *ABCB4* DEFICIENT MICE

Katrin Hochrath[1*], Sabrina Ehnert[2*], Cheryl L. Ackert-Bicknell[3], Yvonne Lau[4], Andrea Schmid[5], Marcin Krawczyk[1], Jan G. Hengstler[6], Jordanne Dunn[3], Kanishka Hitthatiya[7], Birgit Rathkolb[8,9,11], Kateryna Micklich[9], Wolfgang Hans[8,11], Helmut Fuchs[8,11], Valérie Gailus-Durner[8,11], Eckhard Wolf[9], Martin Hrabě de Angelis[8,11,], Steven Dooley[10], Beverly Paigen[3], Britt Wildemann[4], Frank Lammert[1] & Andreas K. Nüssler[2]

[1]Department of Medicine II, Saarland University Medical Center, Homburg, Germany; [2]Department of Trauma Surgery, University of Tübingen, Tübingen, Germany; [3]The Jackson Laboratory, Bar Harbor, ME, USA; [4]Julius Wolff Institut, Berlin-Brandenburg Center for Regenerative Therapies, Charité-Universitätsmedizin Berlin, Berlin, Germany; [5]Department of Traumatology, MRI, Technische Universität München, Munich, Germany; [6]Leibniz Research Centre for Working Environment and Human Factors (IfADo), Dortmund TU, Dortmund, Germany; [7]Institute of Pathology, University Hospital Bonn, Friedrich-Wilhelms-Universität Bonn, Germany; [8]German Mouse Clinic, Institute of Experimental Genetics, Helmholtz Zentrum München, German Research Centre for Environmental Health, Neuherberg, Germany; [9]Institute of Molecular Animal Breeding and Biotechnology, Ludwig-Maximilians-Universität München, Munich, Germany; [10]Molecular Hepatology – Alcohol Associated Diseases, Department of Medicine II, Medical Faculty Mannheim at Heidelberg University, Mannheim, Germany; [12]Member of German Center for Diabetes Research (DZD), Neuherberg, Germany;

[*]Contributed equally

BONE 2013; 55:501-511

ABSTRACT

Hepatic osteodystrophy (HOD) denotes the alterations in bone morphology and metabolism frequently observed in patients with chronic liver diseases, in particular in case of cholestatic conditions. The molecular mechanisms underlying HOD are only partially understood. In the present study, we characterized the bone phenotypes of the ATP-binding cassette transporter B4 knockout mouse (*Abcb4*$^{-/-}$), a well-established mouse model of chronic cholestatic liver disease, with the aim of identifying and characterizing a mouse model for HOD. Furthermore, we investigated the influence of vitamin D on bone quality in this model. The bone morphology analyses revealed reduced bone mineral contents as well as changes in trabecular bone architecture and decreased cortical bone densities in *Abcb4*$^{-/-}$ mice with severe liver fibrosis. We observed dysregulation of genes involved in bone remodeling (osteoprotegerin, osteocalcin, osteopontin) and vitamin D metabolism (7-dehydrocholesterol reductase, Gc-globulin, *Cyp2r1, Cyp27a1*) as well as alterations in calcium and vitamin D homeostasis. In addition, serum RANKL and TGF-β levels were increased in *Abcb4*$^{-/-}$ mice. Vitamin D dietary intervention did not restore the bone phenotypes of *Abcb4*$^{-/-}$ animals. We conclude that the *Abcb4*$^{-/-}$ mouse provides an experimental framework and a preclinical model to gain further insights into the molecular pathobiology of HOD and to study the systemic effects of therapeutic interventions.

INTRODUCTION

Patients with chronic liver disease frequently demonstrate alterations in bone mineral metabolism, leading to osteopenia and osteoporosis. The metabolic bone disease that causes defective bone remodeling in the setting of chronic liver diseases is termed hepatic osteodystrophy (HOD) [1, 2]. To date, the exact prevalence of HOD is unknown. However previous studies estimated that up to 75% of all patients with chronic liver disease suffer from severe osteoporosis [3, 4].

Depending on the etiology of the liver disease, different patterns of progressive bone diseases can be detected. Specifically, chronic cholestasis appears to affect bone metabolism and structure. Indeed, the reported prevalence of osteopenia and osteoporosis in chronic viral hepatitis is approximately 20%, whereas up to 60% of patients with chronic cholestatic diseases display decreases in bone mass [2, 5]. Low bone mass and diseases associated structural deterioration in patients with chronic cholestasis results in increased frequency of fractures of spine, hip and femoral neck as well as other peripheral fractures [1]. However, it is well understood that in addition to low bone mass, other factors such as bone geometry and altered states of bone turnover, contribute to the risk of fracture [6]. In patients with chronic liver diseases fractures do severely affect the quality of life and result in increased morbidity, which in turn compromises long-term prognosis.

HOD, once it has developed, is difficult to treat and special care is required to support the healing of existing fractures [7]. Better understanding of the pathogenesis of HOD is essential to develop adequate treatment strategies. To date several factors have been identified to be associated with HOD, but the pathobiological mechanisms have yet to be fully defined. In particular, bilirubin, insulin-like growth factor 1 (IGF-1) deficiency and the receptor activator of nuclear factor κB ligand (RANKL) - osteoprotegerin (OPG) system have been investigated [6]. Distorted calcium and vitamin D homeostasis seem to play a prominent role in cholestasis-induced bone disease. In short, vitamin D represents

a key regulator of calcium homeostasis and is therefore essential for bone formation and metabolism. It can be absorbed from food or synthesized endogenously from cholesterol derivatives by ultraviolet irradiation in the skin. Here, 7-dehydrocholesterol is converted to cholecalciferol, which then undergoes 25-hydroxylation in hepatocytes, a process mediated primarily by cytochrome P450 enzyme CYP2R1 as well as CYP27A1, CYP2J2 and CYP3A4 [8]. The hydroxylation product, 25-hydroxyvitamin D (25(OH)-vitamin D, also termed calcidiol), enters the systemic circulation, where it is transported by vitamin D binding-protein, (also known as Gc, group-specific component or Gc-globulin) [9]. Calcidiol undergoes further hydroxylation by CYP27B1 mainly, but not exclusively, in the kidney. The resulting hormonal metabolite of vitamin D, 1,25-dihydroxyvitamin D ($1,25(OH)_2$-vitamin D) is, known to act on genes involved in bone metabolism, such as *BGLAP* (osteocalcin), *RANKL* (a.k.a. tumor necrosis factor ligand superfamily member 11, *TNFSFF11*) and *SPP1* (osteopontin) [10].

The ATP-binding cassette transporter B4 knockout mouse (*Abcb4*$^{-/-}$) is a well-established mouse model of chronic liver diseases with a distinct and well-characterized hepatic phenotype. Due to the lack of the hepatobiliary phosphatidylcholine floppase ABCB4, the mice develop bile acid-induced liver damage, leading to sclerosing cholangitis and biliary fibrosis [11-13]. Since, to our knowledge, there are no data outlining the bone phenotype of these mice, we sought to characterize *Abcb4*$^{-/-}$ mice with regard to bone mass, structure and metabolism, with the goal of ascertaining the suitability of the *Abcb4*$^{-/-}$ mouse as a model for HOD. Second, we investigated the influence of vitamin D treatment on bone quality in this new model.

EXPERIMENTAL PROCEDURES

Generation of BALB-*Abcb4*$^{-/-}$ mice

To generate the fibrosis-susceptible BALB-*Abcb4*$^{-/-}$ mouse line, the FVB-*Abcb4*^{tm1Bor} strain was backcrossed into the BALB/cJ background for more than 10 generations. BALB/cJ inbred mice were obtained from Charles River (Sulzfeld, Germany). Mice were kept in 12-h light-dark cycles and were provided with water and standard diet (Altromin 1314, Lage, Germany) *ad libitum*. Temperature and humidity were regulated to 22 ± 1°C and 55 ± 5%, respectively.

To confirm the *Abcb4*$^{-/-}$ genotype, we used the polymerase chain reaction (PCR) of tail DNA with *neo* (5'-CTT GGG TGG AGA GGC TAT TC-3', 5'-AGG TGA GAT GAC AGG AGA TC-3') and *Abcb4* (5'-CAC TTG GAC CTG AGG CTG TG-3', 5'-TCA GGA CTC CGC TAT AAC GG-3') specific primer pairs. The PCR reaction contained 10× PCR buffer (Applied Biosystems, Darmstadt, Germany), 2 mM $MgCl_2$, 10 µM dNTPs, 10 µM primer, 1.25 U *Taq* DNA polymerase (Invitrogen, Darmstadt, Germany), and 20 - 100 ng DNA in 25 µl-reactions. PCR cycling conditions were 30 s @ 94°C, 60 s @ 55°C and 30 s @ 72°C for 35 cycles, and a final extension step of 10 min @ 72°C.

The experimental protocols were performed with permission of the federal states of Baden-Württemberg, Bavaria and Saarland according to §8 of the German Law for the Protection of Animals and the Directive 2010/63/EU of the European Parliament.

Phenotypic characterization of hepatic fibrosis

Histopathology and hydroxyproline assay

Liver samples for histopathological evaluation were fixed in 4% neutral buffered formalin at 4°C for 24 h and embedded in paraffin. Sections (2 - 5 µm) were stained with hematoxylin-eosin (H&E), Masson Goldner trichrome, and Sirius red.

Liver injury was scored at 5, 15, 20, 30, and 44 weeks of age in groups of 4 animals per genotype and point in time. In detail, slices of the left lateral, the right, the median and the caudate liver lobes were scored (0 - 20) separately based on the presence of periductal connective tissue, edema, inflammatory infiltrations, periportal fibrosis, spongy or bridging necrosis, connective tissue septa, proliferation, atrophy and diminution of bile canaliculi, and biliary cirrhosis.

Liver fibrosis was quantified in 15-week-old mice using an histomorphometric semi-automatic system for image analysis (Leica microscope, equipped with Leica application suite software; Wetzlar, Germany). The percentage of collagenous area was calculated from 10 microscopic fields (magnification 100×) randomly chosen in each liver section. Hepatic fibrosis was staged according to Batts and Ludwig [14] and the Ishak [15] scoring systems. The F-scores were defined as follows: 0, no fibrosis; 1, scatter periportal and perineoductular fibrosis; 2, periportal, perineoductular fibrosis (complete lamellae with beginning septa); 3, periportal, perineoductular fibrosis with portal-portal septa and 4, complete cirrhosis.

In addition, hepatic collagen contents were quantified calorimetrically via the collagen specific amino acid hydroxyproline (Hyp), as described by Jamall *et al*. [16, 17].

Clinical chemical and enzyme-linked immunosorbent assays

Blood samples for chemical analyses were obtained from isoflurane-anesthetized mice by puncturing the retro-orbital sinus with capillaries and subsequently collected in heparinized tubes. Plasma alanine aminotransferase (ALT), lactate dehydrogenase (LDH) and alkaline phosphatase (AP) activities as well as calcium and inorganic phosphate concentrations were measured with the Olympus AU 400 autoanalyzer (Olympus, Hamburg, Germany) using adapted reagent kits (Olympus, Hamburg, Germany) or Hitado (Möhnesee, Germany) kits, alternatively.

Serum 25(OH)-vitamin D levels were determined using the chemiluminescence immunoassay LIAISON® 25 OH VitaminD TOTAL assay (DiaSorin, Dietzenbach, Germany). Transforming growth factor- β (TGF-β) levels were measured by TGF-β-receptor cells (MFB-F11), provided by Dr. Ina Tesseur [18] with slight modifications as described [19]. Each sample was measured in triplicate, using active recombinant human TGF-β_1 as control. RANKL and OPG concentrations in serum were measured in duplicates by enzyme-linked immunosorbent assay (ELISA) (Quantikine mouse RANK ligand and OPG immunoassays, R&D Systems, Minneapolis, USA).

Reverse transcription and quantitative real-time PCR

Total mRNA from grinded snap frozen liver tissue specimens was isolated using peqGOLD TriFast™ (Peqlab, Erlangen, Germany) or RNeasy Mini kits (Qiagen, Hilden, Germany). cDNA was synthesized from 1 to 2 µg RNA using cDNA reverse transcription (RT) kits from Applied Biosystems (Carlsbad, USA) or Fermentas (St. Leon-Rot, Germany). Table 1 summarizes primer sequences (5' - 3') and RT-PCR conditions. Products, resolved by gel electrophoresis in a 2 % (w/v) agarose gel, were visualized with ethidium bromide. Densitometric analysis of signals was performed using Image J software (NIH, Bethesda, USA).

mRNA transcript levels were determined by reverse transcriptase quantitative real-time PCR (qPCR; *TaqMan*, Applied Biosystems, Carlsbad, USA), with one cycle for 10 min @ 95°C, followed by 45 cycles with 30 s @ 95°C and 60 s @ 60°C. The relative expression level of each gene was calculated by the ΔΔct-method [20], utilizing 18S RNA as endogenous control, and in relation to wild-type controls similar in age and gender. The relative quotient (RQ, $2^{-\Delta\Delta ct}$) was normalized to the values of BALB/cJ controls.

Table 1: Primer sequences and PCR conditions for RT-PCR

Gene	GeneBank accession number	Forward primer	Reverse primer	T_m [°C]	Product length [bp]
Actb	NM_001101.3	CGACAACGGCT CCGGCATGT	GCACAGTGTGG GTGACCCCG	64	461
Bglap	MN_001037939.1	ACCCTGGCTGCG CTCTGTCT	CCAGGGTCCTGG ACATGGGGA	58	241
Cyp24a1	MN_009996.3	TGGCCACTGCTG GGCAGC	TTTGAAAATGGT GTCCCAGGCCA	58	651
Cyp27a1	MN_024264.4	GTGGACACGAC ATCCAACAC	ATGATCCGGGA GTTTGTGG	60	212
Cyp27b1	MN_010009.2	CGCCTCTGCCGA GACTGGGA	CTCCCCCAGCCA GCGAGCTG	58	555
Cyp2r1	MN_177382.3	GGGAGGCTTACT CAATTCCA	GCAATGATGAG TTCACCCACT	60	567
Dhcr7	MN_007856.2	ATGGGCGCTGCC TCATCTGG	GATTCCAGGCA GCAGGCGGT	60	329
Gc	MN_008096.2	AGAGGAGGTGC TGCAAGACT	GCAGCATATTGT GAGCAGACTC	60	707
Spp1	MN_009263.2	GCAGTCTTCTGC GGCAGGCA	CGGCCGTTGGG GACATCGAC	58	487
Tnfrsf11b	MN_008764.3	TGTGCTGCGCAC TCCTGGTG	GGTGCGGTTGCA CTCCTGCT	60	287
Vdr	MN_000376.2	GCCTGCCGGCTC AAACGCTG	CAGCCAGGTGG GGCAGCATG	58	463

Abbreviations**:** *Actb*, β-actin; *Bglap*, bone γ-carboxyglutamate protein (osteocalcin); *Cyp*, cytochrome P450; *Dhcr7*, 7-dehydrocholesterol reductase; *Gc*, group specific component; *Spp1*, secreted phosphoprotein 1 (osteopontin); *Tnfrsf11b*, tumor necrosis factor receptor superfamily, member 11b (osteoprotegerin); *Vdr*, vitamin D receptor.

Phenotypic characterization of hepatic osteodystrophy

Dual-energy x-ray absorptiometry (DXA)

Phenotypic DXA analyses were performed at the German Mouse Clinic (GMC, [21, 22]) in *Abcb4*$^{-/-}$ mice and wild-type control animals at the age of 15 to 17 weeks (10 animals per genotype and sex). After isoflurane anesthesia, weight and length of each mouse were recorded. Bone mineral content (BMC) and areal bone mineral density (BMD) of the whole body, excluding the skull, was ascertained using a Sabre X-ray bone densitometer (Norland Medical Systems, Hampshire, UK), using a scan speed of 20 mm/s, a resolution of 0.5 mm x 1.0 mm, and a histogram averaging width (HAW) setting of 0.02. The calibration of the system was performed using the QC and QA phantoms supplied by the manufacturer.

Micro-computed tomography (μCT) and histology

Bones of knockout and wild-type mice at the ages of 5, 15, 20, 30 and 44 weeks were collected (4 animals per genotype and point in time). The bone structure and the mineralization of mouse femora were determined by μCT scans on a Viva μCT40 (Scanco Medical, Wangen-Brüttisellen, Switzerland). Femora were placed into phosphate buffered saline-filled reaction tubes and fixed by Pasteur pipettes. To assess the trabecular bones, the distal and mid metaphyses were scanned with standard parameters (70 kV, 114 μA, 10.5 μm voxel size). The volume of interest (VOI) included 135 slices at the distal area and 50 scans in the middle of the femur. A global threshold was used to separate mineralized tissue from bone marrow and soft tissues: This was set to 429 hydroxyapatite (HA) mg/cm^3.

From these measurements the following parameters were determined: bone volume (BV), total volume (TV), bone volume fraction (BV/TV), trabecular number, trabecular separation, trabecular thickness, connective density, and the structure-model index, which defines the trabecular structure (disk-shape: 0 to rod-shape: 3) [23].

Femura of these animals were used to visualize mineralized tissue. Therefore, femoral bones of knockout and wild-type mice (4 animals per point in time) were embedded after formalin fixation and dehydration into polymethylmethacrylate (Technovit 9100; Heraeus Kulzer, Wehrheim, Germany). Longitudinal sections (6 μm) were cut and stained by the use of von Kossa staining (3% silver nitrate and 5% sodium thiosulfate).

Peripheral quantitative computed tomography (pQCT)

The hind axial skeleton with the attached musculature was fixed in 10% neutral buffered formalin overnight and placed subsequently in 95% ethanol until analysis (6 - 14 animals per genotype and sex, at 15 - 17 weeks of age). The total femur bone density was quantified using the SA Plus densitometer (Orthometrics, Stratec SA Plus Research Unit, White Plains, USA). The SA Plus instrument was calibrated using HA standards (50 - 1000 mg/mm^3) with cylindrical diameters of

2.4 mm and lengths of 24 mm to approximate mouse femurs. Quality control was performed with a phantom supplied by the manufacturer. The precision of the SA Plus for repeated measurements of a single femur was found to be 1.2 - 1.4%. As thresholds to separate bone from soft tissue, we used 710 and 570 HA mg/cm^3 for cortical bone areas and surfaces, respectively; to determine mineral contents, a second analysis was carried out with thresholds of 220 and 400 HA mg/cm^3 to include mineral from most partial voxels (0.07 mm) in the analysis. Isolated femurs were scanned at seven locations at 2 mm intervals, beginning 0.8 mm from the distal ends of the epiphyseal condyles. Density values were calculated from the summed areas and associated mineral contents.

Vitamin D intervention study

In parallel experiments, we performed a vitamin D dietary intervention study in *Abcb4*$^{-/-}$ mice on the FVB/N background. At 4 weeks of age, FVB-*Abcb4*$^{-/-}$ and wild-type mice were assigned to three intervention groups. These groups encompassed a total of 6 to 14 mice per genotype and sex. Mice were fed one of: a control vitamin D diet (600 IU vitamin D/kg food), a vitamin D-sufficient diet (2,400 IU vitamin D/kg food), or a vitamin D-deficient diet (100 IU vitamin D/kg food). Apart from vitamin D concentrations, the diets (Altromin, Lage, Germany) were otherwise equal in nutrient and energy contents. The dietary interventions were continued until the age of 15 to 17 weeks.

Statistics

Phenotypic data of mice are given as means ± standard errors of the mean (SEM) and assessed by one-way analysis of variance (ANOVA) with post-hoc multiple comparison tests (Bonferroni) or Student's t-tests. For bone data acquired by pQCT, analysis of covariance (ANCOVA) was used.

To determine whether *Abcb4*$^{-/-}$ mice display a bone phenotype, a subtractive model fitting was performed. All covariates (body weight, femoral length, genotype) were initially considered and then removed in a step-wise fashion until only significant factors remained.

For all tests, p-values < 0.05 were regarded as significant, unless otherwise stated. Statistical analyses were performed using SPSS 20 (IBM, Ehningen, Germany) and GraphPad Prism (GraphPad Sofware, San Diego, USA).

RESULTS

Abcb4$^{-/-}$ mice with severe liver injury show alteration of the bone structure and density

The phenotypic characterization of hepatic fibrosis in *Abcb4*$^{-/-}$ mice showed that liver damage increased most rapidly in the first 15 weeks of life (average liver damage score 15.5 ± 0.8 out of 20). Later on the rate of liver injury progressed slowly until the age of 44 weeks (average liver damage score 18.3 ± 0.7) (Fig. 1). Liver pathology was reflected by significantly elevated serum activities of liver enzymes, including alanine aminotransferase and alkaline phosphatase (Fig. 2).

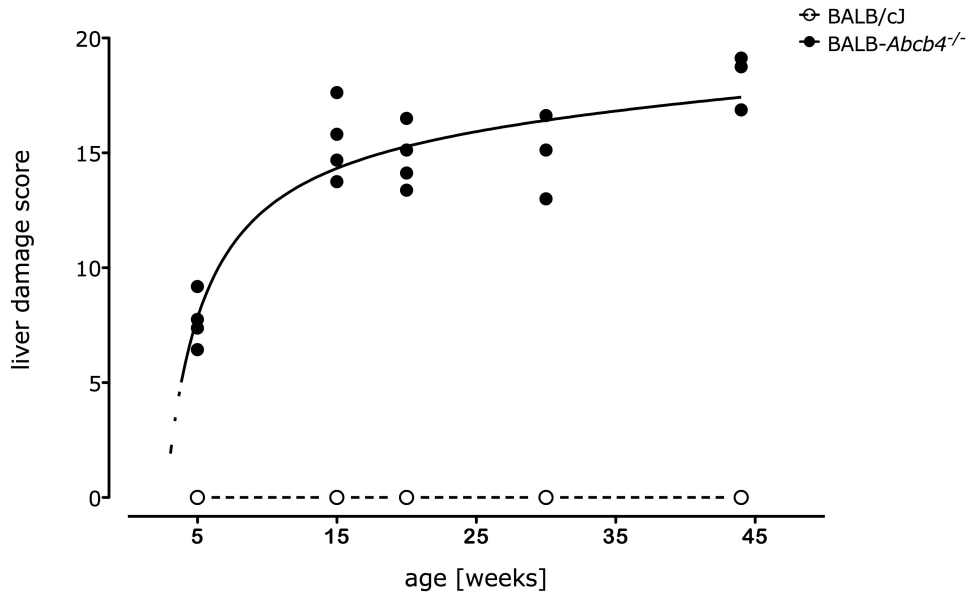

Figure 1: Liver damage score in BALB-*Abcb4*$^{-/-}$ and BABL/cJ wild-type mice. Hepatic injury was scored in liver slices stained with Masson Goldner trichrome based on the presence of periductal connective tissue, edema, inflammatory infiltrations, periportal fibrosis, spongy or bridging necrosis, connective tissue septa, proliferation, atrophy and diminution of bile canaliculi, and biliary cirrhosis as described in experimental procedures.
N = 4 per genotype and time point.

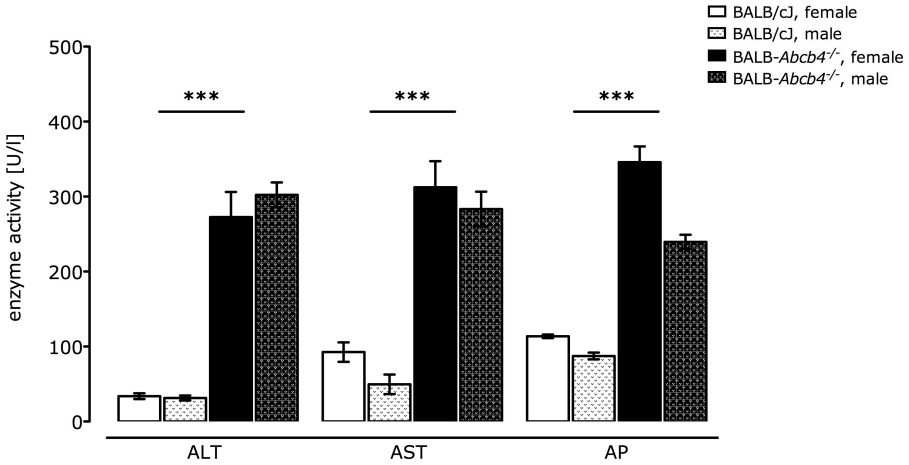

Figure 2: Liver enzyme activities in plasma samples from BALB-*Abcb4*$^{-/-}$ and BABL/cJ wild-type mice at 14 weeks of age. N = 10 per genotype and sex; *** $p < 0.001$. Abbreviations: ALT, alanine aminotransferase; AP, alkaline phosphatase; AST, aspartate aminotransferase.

Whole-body densitometry (DXA) was employed to determine whether bone content and density were affected in *Abcb4*$^{-/-}$ mice at 15 weeks of age. This analysis revealed a significant reduction of whole body bone mineral contents (BMC) in *Abcb4*$^{-/-}$ males (Fig. 3A) and of the bone fractions of the total tissue weights in knockout females (Fig. 3B) in comparison to wild-type controls. However, whole body areal BMD did not differ (Fig. 3C).

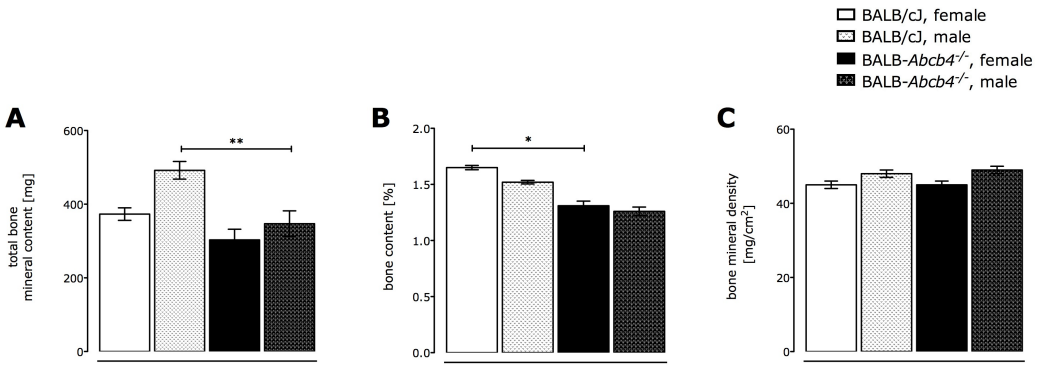

Figure 3: DXA results. Total bone mineral contents (**A**), bone fractions of the total tissue weights (**B**) and areal bone mineral density (C) in BALB-*Abcb4*$^{-/-}$ and BABL/cJ wild-type mice at the age of 15-17 weeks. N = 10 per genotype and sex; * $p < 0.05$, ** $p < 0.01$.

Serial micro-computed tomography (μCT) scanning of *Abcb4*$^{-/-}$ mice revealed alternations in the trabecular bone compartment during the progression of liver disease. The alterations in bone structure were reflected by significantly decreased trabecular numbers (Fig. 4A) and increased trabecular separation (Fig. 4B) in knockout mice at the age of 20 weeks. A similar trend was observed at later time points. In addition, connective density and trabecular tissue mineral density were significantly lower in *Abcb4*$^{-/-}$ mice as compared to controls at 20 and 30 weeks, respectively. The μCT analysis revealed significant changes in trabecular bone volume fractions in young knockout mice (i.e. 5 weeks of age), but not in older animals. However, trabecular thickness did not differ between *Abcb4*$^{-/-}$ and wild-type mice. Supplementary table 1 summarizes all parameters for trabecular bones as measured by μCT.

Femur sections after von Kossa staining (Fig. 4C) complement the μCT results. In both groups, the trabeculae of young knockout (Fig. 4C, a) and wild-type (Fig. 4C, d) mice were found close to the cartilage growth plate arranged mainly in parallel order. At increasing age, changes in trabecular order and connectivity were observed with reduced mineralization of the trabecular bone meshwork in *Abcb4*$^{-/-}$ mice (Fig. 4C, a – c) as compared to wild-type animals (Fig. 4C, d – f).

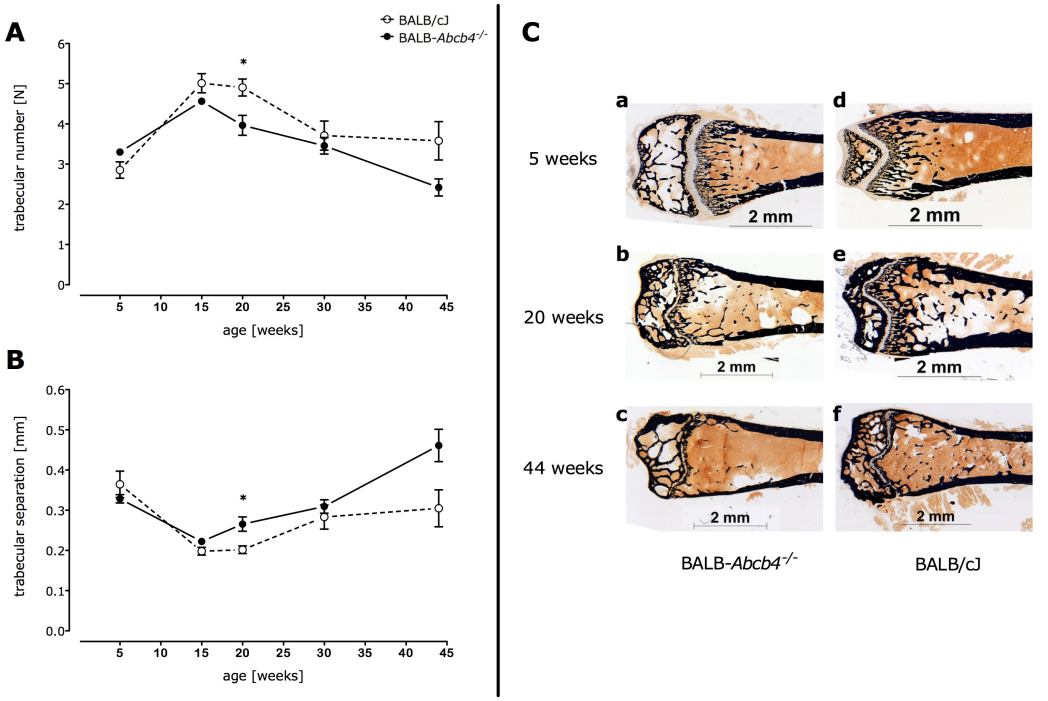

Figure 4: Trabecular bone morphometry and meshwork. Trabecular numbers (**A**) and trabecular separation (**B**) in BALB-*Abcb4*$^{-/-}$ and BABL/cJ wild-type mice at the age of 5-44 weeks, determined by µCT. N = 4 per genotype and time point; * $p < 0.05$, ** $p < 0.01$. Histological femoral slices (von Kossa) (**C**) of BALB-*Abcb4*$^{-/-}$ (a-c) and BABL/cJ (d-j) mice at the age of 5, 20 and 44 weeks. Mineralized cartilage and bone stained in black, non-mineralized cartilage and connective tissue in brown.

Abcb4$^{-/-}$ mice display decreased femoral mineral contents and volumes as well as lower cortical bone densities

Detailed analyses of femurs by pQCT demonstrated a significant reduction in femoral mineral contents (Fig. 5A) and commensurately in total femoral volumes (Fig. 5B) in both female and male *Abcb4*$^{-/-}$ mice in comparison to wild-type controls at 15 weeks of age. As a result, total femoral volume BMD, which is the amount of mineral per unit volume of the entire femur, was not affected by genotype (Fig. 5C).

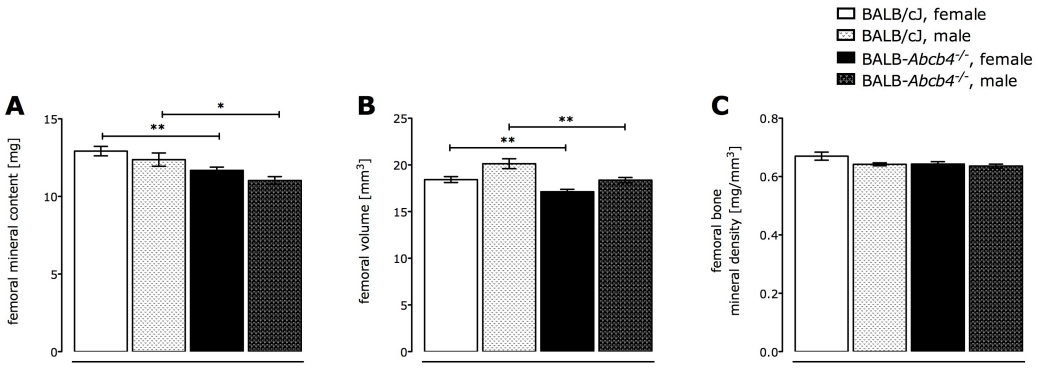

Figure 5: Bone density parameters of the femur. Femoral mineral contents (**A**), femoral volumes (**B**) and bone mineral density (**C**) of BALB/cJ wild-type and BALB-*Abcb4*$^{-/-}$ mice at the age of 15-17 weeks, determined by pQCT. N = 6-14 per genotype and sex;
* $p < 0.05$, ** $p < 0.01$.

Interestingly, cortical density, which reflects the material density of the bone, was significantly decreased in female knockout mice as compared to wild-type mice (1.166 ± 0.004 *vs.* 1.177 ± 0.004 mg/mm^3; $p < 0.05$) (Fig. 6A). Additionally, as illustrated in Fig. 6B, the circumference of the bone at the exact mid-diaphysis (periosteal circumference) of female *Abcb4*$^{-/-}$ animals was significantly lower in comparison to controls. Accordingly, we detected a trend for a decrease of the mid-diaphysial endosteal circumference in these mice (3.00 ± 0.04 *vs.* 3.11 ± 0.04 mm; $p = 0.06$), resulting in no significant differences in the thickness of the cortical bone between knockout and wild-type controls.

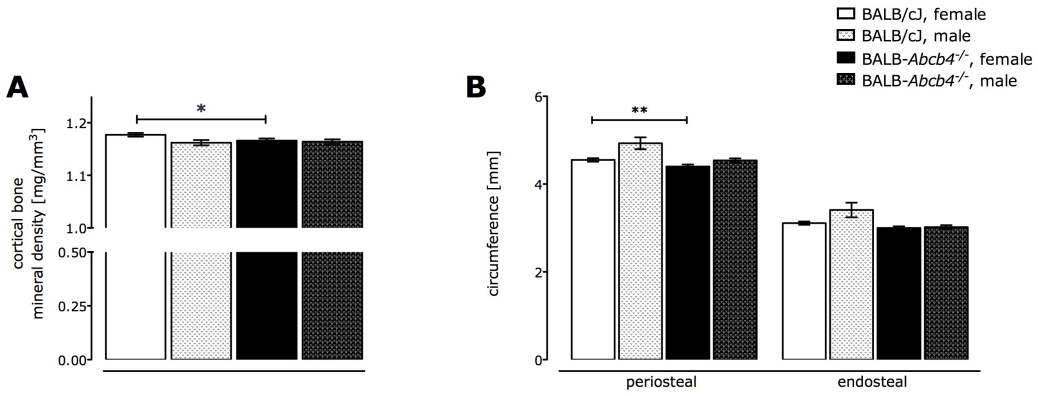

Figure 6: Bone material density. Cortical bone mineral density (**A**) and periosteal and endosteal circumferences of the femur at the mid-diaphysis (**B**) of BALB/cJ and BALB-*Abcb4*$^{-/-}$ mice at the age of 15-17 weeks, determined by pQCT.
N = 6-14 per genotype and sex; * $p < 0.05$, ** $p < 0.01$.

Abcb4$^{-/-}$ mice present with distorted calcium homeostasis and vitamin D metabolism

In comparison to controls, *Abcb4*$^{-/-}$ mice show lower plasma calcium concentrations (male: 2.24 ± 0.01 *vs.* 2.15 ± 0.03 mmol/l, $p < 0.05$; female: 2.22 ± 0.02 *vs.* 2.18 ± 0.02 mmol/l, $p > 0.05$), whereas phosphate levels were markedly increased in both sexes ($p < 0.01$; Fig. 7A). Consistent with the alteration in calcium-phosphate homeostasis, 25(OH)-vitamin D serum concentrations (Fig. 7B) are almost 50% lower in *Abcb4*$^{-/-}$ than in wild-type controls.

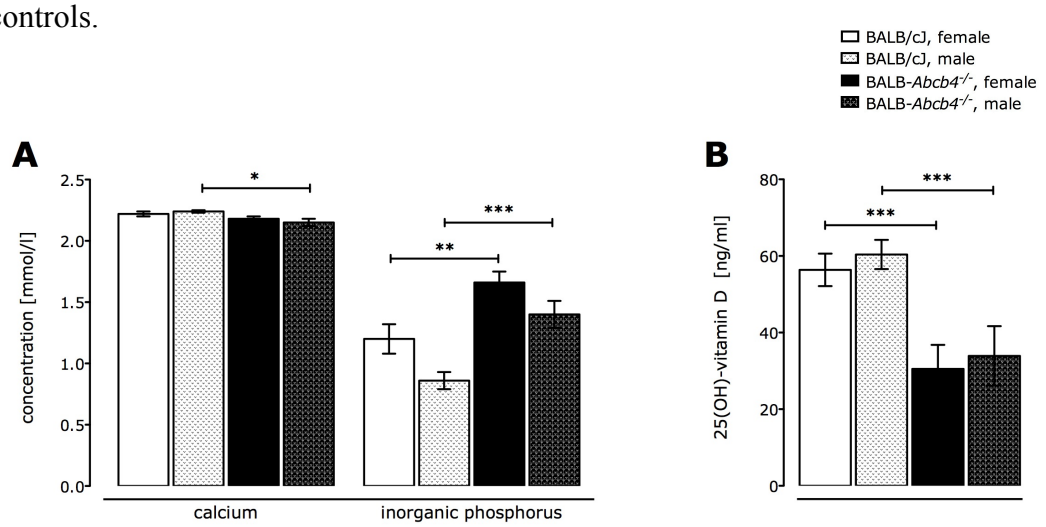

Figure 7: Calcium and phosphate plasma concentrations (**A**) and 25-hydroxyvitamin D serum levels (**B**) in BALB/cJ and BALB-*Abcb4*$^{-/-}$ mice at the age of 15-17 weeks.
N = 9-14 per genotype and sex; * < 0.05, *** 0.001.

Subsequently, we examined gene expression of key enzymes in vitamin D metabolism. *Abcb4*$^{-/-}$ animals show significantly ($p < 0.001$) higher hepatic expression of *Dhcr7,* which converts the vitamin D precursor 7-dehyrocholesterol to cholesterol, at the age of 5 weeks and a trend to higher steady-state mRNA levels at every consecutive time-point in comparison to controls (Fig. 8A). As illustrated in panels B and C of Fig. 8, *Abcb4*$^{-/-}$ animals are also characterized by markedly reduced hepatic expression of *Cyp2r1* and *Cyp27a1*. In line with these findings, the expression of the vitamin D binding protein *Gc* is constantly low in *Abcb4*$^{-/-}$ as compared to wild-type controls, with significant differences in

expression levels at early age (from 5 to 15 weeks of age; Fig. 8D). This expression pattern acts in concert to decrease vitamin D levels in *Abcb4*$^{-/-}$ mice.

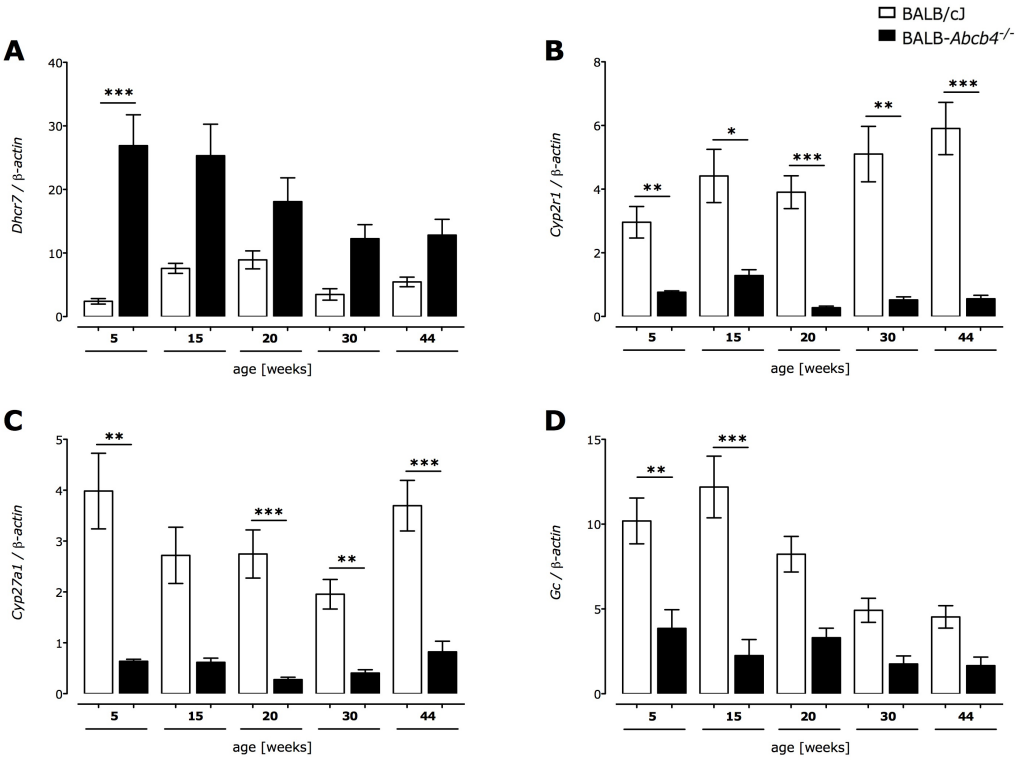

Figure 8: Hepatic expression of key genes involved in vitamin D metabolism. mRNA steady-state levels of genes encoding 7-dehydrocholesterol reductase (*Dhrc7*) (**A**), vitamin D 25-hydroxylase (*Cyp2r1*) (**B**), sterol 27-hydroxylase (*Cyp27a1*) (**C**), and vitamin D binding protein (*Gc*) (**D**) in BALB/cJ wild-type and BALB-*Abcb4*$^{-/-}$ mice at the age of 5-44 weeks. All expression levels are presented relative to β-*actin* expression (RT-PCR).
N = 4 per genotype and time point; * $p < 0.05$, ** $p < 0.01$, *** $p < 0.001$.

Abcb4$^{-/-}$ mice have altered gene expression of bone modeling markers

Next we examined expression levels of genes associated with bone turnover. Specifically, levels of *tumor necrosis factor receptor superfamily, member 11b* (*Tnfrsf11b,* also known as OPG, an inhibitor of osteoclasteogenesis), *bone γ-carboxyglutamate protein* (*Bglap,* alias 'osteocalcin', a marker of osteoblastogenesis) and *secreted phosphoprotein* (*Spp1*, also named 'osteopontin', a component of the bone matrix) in livers and bones of *Abcb4*$^{-/-}$ and wild-type animals. Interestingly, the hepatic expression of *Tnfrsf11b*, the natural antagonist

of RANKL, increased markedly in *Abcb4*$^{-/-}$ animals until 20 weeks of age and was significantly ($p < 0.05$) lower than in wild-type controls afterwards (Fig. 9A). In contrast, the expression levels of osteocalcin in liver increased in a time-shifted fashion, starting with significantly ($p < 0.001$) higher and later on lower expression in knockout mice as compared to controls at the age of 20 and 44 weeks, respectively (Fig. 9B). Gene expression levels of *Spp1* in liver did not significantly vary between *Abcb4*$^{-/-}$ mice and controls (data not shown).

In contrast to these data, bone expression levels of *Spp1* decreased significantly ($p < 0.05$) with age, starting at 30 weeks, in *Abcb4*$^{-/-}$ mice, whereas expression levels of wild-type controls remained constant (Fig. 9C). Bone expression of osteocalcin was markedly lower in *Abcb4*$^{-/-}$ mice as compared to controls at every age, with the largest difference in relative expression detected at the age of 5 weeks ($p < 0.001$; Fig. 9D).

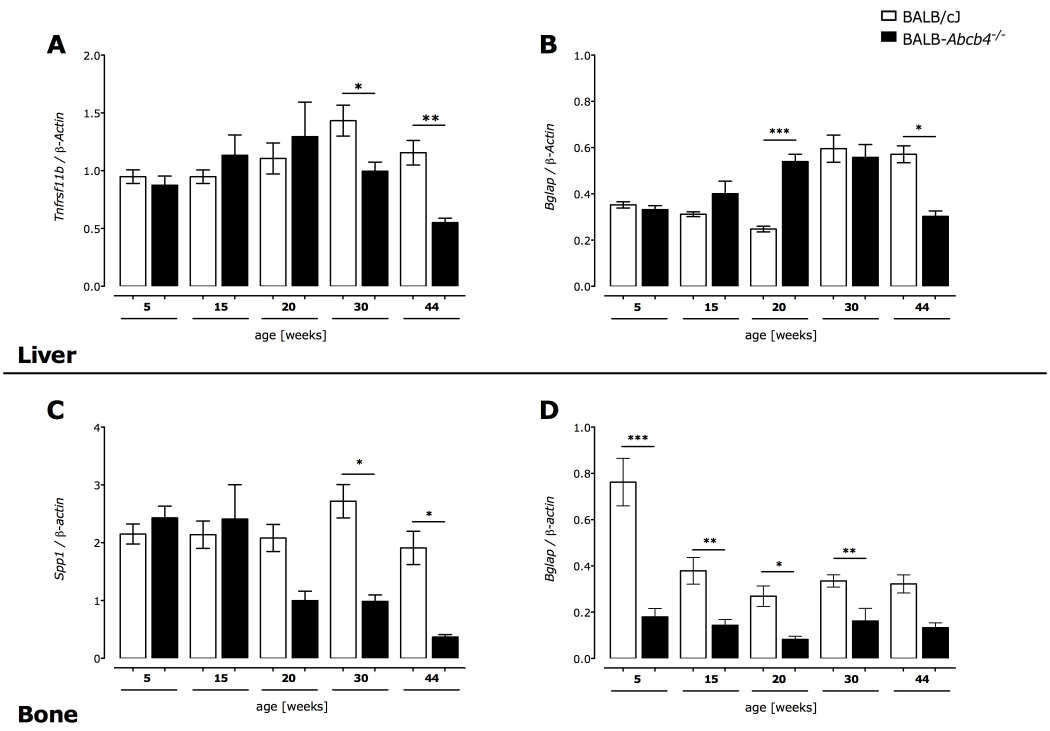

Figure 9: Expression of genes involved in bone metabolism. Hepatic steady-state mRNA levels of *Tnfrsf11b* coding osteoprotegerin (OPG) (**A**), and *bone γ-carboxyglutamate protein* (*Bglap*, osteocalcin) (**B**), as well as bone steady-state mRNA levels of *secreted phosphoprotein 1* (*Spp1*, osteopontin) (**C**), and *Bglap* (**D**) in BALB/cJ wild-type and BALB-*Abcb4*$^{-/-}$ mice at the age of 5-44 weeks. All expression levels are presented relative to β-*actin* expression (RT-PCR). N = 4 per genotype and time point; * $p < 0.05$, ** $p < 0.01$, *** $p < 0.001$.

Abcb4$^{-/-}$ mice show increased systemic TGF-β and RANKL levels

As shown in Fig. 10A, *Abcb4*$^{-/-}$ animals displayed elevated serum levels of activated TGF-β as compared to wild-type mice. Whereas TGF-β concentrations increased in *Abcb4*$^{-/-}$ animals until the age of 30 weeks (from 3.4 ± 0.3 at week 5 to 11.6 ± 2.0 ng/ml at week 30) and subsequently declined to basal levels (4.3 ± 0.1 ng/ml at week 45), the levels continuously decreased throughout the life span of controls (from 2.4 ± 0.2 ng/ml to 0.1 ± 0.1 ng/ml). Of note, *Abcb4*$^{-/-}$ mice exhibited strikingly higher concentrations of the osteoclastogenesis inducing factor RANKL in serum as compared to controls (258 ± 39 *vs*. 120 ± 10 pg/ml at

week 15, $p < 0.01$; Fig. 10B), whereas serum levels of OPG did not differ (2894 ± 308 *vs*. 3140 ± 131 pg/ml; $p > 0.05$).

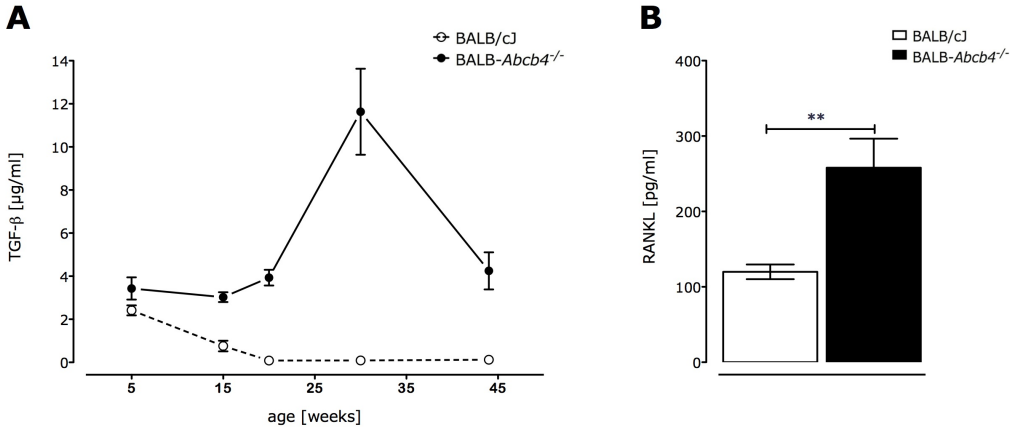

Figure 10: Active TGF-β serum levels measured by cell-based bioassay in BALB-*Abcb4*$^{-/-}$ and BALB/cJ wild-type mice. N = 4 per genotype and time point (**A**). RANKL serum concentration measured by ELISA in BALB-*Abcb4*$^{-/-}$ and BALB/cJ wild-type mice at the age of 15-17 weeks. N = 8-9 per genotype; ** $p < 0.01$ (**B**).

Vitamin D supplementation does not restore bone phenotypes in *Abcb4*$^{-/-}$ mice

The influence of the vitamin D dietary interventions on bone phenotypes was determined in *Abcb4*$^{-/-}$ female mice. The femoral bone mineral densities were significantly ($p < 0.05$) affected by vitamin D treatment. As illustrated in Fig. 11A, *Abcb4*$^{-/-}$ mice that were fed the vitamin D insufficient diet showed a significantly ($p < 0.001$) decreased mineral density as compared to knockout mice receiving the control diet (0.66 ± 0.01 *vs*. 0.70 ± 0.11 mg/mm^3). Fig. 11B illustrates that cortical bone mineral densities measured by pQCT were also significantly ($p < 0.001$) influenced by vitamin D intervention. Interestingly, both *Abcb4*$^{-/-}$ mice that received vitamin D -deficient (100 IU/kg) and mice that received vitamin D -supplemented diets (2,400 IU/kg) displayed reduced cortical bone mineral density in comparison to corresponding controls (1.11 ± 0.01 and 1.12 ± 0.01 *vs*. 1.14 ± 0.01; $p < 0.001$), and a similar pattern was observed for femoral bone mineral densities (Fig. 11). However, cortical thickness and

periosteal circumference were not affected by the vitamin D diets in *Abcb4*$^{-/-}$ mice (data not shown). Moreover, no changes of bone phenotypes were observed in wild-type mice fed any of the three vitamin D diets (data not shown).

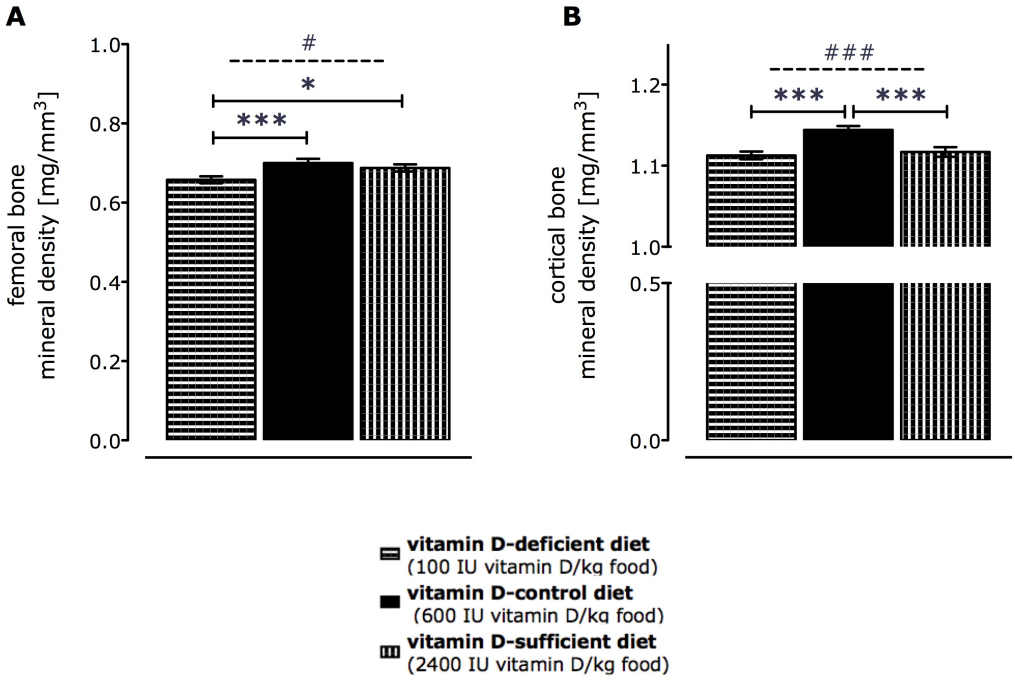

Figure 11: Femoral bone mineral density (**A**) and cortical bone mineral density (**B**) measured by pQCT in FVB-*Abcb4*$^{-/-}$ female mice at 16–18 weeks of age after vitamin D dietary intervention (vitamin D -deficient versus control versus vitamin D -supplemented diet). The patterns of the bars correspond to the three dietary regimens (100 IU vitamin D/kg food, horizontal lines; 600 IU vitamin D/kg food, black bars; 2,400 IU vitamin D/kg food, vertical lines). The dashed lines above the bars illustrate the vitamins D diet intervention effect over all groups ($^{\#}$ $p < 0.05$, $^{\#\#\#}$ $p < 0.001$); the solid lines indicate significant differences between specific dietary groups (* $p < 0.05$, *** $p < 0.001$). N = 8-11 per group.

DISCUSSION

Metabolic bone diseases are common complications of chronic cholestatic liver diseases. Nevertheless, the underlying mechanisms are still to be fully characterized. This is, at least in part, due to the lack of a representative preclinical model that allows the in-depth analysis of the association between liver disease and abnormal bone metabolism. Hence, the present study was designed to establish the *Abcb4*$^{-/-}$ mouse as a novel model for hepatic osteodystrophy and to characterize the systemic consequences of chronic cholangiopathy on bone morphology and metabolism. To date, the phenotypic analyses of *Abcb4*$^{-/-}$ mice have focused exclusively on the hepatic alterations caused by deficiency of the hepatobiliary phospholipid transporter. The present study is the first demonstrating that *Abcb4*$^{-/-}$ animals develop osteodystrophy accompanied by alterations of bone structure and density.

Abcb4$^{-/-}$ mice are characterized by chronic hepatobiliary injury as a result of low phospholipid concentrations in bile [11, 12]. Consequently, *Abcb4*$^{-/-}$ mice develop age-dependent chronic cholangitis and biliary fibrosis in response to persistent inflammation. Consistent with previously published reports [24-26], we detected marked liver damage that rapidly increased up to the age of 15 weeks with slower progression afterwards. In parallel, we observed initial changes of the bone in *Abcb4*$^{-/-}$ mice up to the age of 15 to 20 weeks. Furthermore, reduced numbers and increased separation of trabeculae, in line with diminished connective density, were observed at 20 weeks of age. In humans, trabecular bone architecture is key in maintaining for bone strength, especially in locations that experience high strain, such as in the proximal femur [27, 28]. Our results suggest that chronic cholestasis induced loss of trabecular bone may lead to decreased bone strength and stability.

The whole body (DXA) and femoral bone analyses (pQCT) demonstrated significantly lower mineral contents in the knockout mice at 15 to 17 weeks of age. It is well established that even minor changes in mineralization can lead to several-fold changes of static strength and elasticity [29]. Detailed analyses

revealed also differences between cortical bone in *Abcb4*$^{-/-}$ female and matched control mice. Cortical bone is usually very compact and constitutes about 80% of bone material. It has been previously demonstrated that cortical thinning and increased cortical porosity are important factors of bone strength [30]. Other studies suggested that weakened cortical bone is primarily responsible for intracapsular hip fracture [31]. Overall, the phenotypic characterization identified reduced bone mineralization and trabecular bone alterations in our mouse model, which could compromise bone strength.

In line with the histomorphological observations, we detected aberrations in calcium-phosphate homeostasis and low vitamin D levels, which are also frequently observed in patients with chronic cholestatic liver diseases [2, 32]. Vitamin D deficiency together with altered gene expression of key enzymes in vitamin D metabolism, especially the low expression of *Cyp2r1* and *Cyp27a1*, implies impairment of vitamin D synthesis or at least a systemic effect compromising vitamin D metabolism under cholestatic conditions. However, the role of calcium and vitamin D in cholestasis-associated bone diseases is not clear. Although the supplementation of vitamin D is generally recommended, there is no unequivocal data confirming the efficacy of vitamin D for preventing bone loss in patients with chronic liver diseases [33, 34], which is in line with the results of vitamin D interventions in our model (Fig. 11). These observations indicate that other mediators of bone remodeling might be critical in this specific model.

In general, a bone disorder is an acquired dissociation between bone formation and resorption caused by an imbalance of osteoblast and osteoclast activity. RANKL and OPG represent two key regulatory molecules that are produced by immature osteoblasts. While RANKL enhances osteoclast activity and therefore bone resorption, OPG as its soluble decoy receptor inhibits osteoclast differentiation. The assessment of these mediators in chronic liver diseases produced previously contradictory results [35]. In our model we observed increased RANKL serum levels in *Abcb4*$^{-/-}$ mice with advanced liver injury, whereas OPG serum levels did not differ from controls. Furthermore, *Abcb4*$^{-/-}$ animals displayed elevated serum levels of TGF-β, which promotes RANKL-

induced osteoclastogenesis [36, 37]. In line with the *Abcb4*$^{-/-}$ model, our recently published clinical study has demonstrated that chronically increased serum levels of TGF-β might be a potential inducer of bone density loss in humans [38].

Osteocalcin is produced by osteoblasts and is a surrogate marker of bone osteoblastic activity and bone remodeling. Low mRNA expression of osteocalcin is consistent with reduced osteoblastogenesis, albeit it might also represent a compensatory response. As highlighted recently [39, 40], osteocalcin - apart from its role in bone remodeling - acts as a hormone that influences energy expenditure. It improves glucose tolerance by increasing β-cell proliferation as well as insulin secretion and sensitivity in mice [41]. Of note, we observed that *Abcb4*$^{-/-}$ animals display improved glucose tolerance [42]. In fact, low levels of osteocalcin might result from an adaptive effect but could also be due the low levels of vitamin D in *Abcb4*$^{-/-}$ animals, which regulates osteocalcin expression at the post-transcriptional level [43].

Together, our data suggest an increase in osteoclastogenesis in bone in the absence of *Abcb4*, co-incident with an impact on osteoblastogenesis. This would result in a net decrease in bone remodeling, which might explain both the decrease in bone volume in these young and growing mice, as well as the reduction of bone in the trabecular bone compartment. Osteopontin modifies the migration and attachment of osteoclasts and their resorptive activity [44] and osteopontin-deficient mice show delayed bone resorption in metaphyseal trabeculae and increased bone rigidity [45]. Osteopontin is expressed by both osteoblasts and osteoclasts, and the lower *Spp1* expression in bones from our mice further supports the hypothesis of an imbalance during bone remodeling in the absence of ABCB4.

Since *Rankl*, *Bglap* and *Spp1* are target genes of 1,25$(OH)_2$-vitamin D and their expression is modulated by 25$(OH)_2$-vitamin D [10], a systemic effect of vitamin D on bone in the setting of cholestasis is likely. Further evidence for differential effects of vitamin D on the bone phenotypes in chronic cholestasis is provided by our feeding experiments in female *Abcb4*$^{-/-}$ mice, which develop more severe fibrosis as compared to males [46]. Interestingly, we found that cortical BMD was

reduced in both mice receiving vitamin D-insufficient and vitamin D-sufficient diets. This observation could be explained, at least in part, by interactions between vitamin D and bile acid metabolism. Circulating bile acid levels are about ten-fold higher in *Abcb4*$^{-/-}$ as compared to wild-type mice (not shown) and in fact, the secondary bile acid lithocholic acid (LCA) is known to have deleterious effects on osteoblast viability and affect the expression of *Bglap* and *Rankl* [47, 48]. Moreover, the treatment with LCA in combination with vitamin D decreases the expression of *Cyp24a1*, encoding the hydroxylase involved in catabolism of vitamin D. Additionally to bile acids, elevated serum bilirubin in the ABCB4 deficient mouse model [24] could also affect bone formation since unconjugated bilirubin is known to impair osteoblast proliferation in a dose-dependent fashion [34].

Although HOD is likely to be caused by multiple environmental and genetic factors, it was beyond the attempt of this study to analyze all of these factors. Our experiments demonstrate that mice lacking the hepatic phospholipid transporter ABCB4, primarily known as model for chronic cholestatic liver disease, develop an osteopenic phenotype. We postulate that the *Abcb4*$^{-/-}$ mouse might be considered as a genetically defined preclinical HOD model to gain further insights into the molecular pathobiology of this disorder and to analyze the systemic effects of therapeutic interventions.

Supplementary data to this study can be found online at:
http://559 dx.doi.org/10.1016/j.bone.2013.03.012.

REFERENCES

1. Diamond T, Stiel D, Lunzer M, Wilkinson M, Roche J, Posen S. Osteoporosis and skeletal fractures in chronic liver disease. Gut l1990;31: 82-7.
2. Gasser RW. Cholestasis and metabolic bone disease - a clinical review. Wien Med Wochenschr l2008;158: 553-7.
3. Guañabens N, Cerda D, Monegal A, Pons F, Caballeria L, Peris P, Parés A. Low bone mass and severity of cholestasis affect fracture risk in patients with primary biliary cirrhosis. Gastroenterology l2010;138: 2348-56.
4. Angulo P, Grandison GA, Fong DG, Keach JC, Lindor KD, Bjornsson E, Koch A. Bone disease in patients with primary sclerosing cholangitis. Gastroenterology l2011;140: 180-8.
5. Pusl T, Beuers U. Extrahepatic manifestations of cholestatic liver diseases: pathogenesis and therapy. Clin Rev Allergy Immunol l2005;28: 147-57.
6. López-Larramona G, Lucendo AJ, Gonzalez-Castillo S, Tenias JM. Hepatic osteodystrophy: An important matter for consideration in chronic liver disease. World J Hepatol l2011;3: 300-7.
7. Goel V, Kar P. Hepatic osteodystrophy. Trop Gastroenterol l2010;31: 82-6.
8. Schuster I. Cytochromes P450 are essential players in the vitamin D signaling system. Biochim Biophys Acta l2011;1814: 186-99.
9. Meier U, Gressner O, Lammert F, Gressner AM. Gc-globulin: roles in response to injury. Clin Chem l2006;52: 1247-53.
10. Haussler MR, Whitfield GK, Kaneko I, Haussler CA, Hsieh D, Hsieh JC, Jurutka PW. Molecular Mechanisms of Vitamin D Action. Calcif Tissue Int l2012;92:77-98
11. Fickert P, Fuchsbichler A, Wagner M, Zöllner G, Kaser A, Tilg H, Krause R, Lammert F, Langner C, Zatloukal K, Marschall HU, Denk H, Trauner M. Regurgitation of bile acids from leaky bile ducts causes sclerosing cholangitis in *Mdr2* (*Abcb4*) knockout mice. Gastroenterology l2004;127: 261-74.
12. Lammert F, Wang DQ, Hillebrandt S, Geier A, Fickert P, Trauner M, Matern S, Paigen B, Carey MC. Spontaneous cholecysto- and hepatolithiasis in *Mdr2-/-* mice: a model for low phospholipid-associated cholelithiasis. Hepatology l2004;39: 117-28.
13. Popov Y, Patsenker E, Fickert P, Trauner M, Schuppan D. *Mdr2* (*Abcb4*)-/- mice spontaneously develop severe biliary fibrosis via massiv dysregulation of pro- and antifibrogenic genes. Journal of Hepatology 2005;43:1045-54.
14. Batts KP, Ludwig J. Chronic hepatitis. An update on terminology and reporting. Am J Surg Pathol l1995;19: 1409-17.
15. Ishak K, Baptista A, Bianchi L, Callea F, de Groote J, Gudat F, Denk H, Desmet V, Korb G, MacSween RN, et al. Histological grading and staging of chronic hepatitis. J Hepatol l1995;22: 696-9.
16. Jamall IS, Finelli VN, Que Hee SS. A simple method to determine nanogram levels of 4-hydroxyproline in biological tissues. Anal Biochem l1981;112: 70-5.
17. Hillebrandt S, Goos C, Matern S, Lammert F. Genome-wide analysis of hepatic fibrosis in inbred mice identifies the susceptibility locus *Hfib1* on chromosome 15. Gastroenterology l2002;123: 2041-51.
18. Tesseur I, Zou K, Berber E, Zhang H, Wyss-Coray T. Highly sensitive and specific bioassay for measuring bioactive TGF-beta. BMC Cell Biol l2006;7: 15.
19. Ehnert S, Seeliger C, Vester H, Schmitt A, Saidy-Rad S, Lin J, Neumaier M, Gillen S, Kleeff J, Friess H, Burkhart J, Stockle U, Nüssler AK. Autologous serum improves yield and metabolic capacity of monocyte-derived hepatocyte-like cells: possible implication for cell transplantation. Cell Transplant l2011;20: 1465-77.
20. Livak KJ, Schmittgen TD. Analysis of relative gene expression data using real-time quantitative PCR and the $2^{-\Delta\Delta CT}$ Method. Methods l2001;25: 402-8.

21. Gailus-Durner V, Fuchs H, Becker L, Bolle I, Brielmeier M, Calzada-Wack J, Elvert R, Ehrhardt N, Dalke C, Franz TJ, Grundner-Culemann E, Hammelbacher S, Hölter SM, Hölzlwimmer G, Horsch M, Javaheri A, Kalaydjiev SV, Klempt M, Kling E, Kunder S, Lengger C, Lisse T, Mijalski T, Naton B, Pedersen V, Prehn C, Przemeck G, Racz I, Reinhard C, Reitmeir P, Schneider I, Schrewe A, Steinkamp R, Zybill C, Adamski J, Beckers J, Behrendt H, Favor J, Graw J, Heldmaier G, Höfler H, Ivandic B, Katus H, Kirchhof P, Klingenspor M, Klopstock T, Lengeling A, Müller W, Ohl F, Ollert M, Quintanilla-Martinez L, Schmidt J, Schulz H, Wolf E, Wurst W, Zimmer A, Busch DH, Hrabě de Angelis M. Introducing the German Mouse Clinic: open access platform for standardized phenotyping. Nat Methods l2005;2: 403-4.
22. Gailus-Durner V, Fuchs H, Adler T, Aguilar Pimentel A, Becker L, Bolle I, Calzada-Wack J, Dalke C, Ehrhardt N, Ferwagner B, Hans W, Holter SM, Holzlwimmer G, Horsch M, Javaheri A, Kallnik M, Kling E, Lengger C, Morth C, Mossbrugger I, Naton B, Prehn C, Puk O, Rathkolb B, Rozman J, Schrewe A, Thiele F, Adamski J, Aigner B, Behrendt H, Busch DH, Favor J, Graw J, Heldmaier G, Ivandic B, Katus H, Klingenspor M, Klopstock T, Kremmer E, Ollert M, Quintanilla-Martinez L, Schulz H, Wolf E, Wurst W, Hrabě de Angelis M. Systemic first-line phenotyping. Methods Mol Biol l2009;530: 463-509.
23. Hildebrand T, Ruegsegger P. Quantification of Bone Microarchitecture with the Structure Model Index. Comput Methods Biomech Biomed Engin l1997;1: 15-23.
24. Smit JJ, Schinkel AH, Oude Elferink RP, Groen AK, Wagenaar E, van Deemter L, Mol CA, Ottenhoff R, van der Lugt NM, van Roon MA, et al. Homozygous disruption of the murine mdr2 P-glycoprotein gene leads to a complete absence of phospholipid from bile and to liver disease. Cell l1993;75: 451-62.
25. Henkel C, Roderfeld M, Weiskirchen R, Berres ML, Hillebrandt S, Lammert F, Meyer HE, Stuhler K, Graf J, Roeb E. Changes of the hepatic proteome in murine models for toxically induced fibrogenesis and sclerosing cholangitis. Proteomics l2006;6: 6538-48.
26. Roderfeld M, Rath T, Voswinckel R, Dierkes C, Dietrich H, Zahner D, Graf J, Roeb E. Bone marrow transplantation demonstrates medullar origin of CD34+ fibrocytes and ameliorates hepatic fibrosis in *Abcb4-/-* mice. Hepatology l2010;51: 267-76.
27. Krug R, Burghardt AJ, Majumdar S, Link TM. High-resolution imaging techniques for the assessment of osteoporosis. Radiol Clin North Am l2010;48: 601-21.
28. Hildebrand T, Laib A, Muller R, Dequeker J, Ruegsegger P. Direct three-dimensional morphometric analysis of human cancellous bone: microstructural data from spine, femur, iliac crest, and calcaneus. J Bone Miner Res l1999;14: 1167-74.
29. Currey JD. The relationship between the stiffness and the mineral content of bone. J Biomech l1969;2: 477-480.
30. Bousson V, Peyrin F, Bergot C, Hausard M, Sautet A, Laredo JD. Cortical bone in the human femoral neck: three-dimensional appearance and porosity using synchrotron radiation. J Bone Miner Res l2004;19: 794-801.
31. Crabtree N, Loveridge N, Parker M, Rushton N, Power J, Bell KL, Beck TJ, Reeve J. Intracapsular hip fracture and the region-specific loss of cortical bone: analysis by peripheral quantitative computed tomography. J Bone Miner Res l2001;16: 1318-28.
32. Grünhage F, Hochrath K, Krawczyk M, Höblinger A, Obermayer-Pietsch B, Geisel J, Trauner M, Sauerbruch T, Lammert F. Common genetic variation in vitamin D metabolism is associated with liver stiffness. Hepatology l2012;56: 1883-91.
33. Collier JD, Ninkovic M, Compston JE. Guidelines on the management of osteoporosis associated with chronic liver disease. Gut l2002;50 Suppl 1: i1-9.
34. Guañabens N, Parés A. Liver and bone. Arch Biochem Biophys l2010;503: 84-94.
35. Mansueto P, Carroccio A, Seidita A, Di Fede G, Craxi A. Osteodystrophy in chronic liver diseases. Intern Emerg Med l2012.
36. Fox SW, Lovibond AC. Current insights into the role of transforming growth factor-beta in bone resorption. Mol Cell Endocrinol l2005;243: 19-26.
37. Pfeilschifter J, Bonewald L, Mundy GR. Characterization of the latent transforming growth factor beta complex in bone. J Bone Miner Res l1990;5: 49-58.

38. Ehnert S, Baur J, Schmitt A, Neumaier M, Lucke M, Dooley S, Vester H, Wildemann B, Stockle U, Nüssler AK. TGF-ß1 as possible link between loss of bone mineral density and chronic inflammation. PLoS One l2010;5: e14073.
39. Neve A, Corrado A, Cantatore FP. Osteocalcin: Skeletal and extra-skeletal effects. J Cell Physiol l2012;228: 1149-53.
40. Booth SL, Centi A, Smith SR, Gundberg C. The role of osteocalcin in human glucose metabolism: marker or mediator? Nat Rev Endocrinol l2013;9: 43-55.
41. Lee NK, Sowa H, Hinoi E, Ferron M, Ahn JD, Confavreux C, Dacquin R, Mee PJ, McKee MD, Jung DY, Zhang Z, Kim JK, Mauvais-Jarvis F, Ducy P, Karsenty G. Endocrine regulation of energy metabolism by the skeleton. Cell l2007;130: 456-69.
42. Hochrath K, Krawczyk M, Goebel R, Langhirt M, Rathkolb B, Micklich K, Rozman J, Horsch M, Beckers J, Klingenspor M, Fuchs H, Gailus-Durner V, Wolf E, Acalovschi M, Volmer DA, Hrabě de Angelis M, Lammert F. The hepatic phosphatidylcholine transporter ABCB4 as modulator of glucose homeostasis. FASEB J l2012;26: 5081-91.
43. Mosavin R, Mellon WS. Posttranscriptional regulation of osteocalcin mRNA in clonal osteoblast cells by 1,25-dihydroxyvitamin D3. Arch Biochem Biophys l1996;332: 142-52.
44. Sodek J, Ganss B, McKee MD. Osteopontin. Crit Rev Oral Biol Med l2000;11: 279-303.
45. Chellaiah MA, Kizer N, Biswas R, Alvarez U, Strauss-Schoenberger J, Rifas L, Rittling SR, Denhardt DT, Hruska KA. Osteopontin deficiency produces osteoclast dysfunction due to reduced CD44 surface expression. Mol Biol Cell l2003;14: 173-89.
46. Van Nieuwerk CM, Groen AK, Ottenhoff R, van Wijland M, van den Bergh Weerman MA, Tytgat GN, Offerhaus JJ, Oude Elferink RP. The role of bile salt composition in liver pathology of *mdr2*$^{-/-}$ mice: differences between males and females. J Hepatol l1997;26: 138-45.
47. Ruiz-Gaspá S, Guañabens N, Enjuanes A, Peris P, Martinez-Ferrer A, de Osaba MJ, Gonzalez B, Alvarez L, Monegal A, Combalia A, Parés A. Lithocholic acid downregulates vitamin D effects in human osteoblasts. Eur J Clin Invest l2010;40: 25-34.
48. Dubreuil M, Ruiz-Gaspà S, Guañabens N, Peris P, Álvarez L, Monegal A, Combalia A, Parés A. Ursodeoxycholic acid increases differentiation and mineralization and neutralizes the damaging effects of bilirubin on osteoblastic cells. Liver International l2013: n/a-n/a.

KAPITEL 4:

VITAMIN D ALS MODULATOR DER FIBROGENESE IN ABCB4-DEFIZIENTEN MÄUSEN

VITAMIN D ALS MODULATOR DER FIBROGENESE IN ABCB4-DEFIZIENTEN MÄUSEN

Vitamin D ist ein Secosteroidhormon, das seine pleiotropen Effekte vorwiegend über den Vitamin D-Rezeptor (VDR) vermittelt. Neben seiner klassischen Rolle als Regulator des Knochenstoffwechsels ist Vitamin D auch in die Modulation des Immunsystems sowie die Zell-Entwicklung und Differenzierung involviert (Cantorna *et al.* 2004, Yang *et al.* 1993, Abe *et al.* 1981). Insbesondere die extra-skelettalen Effekte könnten relevant sein für die Pathogenese und die Behandlung chronischer Lebererkrankungen, da unter diesen Patienten ein Vitamin D-Mangel, unabhängig von der Ätiologie der Erkrankung, weit verbreitet ist. Während etwa 40% der gesunden westeuropäischen Bevölkerung eine Vitamin D-Unter-versorgung aufweisen (< 30 ng/ml), sind es bis zu 90% bei Patienten mit einer chronischen Lebererkrankung (Zittermann 2010, Arteh *et al.* 2010). Zudem weisen Patienten mit einem Vitamin D-Mangel eine stärker ausgeprägte Leberfibrose und eine erhöhte Sterblichkeit auf (Petta *et al.* 2010, Putz-Bankuti *et al.* 2012). Weitere Analysen zeigen eine inverse Korrelation von Vitamin D-Serumkonzentrationen mit der Ausprägung der Lebererkrankung (Arteh *et al.* 2010, Fisher and Fisher 2007). Ungeachtet dieser Beobachtungen liegen nur wenige Studien vor, die den protektiven Schutz von Vitamin D bei chronischen Lebererkrankungen untersuchen (Song and Rockey 2013). Dies ist vermutlich auch auf den Mangel an adäquaten präklinischen Modellen zurück zuführen, in denen die Effekte einer Vitamin D-Supplementation untersucht werden können.

Vorarbeiten anderer Arbeitsgruppen lassen vermuten, dass speziell bei cholestatischen Lebererkrankungen Vitamin D und sein Rezeptor eine potentiell regulierende Rolle spielen. Dazu zählt die Tatsache, dass in der Leber die Expression von VDR primär auf Nicht-Parenchym-Zellen und Epithelzellen der Gallengänge limitiert ist (Gascón-Barre *et al.* 2003). Des Weiteren konnte nach-gewiesen werden, dass spezifische Gallensäuren wie die Lithocholsäure als Liganden und Aktivatoren des VDR fungieren (Makishima *et al.* 2002).

Ziel der hier dargestellten Studie war es daher, den Einfluss von Vitamin D auf die biliäre Leberfibrose in der *Abcb4*$^{-/-}$-Maus zu untersuchen. Zu diesem Zweck wurden *Abcb4*$^{-/-}$-Mäuse und Kontrolltiere über 12 Wochen mit einer Vitamin D-Mangeldiät, einer Vitamin D- supplementierten oder regulären Kontroll-Diät (100, 2400 oder 600 IU Cholecalciferol/kg Futter) gefüttert. Im Anschluss an die Diät erfolgte eine umfangreiche Analyse der Tiere in Hinblick auf ihre Leberphänotypen. Zusätzlich wurden die Vitamin D-Konzentrationen im Serum sowie die hepatische mRNA-Expression von VDR, von Enzymen des Vitamin D- und Gallensäurestoffwechsels und das Adhäsionsprotein E-Cadherin quantifiziert.

Die Ergebnisse dieser Studie zeigen, dass die Vitamin D-Konzentrationen im Serum vom Genotyp und der verabreichten Diät abhängig sind. So finden sich bei *Abcb4*$^{-/-}$-Tieren, die eine Kontroll-Diät erhalten haben, geringere Vitamin D-Konzentrationen im Vergleich zu gesunden Wildtyp-Mäusen. Die Untersuchung des Leberphänotyps belegt, dass sich die hepatischen Kollagenkonzentrationen und die weitere Ausprägung der Fibrose zwischen den Diätgruppen unterscheiden. Nach Verabreichung einer Vitamin D-Mangeldiät entwickeln *Abcb4*$^{-/-}$-Mäuse eine deutlich stärker ausgeprägte Fibrose und höhere Kollagenwerte im Vergleich zu Tieren, die über ihr Futter mehr Vitamin D erhalten haben. Das Fibrosestadium von ABCB4-defizienten Mäusen, denen eine Kontroll- oder eine hochdosierte Vitamin D-Diät gefüttert worden ist, unterscheidet sich nicht, allerdings zeigen Tiere unter der hochdosierten Diät niedrigere Transaminasenaktivitäten.

Die Vitamin D/VDR-Signalachse ist bei *Abcb4*$^{-/-}$-Tieren ebenfalls beeinträchtigt. Ein Anstieg der hepatischen *Vdr*-Expression findet sich bei allen ABCB4-defizienten Mäusen. Interessanterweise zeigen Knockout-Mäuse nach einer Vitamin D-Mangeldiät, parallel zu der stärksten Fibroseausprägung, die niedrigsten *Vdr*-Expressionslevel. Eine Vitamin D-Diät-abhängige Regulation von E-Cadherin in der Leber konnte nicht nachgewiesen werden.

Zusammenfassend belegen die Daten, dass Vitamin D einen modulierenden Effekt auf die Fibrogenese in ABCB4-defizienten Mäusen hat und die Ausprägung der biliären Fibrose durch den Vitamin D-Status beeinflusst wird. Während ein

Vitamin D-Mangel mit einer vermehrten Kollagenablagerung und stärkerer Fibrose assoziiert ist, reduziert eine ausreichende Vitamin D-Versorgung die Leberfibrose. Über die hochdosierte Vitamingabe lässt sich jedoch nur ein moderater zusätzlicher Effekt erzielen. Übertragen auf Patienten mit chronisch cholestatischen Lebererkrankungen, lässt diese Studie vermuten, dass durch die Behebung eines Vitamin D-Mangels, ein anti-fibrotischer Effekt erzielt werden kann, dass eine exzessive Vitamin D-Dosis jedoch keine darüber hinausführenden therapeutischen Effekte haben könnte.

Die immunhistologischen Analysen von E-Cadherin und Zytokeratin für diese Studie wurde von Dr. Marion Pollheimer und Prof. Dr. Peter Fickert (Institut für Pathologie, Medizinische Universität Graz) durchgeführt. Die histopathologische Anfertigung und Bewertung der Leberschnitte wurden mit freundlicher Unterstützung von Dr. Kanishka Hittatiya (Pathologisches Institut, Universitätsklinikum Bonn) vorgenommen.

VITAMIN D MODULATES BILIARY FIBROSIS IN ABCB4 DEFICIENT MICE

Katrin Hochrath[1], Caroline S. Stokes[1], Jürgen Geisel[2], Marion J. Pollheimer[3], Peter Fickert[3,4], Steven Dooley[5] and Frank Lammert[1]

[1]Department of Medicine II and [2]Institute of Clinical Chemistry and Laboratory Medicine, Saarland University Medical Center, Homburg, Germany; [3]Insititute of Pathology Medical University Graz, Graz, Austria; [4]Division of Gastroenterology and Hepatology, Department of Internal Medicine, Medical University of Graz, Graz, Austria; [5]Division of Molecular Hepatology - Alcohol Associated Diseases, Department of Medicine II, Medical Faculty Mannheim, University of Heidelberg, Mannheim, Germany

Hepatology International 2014; 1-10

ABSTRACT

Purpose: Impaired vitamin D receptor signaling represents an aggravating factor during liver injury and recent studies suggest that vitamin D might exert a protective role in chronic hepatobiliary diseases. We hypothesized that vitamin D supplementation would ameliorate liver fibrosis in ATP-binding cassette transporter B4 knockout (*Abcb4*$^{-/-}$) mice as preclinical model of sclerosing cholangitis.

Methods: *Abcb4*$^{-/-}$ and wild-type mice were fed regular chow diet (600 IU vitamin D/kg food) or diets with lower (100 IU/kg) and higher (2,400 IU/kg) vitamin D concentrations for 12 weeks. Serum 25-hydroxyvitamin D concentrations were measured by chemiluminescence immunoassays. Liver injury and biliary fibrosis were assessed by liver enzyme activities, histopathology and hepatic collagen contents. Hepatic mRNA expression of markers for fibrosis, vitamin D and bile acid metabolism were analyzed by quantitative PCR.

Results: Different vitamin D concentrations were observed depending on genotype and diet group, with *Abcb4*$^{-/-}$ mice on the control diet showing lower vitamin D concentrations compared to wild-type mice. *Abcb4*$^{-/-}$ animals on the low vitamin D diet demonstrated most advanced liver fibrosis and highest hepatic collagen contents. Feeding *Abcb4*$^{-/-}$ mice high vitamin D diet enriched serum vitamin D levels, lowered liver enzyme activities, altered expression levels of profibrogenic genes and ameliorated, in part, liver injury.

Conclusions: This is the first report to demonstrate that fibrogenesis in the established *Abcb4*$^{-/-}$ model is influenced by vitamin D supplementation. Since vitamin D modulates sclerosing cholangitis *in vivo*, we speculate that sufficient vitamin D intake might improve liver damage and induce anti-fibrotic effects in chronic cholestasis in humans.

INTRODUCTION

Vitamin D deficiency occurs in up to 90% of patients with chronic liver diseases, irrespective of the underlying etiology of liver injury [1, 2]. Moreover, in these patients, low vitamin D levels are associated with increased grades of necroinflammation and stages of fibrosis and a heightened mortality risk [3-6]. Despite these observations, and in particular the inverse correlation between vitamin D levels and the severity of liver diseases, to date few studies have investigated the beneficial and adverse effects of vitamin D supplementation in chronic liver diseases [7-9]. Therefore, data regarding the efficacy of vitamin D supplementation are still lacking and preclinical models for assessing the effects of vitamin D are needed.

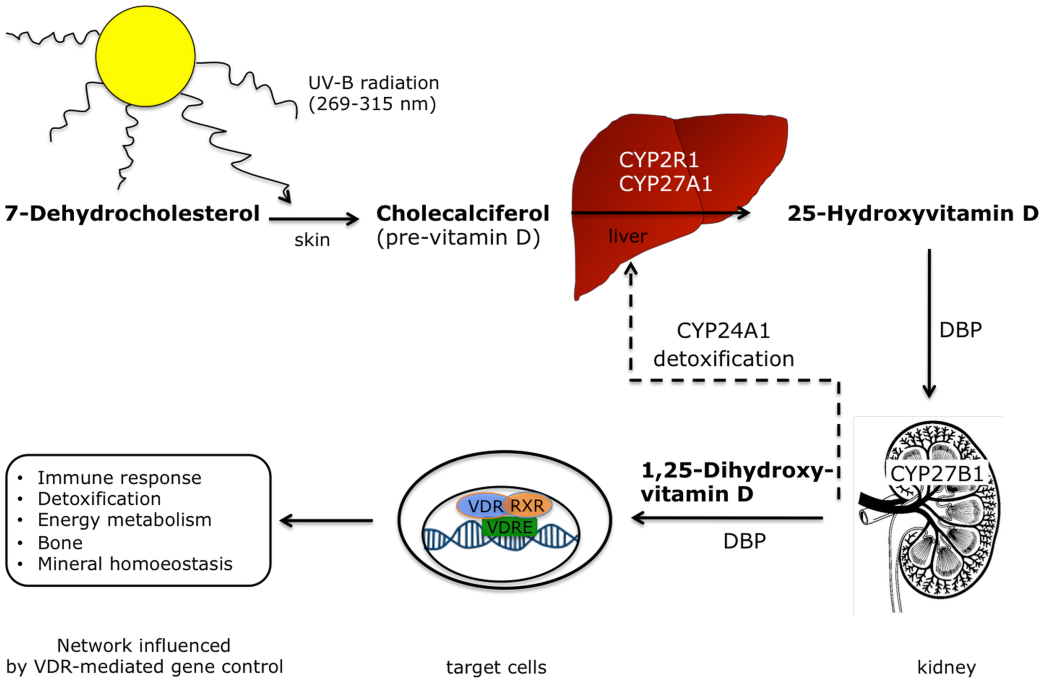

Figure 1: Vitamin D metabolism overview.
Abbreviations: CYP27A1, cytochrome P450, family 27, subfamily A, polypeptide 1; CYP27B1, cytochrome P450, family 27, subfamily B, polypeptide 1; CYP2R1, cytochrome P450, family 2, subfamily R, polypeptide 1; RXR, retinoid X receptor; DBP, vitamin D-binding protein; VDR, vitamin D receptor; VDRE, vitamin D response element

Vitamin D is a steroid hormone with pleiotropic effects that undergoes hydroxylation in liver and kidney [6]. The major circulating form, 25-hydroxyvitamin D, is bound to vitamin D binding protein, whereas effects of 1α,25-dihydroxyvitamin D on target genes in many organs are mediated by a ligand-activated nuclear receptor, vitamin D receptor (VDR) [10], which forms a heterodimer with the retinoid X receptor (RXR) to modulate processes and networks ranging from immune responses to mineral homoeostasis (Figure 1).

In the liver, VDR expression is restricted to non-parenchymal cells and biliary epithelial cells [11]. Besides activation of VDR by vitamin D, lithocholic acid and its derivatives have been demonstrated to function as VDR ligands and activators [12]. Furthermore, regulation of bile acid synthesis and enzymes responsible for bile acid detoxification are influenced by vitamin D-VDR-signaling [13-15]. These findings collectively point to a potential modulatory role of vitamin D-VDR-signaling in biliary-type liver injury.

Hence, we hypothesized that vitamin D supplementation ameliorates liver fibrosis *in vivo* by phenotyping *Abcb4* (ATP-binding cassette transporter, subfamily B, member 4) knockout (*Abcb4*$^{-/-}$, also known as *Mdr2*$^{-/-}$) mice, an established and highly reproducible model of sclerosing cholangitis [16-18]. *Abcb4*$^{-/-}$ mice lack the hepatocanalicular phosphatidylcholine floppase ABCB4 and develop sclerosing cholangitis and liver fibrosis [19]. The disease caused by mutations of the orthologous human gene is called progressive familial intrahepatic cholestasis (PFIC type 3), which resembles primary sclerosing cholangitis.

MATERIAL AND METHODS

Animals

FVB/N-*Abcb4*^{tm1bor} mice and FVB/NJ control mice were obtained from the Jackson Laboratory (Bar Harbor, USA). The mice were housed and bred in individually ventilated cages with a 12-hour light-dark cycle under incandescent lighting free from UVB radiation. Temperature and humidity were regulated at 22 ± 1°C and 55 ± 5%, respectively. Water and food were provided *ad libitum*. Mice were genotyped by polymerase chain reaction (PCR) of tail DNA using *neo* (5´-CTT GGG TGG AGA GGC TAT TC -3´; 5´-AGG TGA GAT GAC AGG AGA TC -3´) and *Abcb4* (5´-CAC TTG GAC CTG AGG CTG TG; TCA GGA CTC CGC TAT AAC GG -3) specific primer pairs. The PCR reaction included PCR buffer (Applied Biosystems, Darmstadt, Germany), 2 mM $MgCl_2$, 10 µM dNTPs, 10 µM primer, 1.25 U *Taq* DNA polymerase (Invitrogen, Darmstadt, Germany), and 20 - 100 ng DNA in 25-µl-reactions. PCR cycling conditions were 94°C/30 s, 55°C/60 s and 72°C/30 s for 35 cycles, and a final extension step of 10 minutes at 72°C.

The animal experiments were performed with permission from the federal state of Saarland according to §8 of the German Law for the Protection of Animals and the Directive 2010/63/EU of the European Parliament. All institutional and national guidelines for the care and use of laboratory animals were followed.

Diets

The vitamin D diets were commenced after weaning in the fourth week of age, coinciding with the initiation of liver pathology including sclerosing cholangitis, which at this point is not yet fully developed [20]. Wild-type controls and *Abcb4*$^{-/-}$ mice of both sexes were divided into three groups, with each receiving a different diet: The control group was fed regular diet, containing 600 IU vitamin D (cholecalciferol)/kg food, which is based on the established nutrient requirements for laboratory mice [21]. The low vitamin D group obtained a diet with 100 IU vitamin D/kg, and the high vitamin D diet group was fed a diet enriched with 2,400 IU vitamin D/kg. All diets were given for 12 weeks. With the exception of vitamin D content, all three diets were otherwise equal in nutrient composition and total energy, and were obtained from Altromin (Lage, Germany; see Supplementary Table 1 - 3 for detailed dietary composition). In total, 113 animals were analyzed, with a minimum of 15 mice per genotype and diet group. Table 1 provides the numbers of animals analyzed per genotype, sex and diet group. Food intake was controlled by monitoring weekly food consumption per cage and did not differ (3 - 4 g/day) between the groups. Survival rates were 100%.

Table 1: Number of animals analyzed per genotype, sex and diet group

	FVB-*Abcb4*$^{-/-}$		**FVB/NJ wild-type**	
Diet	Female	Male	Female	Male
Low vitamin D diet (100 IU/kg food)	11	9	6	9
Control vitamin D diet (600 IU/kg food)	10	7	10	9
High vitamin D diet (2,400 IU/kg food)	12	11	9	11

Phenotypic characterization of biliary fibrosis

For histopathological evaluation, liver samples were preserved in 4% neutral-buffered formaldehyde solution at 4°C and embedded in paraffin. Paraffin sections (2 μm) were stained with hematoxylin-eosin (H&E), or Sirius red for the detection of collagen. The stages of liver fibrosis and relative collagen areas were assessed by a pathologist blinded to the study protocol, using a semiautomatic system for image analysis (Stingray F146C IRF Medical camera, ½" type progressive scan CCD, Germany) and HistoQuant image morphometry software (3DHistech, Budapest, Hungary). Hepatic fibrosis was staged (F-score) using a scale adapted from the Batts and Ludwig, and Ishak scoring systems [22, 23]. The F-scores are subdivided into five classes: 0 = no fibrosis; 1 = scatter periportal and perineoductular fibrosis; 2 = periportal, perineoductular fibrosis; 3 = periportal, perineoductular fibrosis with portal-portal septa; and 4 = complete cirrhosis.

Relative collagen content was determined as the mean percentage of the collagen stained area to the whole area (field of view). Therefore, we screened representative microscopic fields (magnification 100×), which were randomly chosen from each liver section (avoiding arteries of a diameter > 100 micrometers) after setting a threshold capturing Sirius red stained areas of collagen. In addition, collagen in liver was quantified by colorimetric measurement of the collagen-specific amino acid hydroxyproline, as described previously [24, 25].

Serum biochemical assays

Blood was collected from the inferior vena cava after harvesting. Samples were left for 10 minutes at room temperature in darkness and centrifuged for 20 minutes at 2000× *g*. Serum was stored at -80°C until analysis. Serum calcium concentrations, alanine aminotransferase (ALT), aspartate aminotransferase (AST) and alkaline phosphatase (AP) activities were measured in Cobas® 8000 analyzer (Roche Diagnostics, Mannheim, Germany) by standardized methods

following the recommendations of the International Federation of Clinical Chemistry. Serum 25-hydroxyvitamin D concentrations were determined using the chemiluminescence immunoassay LIAISON® 25 OH Vitamin D TOTAL Assay (DiaSorin, Minnesota, USA).

Gene expression analyses by quantitative real-time PCR

Hepatic mRNA expression levels of individual genes were determined by quantitative real-time PCR (qPCR) (*TaqMan*, Applied Biosystems), using 1 µg RNA for reverse transcription and 18S RNA as endogenous control, with one cycle at 95°C for 10 minutes, followed by 45 cycles at 95°C/30 s and 60°C/60 s. The sex-specific expression levels were calculated by the ΔΔct-method [26] in relation to counterpart wild-type controls (e.g. $\Delta\Delta ct_{Col1\alpha2}$ = $\Delta ct_{Col1\alpha2}$ *Abcb4*$^{-/-}$ female on low vitamin D diet - mean $\Delta ct_{Col1\alpha2}$ wild-type female on low vitamin D diet). The relative quotient (RQ, $2^{-\Delta\Delta ct}$) for each sample was normalized to sex-specific wild-type mice fed the control diet. The *TaqMan* (Applied Biosystems) expression assay IDs were: *Col1α2*, Mm01165187_m1; *Cramp*, Mm00438285_m1; *Cyp2r1*, Mm01159413_m1; *Cyp7a1*, Mm00484150_m1; *Cyp8b1*, Mm00501637_s1; *Cyp27a1*, Mm00470430_m1; *Tgf-β1*, Mm03024053_m1; *Timp1*, Mm00441818_m1; and *Vdr*, Mm00437297_m1.

Immunofluorescence microscopy for cytokeratin 19 and E-cadherin

Double immunofluorescence staining for cytokeratin 19 (CK19) and E-cadherin was performed on acetone-fixed (-20°C, 10 minutes) cryosection of liver tissue (4 - 6 animals per genotype and diet group) CK19 was detected using a monoclonal rabbit anti-Troma-III antibody (1:500) [27]. In addition, slides were incubated with a monoclonal rabbit antibody anti-E-cadherin (1:200; #3195, Cell Signaling Technology, Massachusetts, USA). Secondary antibodies were conjugated to fluor 488-goat anti-rabbit (1:100) or tetramethylrhodamine isothiocyanate 565-anti-rabbit antibody (1:50) [19].

Statistics

The results were analyzed using SPSS 20.0 (IBM, Ehningen, Germany). Quantitative data are presented as means ± standard errors (SE) or median and ranges, as appropriate. All data were analyzed for the effects of diet and genotype. Means were compared with Student t-tests or one-way analyses of variance (ANOVA), followed by *post hoc* Bonferroni correction. The medians of non-parametric data were compared with Mann-Whitney U or Kruskal-Wallis tests, respectively. Two-way ANOVA was applied to assess the interaction of diet and sex after exclusion of extreme values. Correlation coefficients were calculated according to Pearson or Spearman as appropriate. P values < 0.05 were considered significant.

RESULTS

Vitamin D supplementation exerts no toxic effects in *Abcb4*$^{-/-}$ mice

After weaning all mice continued to develop normally and displayed no obvious signs of developmental or behavioral abnormalities. Body weight and liver-to-body weight ratios were not affected by dietary composition, with the exception of female *Abcb4*$^{-/-}$ mice on the high vitamin D diet displaying increased body weight compared to knockout mice on the control diet (24.6 ± 0.9 g *vs*. 20.2 ± 0.9 g, $p < 0.01$). Serum calcium levels were slightly higher in *Abcb4*$^{-/-}$ mice as compared to wild-type controls in all dietary groups, and no hypercalcemia was induced (Supplementary figure 2).

Vitamin D serum concentrations depend on genotype, sex and diet

As shown in Figure 2A, mice displayed different serum vitamin D concentrations depending on genotype and diet group. On the low vitamin D diet, both strains displayed serum vitamin D levels < 10 ng/ml. *Abcb4*$^{-/-}$ mice on the control diet showed significantly ($p < 0.01$) lower vitamin D concentrations compared to FVB/NJ wild-type mice on this diet (38.4 ± 1.9 *vs.* 46.8 ± 1.7 ng/ml). In contrast, *Abcb4*$^{-/-}$ mice on the high vitamin D diet demonstrated significantly ($p < 0.001$) increased vitamin D levels in comparison to wild-type counterparts (67.2 ± 2.4 *vs.* 42.0 ± 2.3 ng/ml). The vitamin D concentrations in female mice were significantly ($p < 0.001$) higher than in male mice in the high vitamin D group and a significant ($p < 0.01$, two-way ANOVA) interaction between sex and diet was observed for vitamin D levels but not for other phenotypes.

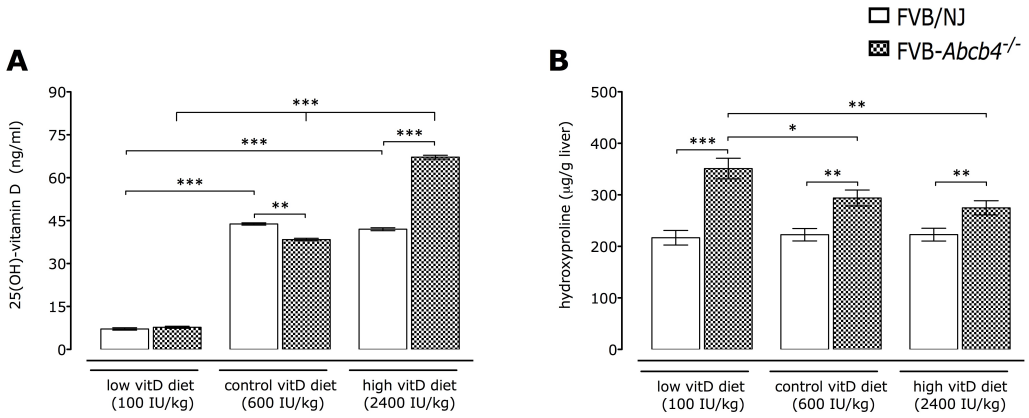

Figure 2: Mean serum 25-hydroxyvitamin D concentrations (**A**) and mean hepatic collagen contents (± SE) as determined via the collagen-specific amino acid hydroxyproline (**B**) in *Abcb4*$^{-/-}$ and wild-type mice fed different vitamin D diets for 12 weeks.
* $p < 0.05$, ** $p < 0.01$, *** $p < 0.001$.

Vitamin D supplementation influences hepatic fibrosis in *Abcb4*$^{-/-}$ mice

Figure 2B illustrates that the quantification of hepatic collagen contents revealed a significant ($p < 0.001$) increase in *Abcb4*$^{-/-}$ mice in all three diet groups as compared to controls. Hepatic collagen contents were highest in *Abcb4*$^{-/-}$ mice receiving the vitamin D-deficient diet, and displayed a dose-related trend towards lower levels in knockout mice on the regular and the high vitamin D diets. In contrast, no impact of diet on hepatic collagen levels was detected in wild-type mice.

Histopathological staging of liver fibrosis revealed no fibrosis (F0) in wild-type mice. Contrary, *Abcb4*$^{-/-}$ mice progressed to fibrosis stage F3. *Abcb4*$^{-/-}$ animals on the low vitamin D diet demonstrated significantly ($p < 0.001$) higher fibrosis scores (median F3, range F2 - F3) compared with knockout mice fed the control or the high vitamin D diets (high vitamin D diet: median F2, range F1 - F3; control diet: median F2, range F0 - F3).

Figure 3A shows that these histopathological observations were reflected by the relative collagen areas, as determined after Sirius red staining. Representative liver sections stained with Sirius red are shown in Figure 3B. As expected, we

observed genotype-dependent differences, with increased collagen areas in *Abcb4*$^{-/-}$ mice as compared to wild-type mice. Collagen areas were significantly ($p < 0.01$) larger in *Abcb4*$^{-/-}$ mice receiving the low vitamin D diet in comparison to those on the control diet (2.47%, range 0.93 - 4.57 *vs.* 2.08%, range 0.05 - 2.62). The lowest collagen areas in *Abcb4*$^{-/-}$ mice were determined in animals fed the high vitamin D diet (2.03%, range 0.69 - 4.31). Interestingly, wild-type mice on the high vitamin D diet also showed significantly ($p < 0.01$) reduced collagen areas (0.18%, range 0.09 - 0.35) in comparison to mice on diets with lower vitamin D concentrations (control diet: 0.38%, range 0.10 - 1.27; low vitamin D diet: 0.31%, range 0.10 - 1.08).

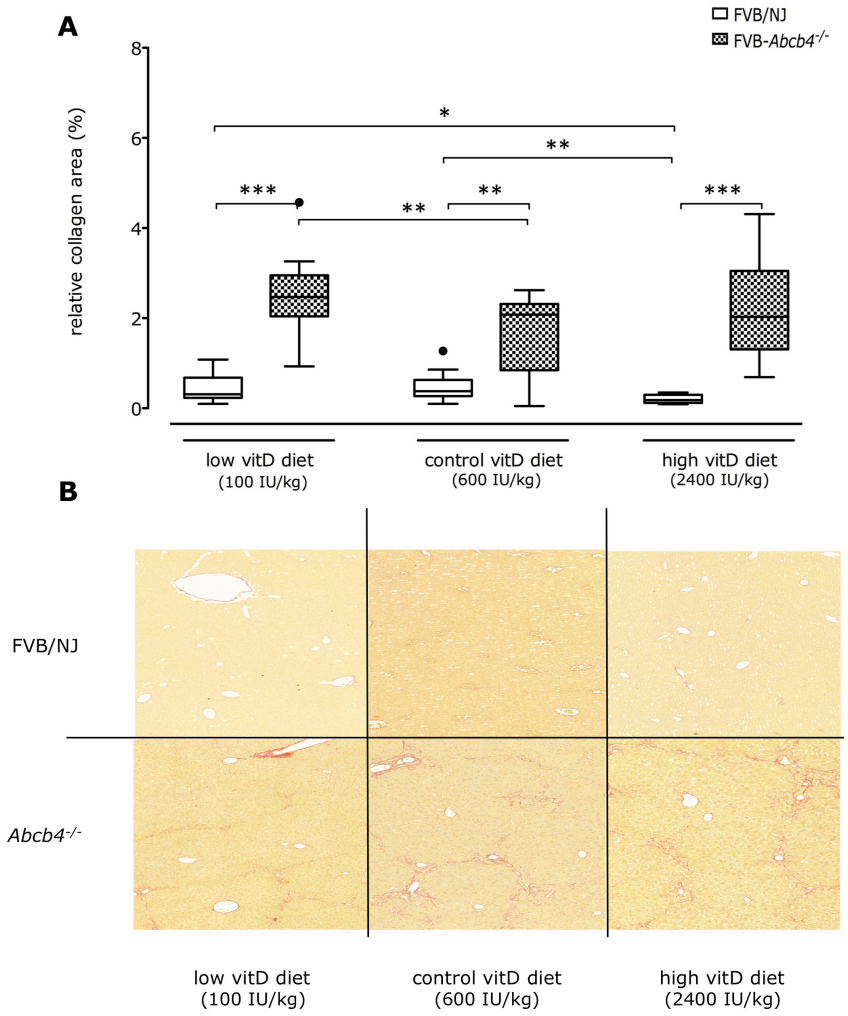

Figure 3: Median relative collagen contents (with 1.5 interquartile ranges) as determined after Sirius red staining (**A**), and representative liver sections (Sirius red stained) (**B**) from *Abcb4*$^{-/-}$ and wild-type mice fed different vitamin D diets for 12 weeks.
* $p < 0.05$, ** $p < 0.01$, *** $p < 0.001$.

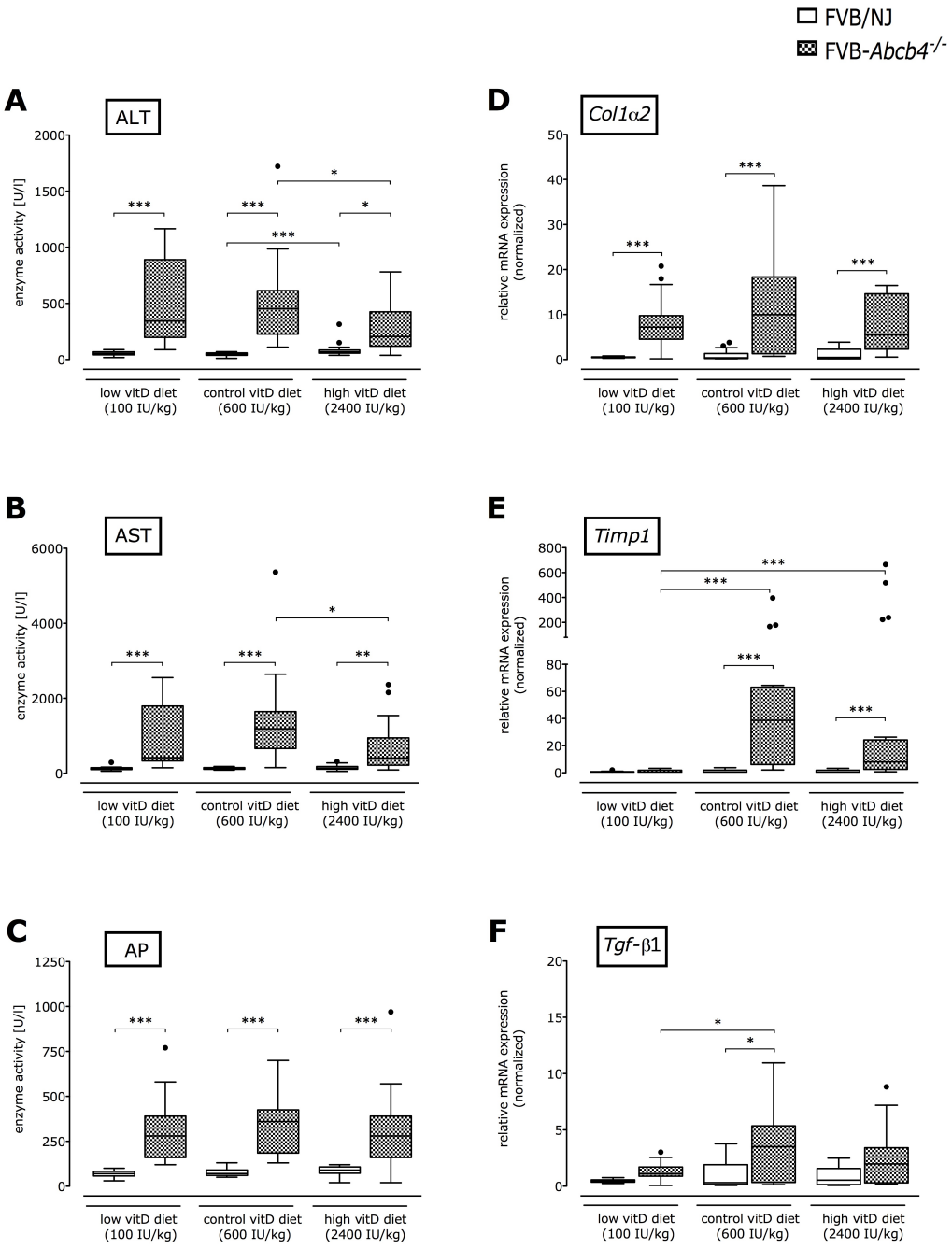

Figure 4: Serum liver enzyme activities. Alanine aminotransferase (ALT) (**A**), aspartate aminotransferase (AST) (**B**) and alkaline phosphatase (AP) (**C**) activities in *Abcb4*$^{-/-}$ and wild-type mice fed different vitamin D diets.
Relative hepatic mRNA expression levels of profibrogenic genes. Collagen type I, *a*2-chain (*Col1a2*) (**D**), tissue inhibitor of matrix metalloproteinase 1 (*Timp1*) (**E**) and transforming growth factor-β1 (*Tgf- β1*) (**F**) in *Abcb4*$^{-/-}$ and wild-type mice fed different vitamin D diets for 12 weeks. Data are normalized based on the expression of wild-type mice fed the vitamin D control diet (600 IU/kg food). Box-plots with whiskers 1.5 interquartile ranges.
* $p < 0.05$, ** $p < 0.01$, *** $p < 0.001$

Serum parameters for liver damage and cholestasis (ALT, AST, AP) were significantly elevated in *Abcb4*$^{-/-}$ compared to corresponding wild-type mice in all diet groups (Figure 4, A - C). Notably, enzymatic activities of both ALT and AST in *Abcb4*$^{-/-}$ mice significantly decreased on the high vitamin D diet as compared to knockout mice fed the control diet. Wild-type mice receiving the high vitamin D diet displayed elevated ALT activities in comparison to those on the control diet (68 U/l, range 37 - 314 *vs*. 48 U/l, range 11 - 77; $p < 0.01$). AP activities did not differ between diet groups in either knockout or wild-type mice (Figure 4C).

Dietary vitamin D affects hepatic expression of profibrogenic genes in *Abcb4*$^{-/-}$ *mice*

Panel D of Figure 4 illustrates that hepatic steady-state mRNA expression levels of collagen type I (*Col1α2*) were significantly ($p < 0.001$) higher in ABCB4 deficient mice as compared to wild-type controls, irrespective of the diet. *Timp1* expression increased significantly ($p < 0.001$) in *Abcb4*$^{-/-}$ mice fed the control or the high vitamin D diets, but not in animals fed the low vitamin D diet, as compared to corresponding wild-type mice (Figure 4E). Figure 4F shows that a similar trend was observed for transforming growth factor (*Tgf*)-*β1* expression, with significantly ($p < 0.05$) reduced levels in *Abcb4*$^{-/-}$ mice on the low vitamin D diet as compared to the control diet. *Tgf-β1* expression correlated significantly ($\rho = 0.92$, $p < 0.01$) with expression of *Vdr* in *Abcb4*$^{-/-}$ mice.

Diet and genotype modify the hepatic expression of *Vdr* and vitamin D hydroxylases

The hepatic gene expression of *Vdr* was increased in ABCB4 deficient mice compared with the corresponding wild-type controls in all diet groups. Similar to *Tgf-β1* and *Timp1* expression, vitamin D deficient *Abcb4*$^{-/-}$ mice displayed lower expression levels of *Vdr* as compared to *Abcb4*$^{-/-}$ mice on the control diet (Figure 5A). Panel B of Figure 5 illustrates that gene expression of the hepatic antimicrobial peptide cathelicidin (*Cramp*) was increased in *Abcb4*$^{-/-}$ animals on

control and low vitamin D diets, whereas knockout mice fed the high vitamin D diet did not differ from wild-type animals. The highest *Cramp* expression levels were observed in vitamin D deficient *Abcb4*$^{-/-}$ mice.

As circulating vitamin D levels depend on *Abcb4* genotype and diet (Figure 2A), we assessed expression differences of the major vitamin D hydroxylase *Cyp2r1* and *Cyp27a1* in liver. The mRNA levels of both enzymes were markedly increased in*Abcb4*$^{-/-}$ mice challenged with low and high vitamin D diets (data not shown). The expression of the genes *Cyp7a1* and *Cyp8b1*, encoding the rate-limiting enzymes for bile acid synthesis and conversion to cholic acid, respectively, tended to decrease in *Abcb4*$^{-/-}$ mice on diets with higher vitamin D contents, but no significant differences were observed (data not shown).

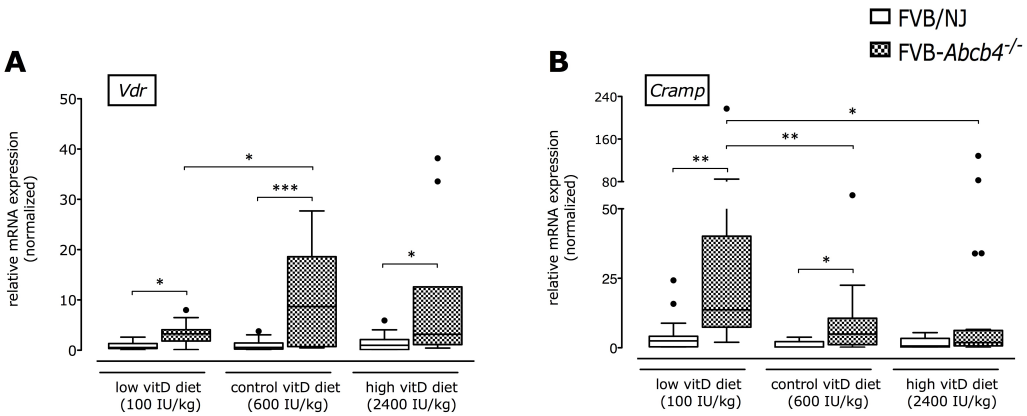

Figure 5: Relative hepatic mRNA expression levels of the vitamin D receptor (*Vdr*) (**A**) and cathelicidin (*Cramp*) (**B**) genes in *Abcb4*$^{-/-}$ and wild-type mice fed different vitamin D diets for 12 weeks. Data are normalized based on the expression of wild-type mice fed the vitamin D control diet (600 IU/kg food). Box-plots with whiskers 1.5 interquartile ranges.
* $p < 0.05$, ** $p < 0.01$, *** $p < 0.001$.

Vitamin D supplementation does not appear to influence hepatic adherens junction integrity

As determined by double immunofluorescence microscopy (Figure 6), genotype-specific changes could be observed. *Abcb4*$^{-/-}$ animals from all vitamin D diet

groups displayed an increase in ductular proliferation, as shown by increased number of K19-positive cholangiocytes and overexpression of E-cadherin. At the hepatocyte level, a diffuse E-cadherin expression within the liver lobe was detected in *Abcb4*$^{-/-}$ mice (Figure 6, D - F), which contrasted with the findings in wild-type controls. However, an influence of dietary vitamin D intake on changes in the E-cadherin distribution pattern on hepatocyte or even on the bile duct level was not apparent in either strain.

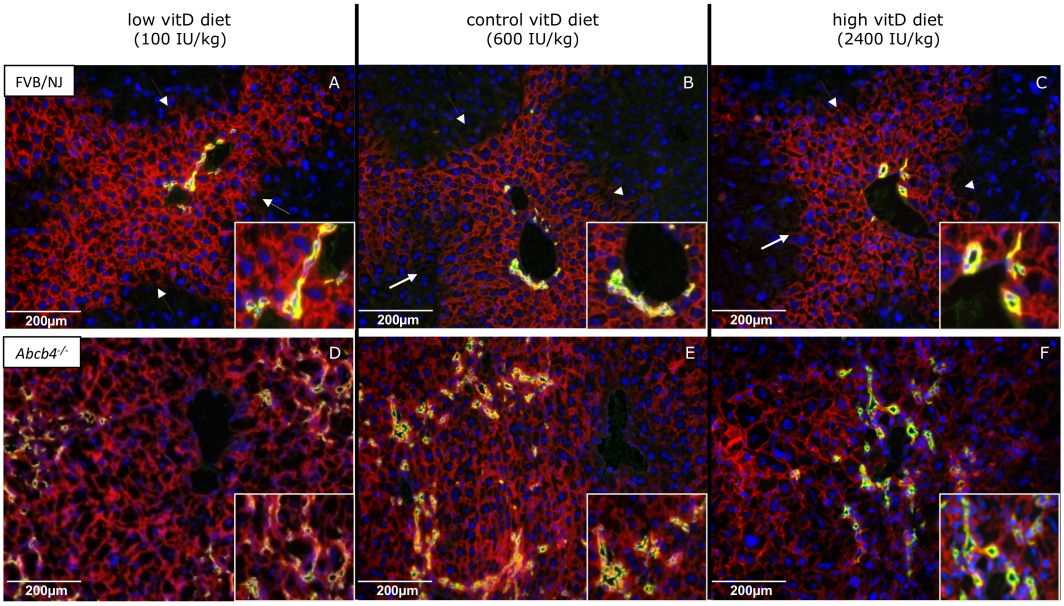

Figure 6: Double immunofluorescence staining for K19 (in green) and E-cadherin (in red) of livers from *Abcb4*$^{-/-}$ and wild-type mice fed different vitamin D diets for 12 weeks. At the hepatocyte level, predominant E-cadherin expression occurs in zone I of the liver lobe in wild-type animals (indicated by white arrows, panels **A** - **C**), whereas diffuse E-cadherin expression is present in *Abcb4*$^{-/-}$ mice (panels **D** - **F**).
Abbreviations: bd, bile duct; pv, portal vein.

DISCUSSION

In this study we examined the modulatory effects of dietary vitamin D supplementation on biliary fibrosis *in vivo* in *Abcb4*$^{-/-}$ mice. The following major results were demonstrated: (i) vitamin D deficiency is associated with increased collagen accumulation and fibrogenesis in this preclinical model; (ii) a vitamin D sufficient diet ameliorates chronic liver injury; and (iii) high dose vitamin D supplementation exerts only a further benefit by reduction of aminotransferase activities. Taken together these findings suggest that low vitamin D levels aggravate liver fibrosis but supranormal vitamin D levels have no additive anti-inflammatory or -fibrotic effects in *Abcb4*$^{-/-}$ mice. This may indicate that vitamin D deficiency should be avoided to decrease the risk of progressive fibrosis in chronic cholangitis and that an adequate vitamin D intake has, at least to some extent, anti-inflammatory and -fibrotic effects. These observations are relevant for future translational studies, because chronic cholestatic liver injury in humans is frequently accompanied by vitamin D deficiency [7, 28]. More specifically, *Abcb4*$^{-/-}$ mice receiving the low vitamin D diet developed more advanced stages of fibrosis as compared to mice consuming diets with higher vitamin D contents. Of note, maximum vitamin D supplementation did not further improve the fibrosis scores in our model, but in comparison to the control group it ameliorated hepatocellular damage, as illustrated by lower serum aminotransferase activities. These observations are also reflected by enhanced hepatic collagen accumulation in *Abcb4*$^{-/-}$ mice with vitamin D deficiency, whereas the lowest collagen contents were observed in mice receiving the high vitamin D diet. The mRNA expression analyses did not identify differences in collagen expression, pointing to vitamin D-dependent post-transcriptional regulatory mechanisms. On the other hand, *in vitro* studies and a rat model of toxin-induced hepatic fibrosis have demonstrated possible anti-fibrotic effects of vitamin D supplementation through diminished hepatic stellate cell (myofibroblast) activation and collagen expression [29-31]. These different observations might be due to the diverse experimental set-ups, in particular homogenous cell cultures *versus* heterogeneous cell populations from

total liver, given that in cholestatic disorders portal fibroblasts are predominantly responsible for hepatic collagen deposition [32].

Despite identical dietary intake, *Abcb4*$^{-/-}$ mice demonstrated lower vitamin D serum concentrations on control chow diet as compared to wild-type mice. Serum vitamin D levels increased markedly in *Abcb4*$^{-/-}$ mice receiving the high vitamin D diet, whereas it remained constant in wild-type mice. These findings allude to a potential dysregulation of intestinal vitamin D uptake. Additionally, we observed higher expression of the vitamin D activating enzymes *Cyp2r1* and *Cyp27a1* in livers of ABCB4 deficient mice on the high vitamin D diet. Vitamin D levels are regulated through degradation via 24-hydroxylase, and vitamin D induces the expression of this enzyme, thus controlling its own catabolism [33, 34]. Of note, bile acids such as lithocholic acid have been shown to decrease this stimulatory effect of vitamin D and influence a broad spectrum of signaling pathways via the nuclear receptors VDR, FXR, and PXR [35-38]. In fact minor changes in bile salt composition have been shown to affect hepatic fibrogenesis in ABCB4 deficient mice [39], although the expression of the genes encoding the rate-limiting enzymes for bile salt synthesis (*Cyp7a1*) and conversion to the hydrophobic cholic acid (*Cyp8b1*) showed no major differences across the groups. Further studies however, would be required to elucidate the molecular mechanisms underlying the genotype-diet interactions.

The expression levels of the fibrosis markers *Col1α2*, *Timp1* and *Tgf-β1* did not strictly correlate with the severity of liver injury and fibrosis. Some of these discrepancies could be related to the fact that we measured mRNA levels in total liver, although vitamin D might exert specific effects on different hepatic cell populations. Altered vitamin D-VDR signaling, which has been reported in cholestatic conditions, was corroborated in this study, as illustrated by increased *Vdr* expression in ABCB4 deficient as compared to wild-type mice. Furthermore, *Vdr* expression was reduced in *Abcb4*$^{-/-}$ mice on the low vitamin D diet, and these animals displayed the highest fibrosis scores. Recently elegant mechanistic studies have demonstrated that the activation of VDR antagonizes TGF-β-induced recruitment of SMAD3 via co-occupation of regulatory sites in key profibrogenic

genes (including *COL1A2*, *TIMP1*, and *TGFB1*) in the presence of TGF-β [31]. In this context it is interesting to note that in comparison to *Abcb4*$^{-/-}$ mice on control diet, our data show lower *Tgf-β1* expression levels both in vitamin D deficiency and upon excess dietary supplementation, illustrating the interaction of vitamin D and TGF-β signaling in the setting of biliary inflammation and fibrosis.

Given the potential anti-inflammatory effects of vitamin D, we also assessed the hepatic expression of the antimicrobial peptide cathelicidin (*Cramp*) [40]. Since the vitamin D response element is absent in the murine *Cramp* promoter (in contrast to humans) [41], we conclude that the decrease of *Cramp* expression upon vitamin D supplementation to levels observed in healthy controls is more likely to reflect the amelioration of hepatic inflammation than direct effects on *Cramp*. Further investigations into the regulation of antimicrobial peptides in sclerosing cholangitis would be interesting but were beyond the scope of this study.

To protect parenchymal liver cells from toxic bile compounds, epithelial cells form a physical barrier by apical junctional complexes (tight junction and adherens junction). Distinct functional and morphological alterations of these junctional complexes have been described in cholestasis in both mice and humans [19, 42]. Since vitamin D has been shown to be involved in the regulation of apical junctional complexes in other organs [43-45], Firrincieli *et al*. [46] have recently investigated the role of VDR in the maintenance of bile duct integrity in mice with biliary-type injury. Their study demonstrated altered E-cadherin staining and loss of cell adhesion in biliary epithelial cells in *Vdr*$^{-/-}$ mice subjected to bile duct ligation [46]. Therefore we also assessed hepatic adherens integrity in our model, which revealed genotype-specific differences in biliary epithelial cell proliferation and E-cadherin staining. However, vitamin D-dependent effects could not be substantiated. Nevertheless, this does not exclude the possibility that truncated E-cadherin might be relevant, which was shown to be present in higher amounts in *Vdr*$^{-/-}$ mice [46].

In conclusion, our findings indicate that vitamin D modulates biliary injury and fibrogenesis *in vivo* and that the severity of biliary fibrosis in *Abcb4*$^{-/-}$ mice is

influenced by vitamin D status. In this model, vitamin D deficiency appears to aggravate liver fibrosis however, the beneficial effects of vitamin D supplementation are limited. We speculate that excess vitamin D supplementation does not fully protect from liver fibrosis but an adequate vitamin D intake abates hepatic injury and confers anti-fibrotic effects in patients with cholestatic liver diseases.

Supplementary data to this study can be found online at:
http://link.springer.com/article/10.1007/s12072-014-9548-2/fulltext.html.

REFERENCES

1. Zittermann A. The estimated benefits of vitamin D for Germany. Mol Nutr Food Res. 2010;54:1164-1171.
2. Grünhage F, Hochrath K, Krawczyk M, Höblinger A, Obermayer-Pietsch B, Geisel J, Trauner M, Sauerbruch T, Lammert F. Common genetic variation in vitamin D metabolism is associated with liver stiffness. Hepatology. 2012;56:1883-1891.
3. Petta S, Camma C, Scazzone C, Tripodo C, Di Marco V, Bono A, Cabibi D, Licata G, Porcasi R, Marchesini G, Craxi A. Low vitamin D serum level is related to severe fibrosis and low responsiveness to interferon-based therapy in genotype 1 chronic hepatitis C. Hepatology 2010;51:1158-1167.
4. Trepo E, Ouziel R, Pradat P, Momozawa Y, Quertinmont E, Gervy C, et al. Marked 25-hydroxyvitamin D deficiency is associated with poor prognosis in patients with alcoholic liver disease. J Hepatol. 2013;59: 344-50..
5. Putz-Bankuti C, Pilz S, Stojakovic T, Scharnagl H, Pieber TR, Trauner M, Obermayer-Pietsch B, Stauber RE. Association of 25-hydroxyvitamin D levels with liver dysfunction and mortality in chronic liver disease. Liver Int. 2012;32:845-851.
6. Stokes CS, Volmer DA, Grünhage F, Lammert F. Vitamin D in chronic liver disease. Liver Int. 2013;33:338-352.
7. Arteh J, Narra S, Nair S. Prevalence of vitamin D deficiency in chronic liver disease. Dig Dis Sci. 2010;55:2624-2628.
8. Fisher L, Fisher A. Vitamin D and parathyroid hormone in outpatients with noncholestatic chronic liver disease. Clin Gastroenterol Hepatol. 2007;5:513-520.
9. Song BJ, Rockey DC. Status of research on vitamin D supplementation in treating or preventing liver fibrosis. Liver Int. 2013;33:653-655.
10. Wang Y, Zhu J, DeLuca HF. Where is the vitamin D receptor? Arch Biochem Biophys. 2012;523:123-133.
11. Gascon-Barré M, Demers C, Mirshahi A, Neron S, Zalzal S, Nanci A. The normal liver harbors the vitamin D nuclear receptor in nonparenchymal and biliary epithelial cells. Hepatology. 2003;37:1034-1042.
12. Makishima M, Lu TT, Xie W, Whitfield GK, Domoto H, Evans RM, Haussler MR, Mangelsdorf DJ. Vitamin D receptor as an intestinal bile acid sensor. Science. 2002;296:1313-1316.
13. Jiang W, Miyamoto T, Kakizawa T, Nishio SI, Oiwa A, Takeda T, Suzuki S, Hashizume K. Inhibition of LXRalpha signaling by vitamin D receptor: possible role of VDR in bile acid synthesis. Biochem Biophys Res Commun. 2006;351:176-184.
14. Schmidt DR, Holmstrom SR, Fon Tacer K, Bookout AL, Kliewer SA, Mangelsdorf DJ. Regulation of bile acid synthesis by fat-soluble vitamins A and D. J Biol Chem. 2010;285:14486-14494.
15. Han S, Li T, Ellis E, Strom S, Chiang JY. A novel bile acid-activated vitamin D receptor signaling in human hepatocytes. Mol Endocrinol. 2010;24:1151-1164.
16. Lammert F, Wang DQ, Hillebrandt S, Geier A, Fickert P, Trauner M, Matern S, Matern S, Paigen B, Carey MC. Spontaneous cholecysto- and hepatolithiasis in *Mdr2*$^{-/-}$ mice: a model for low phospholipid-associated cholelithiasis. Hepatology. 2004;39:117-128.
17. Fickert P, Wagner M, Marschall HU, Fuchsbichler A, Zollner G, Tsybrovskyy O, Zatloukal K, Liu J, Waalkes MP, Cover C, Denk H, Hofmann AF, Jaeschke H, Trauner M. 24-norUrsodeoxycholic acid is superior to ursodeoxycholic acid in the treatment of sclerosing cholangitis in *Mdr2* (*Abcb4*) knockout mice. Gastroenterology. 2006;130:465-481.
18. Moustafa T, Fickert P, Magnes C, Guelly C, Thueringer A, Frank S, Kratky D, Sattler W, Reicher H, Sinner F, Gumhold J, Silbert D, Fauler G, Hofler G, Lass A, Zechner R, Trauner M. Alterations in lipid metabolism mediate inflammation, fibrosis, and proliferation in a mouse model of chronic cholestatic liver injury. Gastroenterology. 2012;142:140-151 e112.

19. Fickert P, Fuchsbichler A, Wagner M, Zollner G, Kaser A, Tilg H, Krause R, Lammert F, Langner C, Zatloukal K, Marschall HU, Denk H, Trauner M. Regurgitation of bile acids from leaky bile ducts causes sclerosing cholangitis in *Mdr2* (*Abcb4*) knockout mice. Gastroenterology. 2004;127:261-274.
20. Mauad TH, van Nieuwkerk CM, Dingemans KP, Smit JJ, Schinkel AH, Notenboom RG, van den Bergh Weerman MA, Verkruisen RP, Groen AK, Oude Elferink RP, van der Valk MA, Borst P, Offerhaus GJA. Mice with homozygous disruption of the mdr2 P-glycoprotein gene. A novel animal model for studies of nonsuppurative inflammatory cholangitis and hepatocarcinogenesis. Am J Pathol. 1994;145:1237-1245.
21. National Research Council. Nutrient Requirements of Laboratory Animals, Fourth Revised Edition. Washington, DC: The National Academies Press. 1995;80-102.
22. Batts KP, Ludwig J. Chronic hepatitis. An update on terminology and reporting. Am J Surg Pathol. 1995;19:1409-1417.
23. Ishak K, Baptista A, Bianchi L, Callea F, De Groote J, Gudat F, Denk H, Desmet V, Korb G, MacSween RN, Phillips MJ, Portmann BG, Poulsen H, Scheuer PJ, Schmid M, Thaler H. Histological grading and staging of chronic hepatitis. J Hepatol. 1995;22:696-699.
24. Jamall IS, Finelli VN, Que Hee SS. A simple method to determine nanogram levels of 4-hydroxyproline in biological tissues. Anal Biochem. 1981;112:70-75.
25. Hillebrandt S, Goos C, Matern S, Lammert F. Genome-wide analysis of hepatic fibrosis in inbred mice identifies the susceptibility locus *Hfib1* on chromosome 15. Gastroenterology. 2002;123:2041-2051.
26. Livak KJ, Schmittgen TD. Analysis of relative gene expression data using real-time quantitative PCR and the $2^{-\Delta\Delta C}{}_T$ method. Methods. 2001;25:402-408.
27. Fickert P, Fuchsbichler A, Marschall HU, Wagner M, Zollner G, Krause R, Zatloukal K, Jaeschke H, Denk H, Trauner M. Lithocholic acid feeding induces segmental bile duct obstruction and destructive cholangitis in mice. Am J Pathol. 2006;168:410-422.
28. Dibble JB, Sheridan P, Hampshire R, Hardy GJ, Losowsky MS. Osteomalacia, vitamin D deficiency and cholestasis in chronic liver disease. Q J Med. 1982;51:89-103.
29. Abramovitch S, Dahan-Bachar L, Sharvit E, Weisman Y, Ben Tov A, Brazowski E, Reif S. Vitamin D inhibits proliferation and profibrotic marker expression in hepatic stellate cells and decreases thioacetamide-induced liver fibrosis in rats. Gut. 2011;60:1728-1737.
30. Potter JJ, Liu X, Koteish A, Mezey E. 1,25-dihydroxyvitamin D3 and its nuclear receptor repress human α1 (I) collagen expression and type I collagen formation. Liver Int. 2013;33:677-686.
31. Ding N, Yu RT, Subramaniam N, Sherman MH, Wilson C, Rao R, Leblanc M, Coulter S, He M, Scott C, Lau SL, Atkins AR, Barish GD, Gunton JE, Liddle C, Downes M, Evans RM. A vitamin D receptor/SMAD genomic circuit gates hepatic fibrotic response. Cell. 2013;153:601-613.
32. Bataller R, Brenner DA. Liver fibrosis. J Clin Invest. 2005;115:209-218.
33. Ohyama Y, Ozono K, Uchida M, Shinki T, Kato S, Suda T, Yamamoto O, Noshiro M, Kato Y. Identification of a vitamin D-responsive element in the 5'-flanking region of the rat 25-hydroxyvitamin D3 24-hydroxylase gene. J Biol Chem. 1994;269:10545-10550.
34. Dhawan P, Peng X, Sutton AL, MacDonald PN, Croniger CM, Trautwein C, Centrella M, McCarthy TL, Christakos S. Functional cooperation between CCAAT/enhancer-binding proteins and the vitamin D receptor in regulation of 25-hydroxyvitamin D3 24-hydroxylase. Mol Cell Biol. 2005;25:472-487.
35. Ruiz-Gaspà S, Guañabens N, Enjuanes A, Peris P, Martinez-Ferrer A, de Osaba MJ, Gonzalez B, Alvarez L, Monegal A, Combalia A, Parés A. Lithocholic acid downregulates vitamin D effects in human osteoblasts. Eur J Clin Invest 2010;40:25-34.
36. Hylemon PB, Zhou H, Pandak WM, Ren S, Gil G, Dent P. Bile acids as regulatory molecules. J Lipid Res. 2009;50:1509-1520.
37. Li T, Chiang JY. Nuclear receptors in bile acid metabolism. Drug Metab Rev. 2013;45:145-155.

38. Chow EC, Magomedova L, Quach HP, Patel R, Durk MR, Fan J, Maeng HJ, Irondi K, Anakk S, Moore DD, Cummins CL, Pang KS. Vitamin D receptor activation down-regulates the small heterodimer partner and increases CYP7A1 to lower cholesterol. Gastroenterology. 2014;146:1048-59.
39. Van Nieuwerk CM, Groen AK, Ottenhoff R, van Wijland M, van den Bergh Weerman MA, Tytgat GN, Offerhaus JJ, Oude Elferink RP. The role of bile salt composition in liver pathology of *mdr2* (-/-) mice: differences between males and females. J Hepatol. 1997;26:138-145.
40. D'Aldebert E, Biyeyeme Bi Mve MJ, Mergey M, Wendum D, Firrincieli D, Coilly A, Fouassier L, Corpechot C, Poupon R, Housset C, Chignard N. Bile salts control the antimicrobial peptide cathelicidin through nuclear receptors in the human biliary epithelium. Gastroenterology. 2009;136:1435-43.
41. Gombart AF, Borregaard N, Koeffler HP. Human cathelicidin antimicrobial peptide (CAMP) gene is a direct target of the vitamin D receptor and is strongly up-regulated in myeloid cells by 1,25-dihydroxyvitamin D_3. FASEB J. 2005;19:1067-77.
42. Sakisaka S, Kawaguchi T, Taniguchi E, Hanada S, Sasatomi K, Koga H, Harada M, Kimura R, Sata M, Sawada N, Mori M, Todo S, Kurohiji T. Alterations in tight junctions differ between primary biliary cirrhosis and primary sclerosing cholangitis. Hepatology. 2001;33:1460-1468.
43. Pálmer HG, González-Sancho JM, Espada J, Berciano MT, Puig I, Baulida J, Quintanilla M, Cano A, de Herreros AG, Lafarga M, Munoz A. Vitamin D_3 promotes the differentiation of colon carcinoma cells by the induction of E-cadherin and the inhibition of β-catenin signaling. J Cell Biol. 2001;154:369-387.
44. Gniadecki R, Gajkowska B, Hansen M. 1,25-dihydroxyvitamin D_3 stimulates the assembly of adherens junctions in keratinocytes: involvement of protein kinase C. Endocrinology 1997;138:2241-2248.
45. Kong J, Zhang Z, Musch MW, Ning G, Sun J, Hart J, Bissonnette M, Li YC. Novel role of the vitamin D receptor in maintaining the integrity of the intestinal mucosal barrier. Am J Physiol Gastrointest Liver Physiol. 2008;294:G208-216.
46. Firrincieli D, Zúñiga S, Rey C, Wendum D, Lasnier E, Rainteau D, Braescu T, Falguières T, Boissan M, Cadoret A, Housset C, Chignard N. Vitamin D nuclear receptor deficiency promotes cholestatic liver injury by disruption of biliary epithelial cell junctions in mice. Hepatology. 2013;58:1401-1412.

KAPITEL 5:

DISKUSSION

DISKUSSION

Als Hauptstoffwechselorgan können Fehlfunktionen der Leber, unabhängig von ihrem Ursprung, den gesamten Organismus beeinträchtigen. Wechselwirkungen chronischer Lebererkrankungen mit dem extrahepatischen Organsystem sind bis heute jedoch nur unzureichend untersucht und verstanden. Im Rahmen dieser Arbeit wurden die systemischen Auswirkungen chronisch cholestatischer Lebererkrankungen in der *Abcb4*-Knockout-Maus, einem etablierten Modell der sklerosierenden Cholangitis und biliären Fibrose (Lammert *et al.* 2004, Fickert *et al.* 2004) analysiert, mit dem Ziel, pathobiologische Mechanismen cholestatischer Erkrankungen besser zu verstehen und potenzielle Determinanten der Fibrogenese zu identifizieren.

Die Ergebnisse der umfangreichen Phänotypisierung von *Abcb4*$^{-/-}$-Mäusen und die detaillierten Analysen verdeutlichen den Einfluss des Transporterdefekts auf multiple metabolische Prozesse. Dazu zählen Effekte auf die Glukose- und Lipidhomöostase sowie den Knochen- und Vitamin D-Stoffwechsel in *Abcb4*$^{-/-}$-Mäusen. Dass die beobachteten Auswirkungen des ABCB4-Defekts in der Maus auch auf den humanen Organismus übertragbar und von klinischer Relevanz sein können, konnte in Teilen bereits nachgewiesen werden. Es ist anzunehmen, dass auch eine Vielzahl weiterer beobachteter Wechselwirkungen auf Patienten mit *ABCB4*-Varianten und cholestatischen Lebererkrankungen transferiert werden kann.

Der Einfluss auf die Glukosehomöostase

Die Charakterisierung des Glukosestoffwechsels in *Abcb4*$^{-/-}$-Mäusen verdeutlicht, dass die *Abcb4*-Defizienz mit einer erhöhten Glukosetoleranz und Veränderungen in der Genexpression von Schlüsselenzymen des Glukosestoffwechsels einhergeht. Dass es sich um einen spezifischen *Abcb4*-Effekt handelt, der nicht unmittelbar mit dem cholestatischen Krankheitsbild zusammenhängt, zeigt die Analyse der humanen Kohorten. Hier wurde eine Assoziation des Glukosespiegels

mit der relativ häufig vorkommenden procholestatischen Genvariante *ABCB4* c.711A>T nachgewiesen. Trägerinnen dieser Variante besitzen ein erhöhtes Risiko, im Verlauf einer Schwangerschaft eine Cholestase zu entwickeln.

Da ABCB4 selektiv Phosphatidylcholin transloziert, ist es wahrscheinlich, dass die Ursache für die beobachteten Effekte auf die Glukosehomöostase im hepatischen PC-Metabolismus zu finden ist. Ein Bindeglied des Phosphatidylcholin- und Glukosestoffwechsels stellt der Transkriptionsfaktor LRH-1 dar. Seine Aktivierung erfolgt über spezifische Phosphatidylcholin-Derivate und reguliert Signalwege des Gallensäurestoffwechsels und der Glukosehomöostase (Lee *et al.* 2011). In der Tat zeigen ABCB4-defiziente Mäuse eine erhöhte hepatische *Lrh-1* Expression. Auch die Expression von LRH-1 Zielgenen wie *Cyp8b1* ist in *Abcb4*$^{-/-}$ -Tieren erhöht. Weiterhin konnten wir die spezifischen Phosphatidylcholin-Liganden (DUPC und DLPC) des LRH-1 Rezeptors in der murinen Leber nachweisen. Unterstützt wird die These eines LRH-1-vermittelten Effekts durch Daten, die eine direkte Beeinflussung der Glucokinase (*Gck*) -Expression auf LRH-1 unter postprandialen Bedingungen nachweisen (Oosterveer *et al.* 2012). Aufgrund der Komplexität der Glukosehomöostase und der vielfältigen regulierenden Einflussgrößen können auch LRH-1-unabhängig vermittelte Signalwege nicht ausgeschlossen werden. Infolge der Cholestase und der erhöhten Gallensäurekonzentration im Blut von *Abcb4*$^{-/-}$-Mäusen wäre auch eine Gallensäurenabhängige Modulation der Glukosehomöostase über die Rezeptoren TGR5 oder FXR denkbar.

TGR5 ist ein G-Protein-gekoppelter Gallensäure-Rezeptor, der über nachgeschaltete Signalwege den Energieverbrauch im Muskel und braunen Fettgewebe reguliert (Watanabe *et al.* 2006). Durch den Einfluss auf die Produktion des gastrointestinalen Hormons Glucagon-like-peptide beeinflusst der Rezeptor zudem den Glukosestoffwechsel (Katsuma *et al.* 2005). *Abcb4*$^{-/-}$-Mäusen zeigen einen leicht erhöhten Sauerstoffverbrauch und damit einen Anstieg der Stoffwechselrate, der auf eine veränderte TGR5-Aktivität hinweisen könnte. Der nukleäre Farnesoid X Rezeptor (FXR, *Nr1h4*) wird ebenfalls über Gallensäuren aktiviert und seine Bedeutung für den Glukosestoffwechsel wurde bereits vielfach

diskutiert (Zhang *et al.* 2006, Ma *et al.* 2006, Wang *et al.* 2008). *Fxr*-Knockout-Mäuse besitzen einen reduzierten hepatischen Glykogengehalt sowie eine verminderte Glukosetoleranz und Insulinsensitivität (Ma *et al.* 2006). Wir konnten jedoch keine Unterschiede in der hepatischen Expression von *Fxr* zwischen *Abcb4*-Knockout- und Wildtyp-Tieren nachweisen. Des Weiteren lag bei Trägerinnen der Genvariante *ABCB4* c.711A>T zum Zeitpunkt der Analyse keine Cholestase vor, so dass ein primär über Gallensäuren vermittelter Einfluss von ABCB4 auf die Glukosehomöostase ausgeschlossen werden kann.

Die Modulation des Lipidstoffwechsels

Die umfangreiche Phänotypisierung der *Abcb4*-Knockout-Mäuse offenbart ebenfalls profunde hepatische und systemische Veränderungen im Lipid-Stoffwechsel, die auf einen vorrangig ABCB4-abhängigen Effekt hindeuten. So weisen *Abcb4*-Knockout-Mäuse, im Gegensatz zu Patienten mit einer extrahepatischen Cholestase, eine Reduktion der Triglycerid- und Cholesterin-Konzentrationen im Plasma auf. *ABCB4*-Polymorphismen im Menschen können jedoch mit einer Abnahme der zirkulierenden Cholesterin-Konzentrationen einhergehen (Acalovschi *et al.* 2009). Das Lipidprofil der Tiere spiegelt neben einer verminderten Sphingomyelin-Konzentration vor allem eine Reduktion in einer Vielzahl von spezifischen PC-Derivaten wider. Das veränderte Verhältnis von Ölsäure (C18:1) zu Sterinsäure (C18:0) in den untersuchten Lipidklassen (Acylcarnitine, Glycerophospholipide, Sphingolipide) und die erhöhte hepatische Expression der Stearoyl-CoA Desaturase (SCD) deuten zudem auf eine gesteigerte Aktivität des Enzyms hin, das die Synthese von einfach ungesättigten Fettsäuren katalysiert. Als Regulator von Fettsäuresynthese (Ntambi and Miyazaki 2004) und Glukosestoffwechsel (Poudyal and Brown 2011) steht die Aktivität der SCD im Zusammenhang mit Übergewicht und Diabetes Typ 2 (Ntambi *et al.* 2002, Wong *et al.* 2011), darüber hinaus ist sie mit der Entstehung des hepatozellulären Karzinoms assoziiert (Budhu *et al.* 2013). Die Regulation der Desaturase erfolgt durch vielfältige hormonelle, diätische- und weitere exogene Faktoren, und zum

Teil vermittelt über das Sterol Regulatory Element-Binding Protein (SREBP1). Unsere Analysen weisen allerdings keine Unterschiede im hepatischen Expressionslevel von *Srebp1* zwischen *Abcb4*$^{-/-}$-Mäusen und Wildtyp-Tieren nach, was eine Regulation durch SREBP1-unabhängige Faktoren wahrscheinlicher macht. Denkbar wäre hier ein Einfluss über Glukose, Dehydroepiandrosteron, Vitamin A und D oder nukleäre Rezeptoren wie LXR und PXR. Da diese Faktoren sowohl in die Regulation der Stearoyl-CoA Desaturase-Aktivität und in die Fibrogenese involviert sind (Ntambi and Miyazaki 2004, Bataller and Brenner 2005, Mallat and Lotersztajn 2013) und/oder im Rahmen der Phänotypisierung der *Abcb4*$^{-/-}$-Mäuse auffällig wurden.

Ergänzend zu den oben dargestellten Veränderungen im Lipidstoffwechsel, zeigt die umfangreiche Studie einer anderen Arbeitsgruppe (Moustafa *et al.* 2012) die Deregulation von Genen der Lipid -Synthese, -Speicherung und -Oxidation in *Abcb4*$^{-/-}$-Mäusen. Die Autoren illustrieren, dass die Reduktion von Leberentzündung und Fibrose in *Abcb4*$^{-/-}$-Tieren durch die modifizierte Gallensäure 24-*Nor*ursodeoxycholsäure zu einem Anstieg des Cholesterin- und Triglyceridspiegels sowie zu einer Normalisierung der Expression zahlreicher Gene des Lipidstoffwechsels führt. Zusammen mit der Studie von Moustafa *et al*. (Moustafa *et al.* 2012) verdeutlicht diese Arbeit, dass die Lipidhomöostase als Einflussgröße in der Pathogenese und Progression cholestatischer Lebererkrankungen eine wichtige Rolle spielt und spezifische Metabolite des Lipidstoffwechsels, insbesondere Phospholipide, einen potenziellen Surrogatmarker für die ABCB4-Defizienz und die dadurch bedingte Cholestase darstellen könnten. Die Eignung des Plasma-Lipidprofils als diagnostischer Marker für die ABCB4-Defizienz bleibt in weiteren Studien zu prüfen.

Die Beeinträchtigung von Struktur und Stoffwechsel des Knochens

Metabolische Knochenerkrankungen sind eine häufige Komplikation bei Patienten mit chronisch cholestatischen Lebererkrankungen, deren zugrundeliegende molekulare Mechanismen unvollständig verstanden sind. Die Charakterisierung

des Knochenphänotypen zeigt erstmalig, dass auch *Abcb4*$^{-/-}$-Mäuse Veränderungen des Knochenstoffwechsels und der Knochenstruktur aufweisen, vergleichbar mit der Pathologie der hepatischen Osteodystrophie im Menschen.

Die parallel zu der Entwicklung der Leberschädigung auftretenden Veränderungen in Struktur und Stoffwechsel der Knochen bei *Abcb4*$^{-/-}$-Mäusen lassen vermuten, dass es sich um einen durch die chronische Cholestase induzierten Effekt handelt. Hierfür sprechen auch die geschlechtsspezifischen Unterschiede mit stärker ausgeprägten Knochen und Leberphänotypen bei weiblichen *Abcb4*$^{-/-}$-Mäusen. Im Detail weisen die morphologischen Untersuchungen eine verminderte Mineralisierung des gesamten Skeletts und eine Beeinträchtigung der trabekulären Knochenarchitektur nach. Zusätzlich findet sich im kortikalen Knochen, der etwa 80% der Knochenmasse ausmacht, eine Abnahme der Dichte bei weiblichen *Abcb4*$^{-/-}$-Mäusen. Da schon geringe Veränderungen in der Mineralisierung erheblich die Belastbarkeit und Elastizität des Knochen beeinflussen (Currey 1969) und die trabekuläre Architektur ebenfalls einen wichtigen Faktor der Knochenstärke darstellt (Krug *et al.* 2010, Hildebrand *et al.* 1999), ist eine Minderung in der Stabilität der Knochen anzunehmen.

Äquivalent zu den morphologischen Analysen entwickeln *Abcb4*$^{-/-}$-Tiere Abweichungen in der Calcium-Phosphat-Homöostase und verminderte Vitamin D-Konzentrationen im Plasma, wie sie auch bei Patienten mit chronischen Lebererkrankungen häufig beobachtet werden (Arteh *et al.* 2010, Grünhage *et al.* 2012). Die reduzierten Vitamin D-Spiegel, zusammen mit der veränderten Genexpression von Schlüsselenzymen des Vitamin D-Stoffwechsels (speziell der 25-Hydroxylasen CYP2R1 und CYP27A1) weisen auf die Beeinträchtigung der Vitamin D-Synthese oder zumindest des Vitamin D-Stoffwechsels unter cholestatischen Bedingungen hin. Die Verabreichung von Vitamin D zur Behebung eines Mangels wird zwar generell bei Patienten mit einer hepatischen Osteodystrophie empfohlen, allerdings liegen keine Daten vor, die eine eindeutige Wirksamkeit von Vitamin D zur Prävention des Knochenmasseverlusts bestätigen (Collier *et al.* 2002, Goel and Kar 2010). In Übereinstimmung hiermit zeigt unsere Interventionsstudie mit verschiedenen Vitamin D-Diäten eine Beeinflus-

sung des Knochenphänotypen bei *Abcb4*$^{-/-}$-Tieren, jedoch keinen Schutz vor einem Qualitätsverlust der Knochen, so dass andere Mediatoren neben Vitamin D für den Umbauprozess des Knochens relevant sein müssen.

Vermittelt wird der Umbauprozess des Knochens hauptsächlich über das Zusammenspiel der Osteoblasten, welche für die Knochenneubildung verantwortlich sind, und den Osteoklasten mit ihrer gewebeabbauenden Eigenschaft. Wichtige Regulatoren des Zusammenspiels und der Aktivität der Zellen sind RANKL und Osteoprotegorin (OPG). RANKL aktiviert die Osteoklasten und damit die Knochenresorption, während OPG als Rezeptor von RANKL die Osteoklastendifferenzierung und den Abbau des Gewebes hemmt. Die Analysen der *Abcb4*$^{-/-}$-Mäuse mit einer fortgeschrittenen Fibrose lassen aufgrund der erhöhten RANKL-Konzentration und der unveränderten OPG-Konzentration im Serum eine gesteigerte Osteoklastogenese vermuten. TGF-β, das die RANKL-induzierte Osteoklastogenese fördert (Fox and Lovibond 2005, Pfeilschifter *et al.* 1990, Yasui *et al.* 2011), ist ebenfalls im Serum der *Abcb4*$^{-/-}$-Tiere erhöht.

Osteocalcin, ein spezifisch von Ostoblasten produziertes Protein der nichtkollagenhaltigen Knochenmatrix, gilt als sensitiver Marker der Osteoblasten-Aktivität und des Umbauprozesses (Neve *et al.* 2012). Die Abnahme der mRNA-Expression von Ostocalcin in den Knochen der *Abcb4*$^{-/-}$-Mäuse steht im Einklang mit einer Reduktion der Osteoblastenbildung und des Knochenaufbaus, wenngleich es sich hierbei auch um einen kompensatorischen Effekt handeln könnte. Interessanterweise konnte gezeigt werden, dass Osteocalcin den Glukosestoffwechsel beeinflusst (Karsenty and Ferron 2012): Als Hormon erhöht es dosisabhängig die Proliferation von β-Zellen sowie die Insulinsekretion im Pankreas und damit die Glukosetoleranz der Maus (Lee *et al.* 2007, Ferron *et al.* 2008). Die regulatorische Bedeutung von Osteocalcin im humanen Glukosestoffwechsel ist allerdings umstritten (Andrews 2013) und ein Anstieg in der Anzahl und Aktivität der Osteoklasten könnte ebenfalls die Glukosetoleranz positiv beeinflussen (Lacombe *et al.* 2013). Zusammenfassend deuten die Daten des Knochenstoffwechsels auf eine verstärkte Osteoklastogenese hin, bei gleichzeitiger

Beeinträchtigung der Osteoblastogenese, infolge der chronischen Cholestase bei ABCB4-Defizienz.

Neben Vitamin D, das die Genexpression von Mediatoren des Knochenstoffwechsels (z.B. *Rankl*, *Spp1*) reguliert (Haussler *et al.* 2012), konnte auch für Gallensäuren regulatorische Effekte (auf *Rankl* und *Bglap*) im Knochenstoffwechsel und ein Einfluss auf die Osteoblastenaktivität bei Menschen nachgewiesen werden (Ruiz-Gaspà *et al.* 2010, Dubreuil *et al.* 2013). Diese regulatorische Interaktion von Vitamin D und Gallensäuren im Knochenstoffwechsel und die Veränderungen beider Stoffwechselvorgänge unter cholestatischen Bedingungen lassen spezifische Pathomechanismen vermuten, die bei Patienten mit chronisch cholestatischen Lebererkrankungen zur hepatischen Osteodystrophie führen. Mit der *Abcb4*$^{-/-}$-Maus steht ein präklinisches Modell zur Verfügung, das es erlaubt, die molekularen Mechanismen der hepatischen Osteodystrophie, wie sie bei Patienten mit cholestatischen Lebererkrankungen auftreten, näher zu untersuchen und systemische Effekte von therapeutischen Interventionen zu prüfen. Eine kürzlich publizierte Studie (Nüssler *et al.* 2014) zeigt, dass die toxisch induzierte Leberfibrose ebenfalls von Veränderungen der Knochenphänotypen begleitet wird. Damit bietet sich die Möglichkeit einer Differenzierung von spezifischen Effekten der chronischen Cholestase und der Identifizierung von Mechanismen, die unabhängig von der Ätiologie der Lebererkrankung sind.

Der Einfluss von Vitamin D auf die biliäre Fibrose

Die Analysen der hepatischen Phänotypen von *Abcb4*$^{-/-}$-Mäusen im Rahmen der Interventionsstudie belegen eine modulierende Wirkung von Vitamin D auf die Leberfibrogenese. So geht ein Vitamin D-Mangel in Knockout-Tieren mit einer erhöhten Kollagen-Ablagerung und Fibrogenese einher, während eine ausreichende Vitamin D-Zufuhr die Leberschädigung reduziert. Über die maximal verwendete Vitamin D-Supplementation kann darüber hinaus nur noch ein moderater Effekt in Form einer niedrigeren Transaminase Aktivität erzielt werden.

Diese Ergebnisse sind im Kontext einer Vitamin D-Unterversorgung bei bis zu 90% der Patienten mit chronischen Lebererkrankungen von besonderer Relevanz (Arteh *et al.* 2010). Die Mechanismen, welche die Vitamin D-Versorgung bei Patienten mit chronischen Lebererkrankungen negativ beeinträchtigen können, sind vielseitig. Dazu zählen eine unzureichende UV-Einwirkung oder Nahrungsaufnahme von Vitamin D-haltigen Lebensmitteln, eine gestörte intestinale Resorption der Nahrung, eine beeinträchtigte Hydroxylierung von Vitamin D (Cholecalciferol) zu 25-Hydroxyvitamin D oder auch ein verstärkter Abbau von 25-Hydroxyvitamin D (Stokes *et al.* 2013). Interessanterweise haben auch *Abcb4*$^{-/-}$-Mäuse im Vergleich zu Wildtyp-Tieren geringere Vitamin D-Serumkonzentrationen nach Erhalt einer Kontroll-Diät. Indes steigt die Vitamin D-Konzentration in *Abcb4*$^{-/-}$-Mäusen, die mit einer hochdosierten Vitamin D-Diät gefüttert wurden, stark an, während die Vitamin D-Konzentration bei Wildtyp-Mäusen konstant bleibt. Diese unerwartete Beobachtung könnte durch eine gestörte Regulation der Vitamin D-Aufnahme verursacht werden. Zusätzlich findet sich bei ABCB4-defizienten Mäusen unter der hochdosierten Diät eine erhöhte Genexpression der 25-Hydroxylasen CYP2R1 und CYP27A1, welche Cholecalciferol zu 25-Hydroxyvitamin D umsetzen. Eine Beeinträchtigung des Vitamin D-Katabolismus kann ebenfalls nicht ausgeschlossen werden. Das für die Initiierung des Vitamin D-Abbaus verantwortliche Enzym, die 24-Hydroxylase CYP24A1, wird durch Vitamin D selbst reguliert. Allerdings können spezifische Gallensäuren wie die Lithocholsäure den stimulierenden Effekt von Vitamin D hemmen. Gallensäuren können zudem ein breites Spektrum an nukleären Rezeptoren aktivieren, dazu zählt der VDR ebenso wie FXR und PXR (Ruiz-Gaspà *et al.* 2010, Hylemon *et al.* 2009, Li and Chiang 2013). Schlüsselenzyme der Gallensäuresynthese (CYP7A1) und des Abbaus (CYP3A4) wiederum werden stark über Vitamin D und seinen Rezeptor reguliert. Tatsächlich konnte nachgewiesen werden, dass schon geringe Änderungen in der Gallensäure-Zusammensetzung die Fibrogenese in *Abcb4*$^{-/-}$-Mäusen beeinflussen (van Nieuwerk *et al.* 1997). CYP27A1 katalysiert neben der 25-Hydroxylierung von Cholecalciferol auch den ersten Schritt des Alternativen-Gallensäure-Synthese-

Signalweges und die Modifikation von Gallensäuren über den klassischen Signalweg der Gallensäuresynthese. Interessanterweise sind weitere Produkte der CYP27A1 (das 27-Hydroxycholesterol) LXR Liganden, welche die Transkription von Genen des Lipidstoffwechsels aktivieren (Hafner *et al.* 2011). Fortführende Studien und detaillierte Analysen der Gallensäure-komposition wären hier interessant und könnten Hinweise zur Aufklärung des molekularen Mechanismus der Genotyp-Diät-Interaktion geben.

Die Verwendung des *Abcb4*$^{-/-}$-Mausmodells und der vorwiegend deskriptive Ansatz unser Studie limitieren die Aussagekraft der Ergebnisse primär auf cholestatische Bedingungen. Allerdings häufen sich die Hinweise, dass ein anti-fibrotischer Effekt von Vitamin D unabhängig von der Ätiologie der Lebererkrankung ist. Zusätzlich weisen diese Studien auf eine limitierte Wirkung hin. Spezifiziert bewirkt die parallele Injektion des aktiven 1,25-Dihydroxyvitamin D und Thioacetamid (zur toxischen Induktion der Fibrose) in der Ratte eine Hemmung der Fibrogenese. Die Entwicklung einer Fibrose kann jedoch nicht vermieden werden (Abramovitch *et al.* 2011). Mittels Phototherapie ist es in einem Modell der nichtalkoholischen Steatohepatitis möglich die Entzündung, Fibrose und Insulin- Resistenz zu reduzieren. Eine moderate Fibrose entsteht jedoch auch in diesem Modell (Nakano *et al.* 2011).

Zusammenfassend demonstriert diese Studie, dass Vitamin D die biliäre Entzündung und Fibrogenese *in vivo* moduliert und dass die Ausprägung der Fibrose vom Vitamin D-Status abhängig ist. In dem untersuchten Modell beschleunigt ein Vitamin D-Mangel die Fibrogenese, allerdings sind die protektiven Effekte einer Vitamin D-Supplementation limitiert. Die Daten deuten an, dass eine exzessive Vitamin D-Aufnahme nicht vor einer Leberfibrose schützt, dass aber bei Patienten mit chronisch cholestatischen Lebererkrankungen ein Vitamin D-Mangel vermieden werden sollte, um das Risiko einer beschleunigten Fibrogenese zu minimieren und das über eine adäquate Vitamin D-Versorgung ein anti-fibrotischer Effekt erzielt werden kann.

In ihrer Gesamtheit belegen die dargestellten Studien die Komplexität und Vielfältigkeit der Auswirkungen des leberspezifischen ABCB4-Defekts auf den

Gesamtorganismus und bieten Hinweise über die Verknüpfung hepatischer und extrahepatischer Symptome bei Patienten mit chronischer Cholestase und biliärer Fibrose. Die erhobenen Daten erweitern zudem maßgeblich die Kenntnisse und das Verständnis pathobiologischer Mechanismen chronisch cholestatischer Lebererkrankungen und identifizieren Vitamin D als potentielle Determinante der Fibrogenese.

LITERATURVERZEICHNIS

1. Abe, E., Miyaura, C., Sakagami, H., Takeda, M., Konno, K., Yamazaki, T., Yoshiki, S., and Suda, T. (1981). Differentiation of mouse myeloid leukemia cells induced by 1 alpha,25-dihydroxyvitamin D3. Proc Natl Acad Sci U S A *78*, 4990-4994.
2. Abramovitch, S., Dahan-Bachar, L., Sharvit, E., Weisman, Y., Ben Tov, A., Brazowski, E., and Reif, S. (2011). Vitamin D inhibits proliferation and profibrotic marker expression in hepatic stellate cells and decreases thioacetamide-induced liver fibrosis in rats. Gut *60*, 1728-1737.
3. Acalovschi, M., Tirziu, S., Chiorean, E., Krawczyk, M., Grünhage, F., and Lammert, F. (2009). Common variants of *ABCB4* and *ABCB11* and plasma lipid levels: a study in sib pairs with gallstones, and controls. Lipids *44*, 521-526.
4. Andrews, N.A. (2013). Skeletal regulation of glucose metabolism: challenges in translation from mouse to man. IBMS BoneKEy *10*.
5. Angulo, P., and Lindor, K.D. (1999). Primary sclerosing cholangitis. Hepatology *30*, 325-332.
6. Arteh, J., Narra, S., and Nair, S. (2010). Prevalence of vitamin D deficiency in chronic liver disease. Dig Dis Sci *55*, 2624-2628.
7. Baghdasaryan, A., Fickert, P., Fuchsbichler, A., Silbert, D., Gumhold, J., Horl, G., Langner, C., Moustafa, T., Halilbasic, E., Claudel, T.*, et al.* (2008). Role of hepatic phospholipids in development of liver injury in *Mdr2* (*Abcb4*) knockout mice. Liver Int *28*, 948-958.
8. Baghdasaryan, A., Claudel, T., Kosters, A., Gumhold, J., Silbert, D., Thuringer, A., Leski, K., Fickert, P., Karpen, S.J., and Trauner, M. (2010). Curcumin improves sclerosing cholangitis in *Mdr2*$^{-/-}$ mice by inhibition of cholangiocyte inflammatory response and portal myofibroblast proliferation. Gut *59*, 521-530.
9. Baghdasaryan, A., Claudel, T., Gumhold, J., Silbert, D., Adorini, L., Roda, A., Vecchiotti, S., Gonzalez, F.J., Schoonjans, K., Strazzabosco, M.*, et al.* (2011). Dual farnesoid X receptor/TGR5 agonist INT-767 reduces liver injury in the *Mdr2*$^{-/-}$ (*Abcb4*$^{-/-}$) mouse cholangiopathy model by promoting biliary HCO^-_3 output. Hepatology *54*, 1303-1312.
10. Bataller, R., and Brenner, D.A. (2005). Liver fibrosis. J Clin Invest *115*, 209-218.
11. Borst, P., and Schinkel, A.H. (1996). What have we learnt thus far from mice with disrupted P-glycoprotein genes? Eur J Cancer *32A*, 985-990.
12. Braet, F., and Wisse, E. (2002). Structural and functional aspects of liver sinusoidal endothelial cell fenestrae: a review. Comparative hepatology *1*, 1.
13. Budhu, A., Roessler, S., Zhao, X., Yu, Z., Forgues, M., Ji, J., Karoly, E., Qin, L.X., Ye, Q.H., Jia, H.L.*, et al.* (2013). Integrated metabolite and gene expression profiles identify lipid biomarkers associated with progression of hepatocellular carcinoma and patient outcomes. Gastroenterology *144*, 1066-1075 e1061.
14. Cantorna, M.T., Zhu, Y., Froicu, M., and Wittke, A. (2004). Vitamin D status, 1,25-dihydroxyvitamin D3, and the immune system. The American journal of clinical nutrition *80*, 1717S-1720S.
15. Cohen-Naftaly, M., and Friedman, S.L. (2011). Current status of novel antifibrotic therapies in patients with chronic liver disease. Therap Adv Gastroenterol *4*, 391-417.
16. Collier, J.D., Ninkovic, M., and Compston, J.E. (2002). Guidelines on the management of osteoporosis associated with chronic liver disease. Gut *50 Suppl 1*, i1-9.
17. Currey, J.D. (1969). The relationship between the stiffness and the mineral content of bone. J Biomech *2*, 477-480.
18. Davit-Spraul, A., Gonzales, E., Baussan, C., and Jacquemin, E. (2009). Progressive familial intrahepatic cholestasis. Orphanet journal of rare diseases *4*, 1.
19. Davit-Spraul, A., Gonzales, E., Baussan, C., and Jacquemin, E. (2010). The spectrum of liver diseases related to *ABCB4* gene mutations: pathophysiology and clinical aspects. Semin Liver Dis *30*, 134-146.

20. Dubreuil, M., Ruiz-Gaspà, S., Guañabens, N., Peris, P., Álvarez, L., Monegal, A., Combalia, A., and Parés, A. (2013). Ursodeoxycholic acid increases differentiation and mineralization and neutralizes the damaging effects of bilirubin on osteoblastic cells. Liver International *33*, 1029-1038.
21. Ferron, M., Hinoi, E., Karsenty, G., and Ducy, P. (2008). Osteocalcin differentially regulates beta cell and adipocyte gene expression and affects the development of metabolic diseases in wild-type mice. Proc Natl Acad Sci U S A *105*, 5266-5270.
22. Fickert, P., Fuchsbichler, A., Wagner, M., Zollner, G., Kaser, A., Tilg, H., Krause, R., Lammert, F., Langner, C., Zatloukal, K.*, et al.* (2004). Regurgitation of bile acids from leaky bile ducts causes sclerosing cholangitis in *Mdr2* (*Abcb4*) knockout mice. Gastroenterology *127*, 261-274.
23. Fickert, P., Wagner, M., Marschall, H.U., Fuchsbichler, A., Zollner, G., Tsybrovskyy, O., Zatloukal, K., Liu, J., Waalkes, M.P., Cover, C.*, et al.* (2006). 24-*nor*Ursodeoxycholic acid is superior to ursodeoxycholic acid in the treatment of sclerosing cholangitis in *Mdr2* (*Abcb4*) knockout mice. Gastroenterology *130*, 465-481.
24. Fisher, L., and Fisher, A. (2007). Vitamin D and parathyroid hormone in outpatients with noncholestatic chronic liver disease. Clinical gastroenterology and hepatology: the official clinical practice journal of the American Gastroenterological Association *5*, 513-520.
25. Forman, B.M. (2005). Are those phospholipids in your pocket? Cell Metab *1*, 153-155.
26. Fowler, C. (2013). Management of patients with complications of cirrhosis. The Nurse practitioner *38*, 14-21; quiz 22-13.
27. Fox, S.W., and Lovibond, A.C. (2005). Current insights into the role of transforming growth factor-beta in bone resorption. Mol Cell Endocrinol *243*, 19-26.
28. Gailus-Durner, V., Fuchs, H., Becker, L., Bolle, I., Brielmeier, M., Calzada-Wack, J., Elvert, R., Ehrhardt, N., Dalke, C., Franz, T.J.*, et al.* (2005). Introducing the German Mouse Clinic: open access platform for standardized phenotyping. Nat Methods *2*, 403-404.
29. Gascón-Barre, M., Demers, C., Mirshahi, A., Neron, S., Zalzal, S., and Nanci, A. (2003). The normal liver harbors the vitamin D nuclear receptor in nonparenchymal and biliary epithelial cells. Hepatology *37*, 1034-1042.
30. Goel, V., and Kar, P. (2010). Hepatic osteodystrophy. Trop Gastroenterol *31*, 82-86.
31. Grünhage, F., Hochrath, K., Krawczyk, M., Höblinger, A., Obermayer-Pietsch, B., Geisel, J., Trauner, M., Sauerbruch, T., and Lammert, F. (2012). Common genetic variation in vitamin D metabolism is associated with liver stiffness. Hepatology *56*, 1883-1891.
32. Hafner, M., Rezen, T., and Rozman, D. (2011). Regulation of hepatic cytochromes p450 by lipids and cholesterol. Curr Drug Metab *12*, 173-185.
33. Haussler, M.R., Whitfield, G.K., Kaneko, I., Haussler, C.A., Hsieh, D., Hsieh, J.C., and Jurutka, P.W. (2012). Molecular Mechanisms of Vitamin D Action. Calcif Tissue Int.
34. Hildebrand, T., Laib, A., Müller, R., Dequeker, J., and Rüegsegger, P. (1999). Direct three-dimensional morphometric analysis of human cancellous bone: microstructural data from spine, femur, iliac crest, and calcaneus. J Bone Miner Res *14*, 1167-1174.
35. Hohenester, S., and Beuers, U. (2011). Phosphatidylcholines as regulators of glucose and lipid homeostasis: Promises and potential risks. Hepatology *54*, 2266-2268.
36. Hylemon, P.B., Zhou, H., Pandak, W.M., Ren, S., Gil, G., and Dent, P. (2009). Bile acids as regulatory molecules. Journal of lipid research *50*, 1509-1520.
37. Iwaisako, K., Brenner, D.A., and Kisseleva, T. (2012). What's new in liver fibrosis? The origin of myofibroblasts in liver fibrosis. J Gastroenterol Hepatol *27 Suppl 2*, 65-68.
38. Iyengar, S.K., Abboud, H.E., Goddard, K.A., Saad, M.F., Adler, S.G., Arar, N.H., Bowden, D.W., Duggirala, R., Elston, R.C., Hanson, R.L.*, et al.* (2007). Genome-wide scans for diabetic nephropathy and albuminuria in multiethnic populations: the family investigation of nephropathy and diabetes (FIND). Diabetes *56*, 1577-1585.
39. Karsenty, G., and Ferron, M. (2012). The contribution of bone to whole-organism physiology. Nature *481*, 314-320.

40. Katsuma, S., Hirasawa, A., and Tsujimoto, G. (2005). Bile acids promote glucagon-like peptide-1 secretion through TGR5 in a murine enteroendocrine cell line STC-1. Biochemical and biophysical research communications *329*, 386-390.
41. Kisseleva, T., Cong, M., Paik, Y., Scholten, D., Jiang, C., Benner, C., Iwaisako, K., Moore-Morris, T., Scott, B., Tsukamoto, H.*, et al.* (2012). Myofibroblasts revert to an inactive phenotype during regression of liver fibrosis. Proc Natl Acad Sci U S A *109*, 9448-9453.
42. Krug, R., Burghardt, A.J., Majumdar, S., and Link, T.M. (2010). High-resolution imaging techniques for the assessment of osteoporosis. Radiol Clin North Am *48*, 601-621.
43. Lacombe, J., Karsenty, G., and Ferron, M. (2013). In vivo analysis of the contribution of bone resorption to the control of glucose metabolism in mice. Mol Metab *2*, 498-504.
44. Lammert, F., Wang, D.Q., Hillebrandt, S., Geier, A., Fickert, P., Trauner, M., Matern, S., Paigen, B., and Carey, M.C. (2004). Spontaneous cholecysto- and hepatolithiasis in *Mdr2*$^{-/-}$ mice: a model for low phospholipid-associated cholelithiasis. Hepatology *39*, 117-128.
45. Lee, N.K., Sowa, H., Hinoi, E., Ferron, M., Ahn, J.D., Confavreux, C., Dacquin, R., Mee, P.J., McKee, M.D., Jung, D.Y.*, et al.* (2007). Endocrine regulation of energy metabolism by the skeleton. Cell *130*, 456-469.
46. Lee, J.M., Lee, Y.K., Mamrosh, J.L., Busby, S.A., Griffin, P.R., Pathak, M.C., Ortlund, E.A., and Moore, D.D. (2011). A nuclear-receptor-dependent phosphatidylcholine pathway with antidiabetic effects. Nature *474*, 506-510.
47. Li, T., and Chiang, J.Y. (2013). Nuclear receptors in bile acid metabolism. Drug metabolism reviews *45*, 145-155.
48. Luxon, B.A. (2011). Bone disorders in chronic liver diseases. Curr Gastroenterol Rep *13*, 40-48.
49. Ma, K., Saha, P.K., Chan, L., and Moore, D.D. (2006). Farnesoid X receptor is essential for normal glucose homeostasis. J Clin Invest *116*, 1102-1109.
50. Makishima, M., Lu, T.T., Xie, W., Whitfield, G.K., Domoto, H., Evans, R.M., Haussler, M.R., and Mangelsdorf, D.J. (2002). Vitamin D receptor as an intestinal bile acid sensor. Science *296*, 1313-1316.
51. Mallat, A., and Lotersztajn, S. (2013). Cellular mechanisms of tissue fibrosis. 5. Novel insights into liver fibrosis. Am J Physiol Cell Physiol *305*, C789-799.
52. Martin, M. (1993). Primary sclerosing cholangitis. Annu Rev Med *44*, 221-227.
53. Mederacke, I., Hsu, C.C., Troeger, J.S., Huebener, P., Mu, X., Dapito, D.H., Pradere, J.P., and Schwabe, R.F. (2013). Fate tracing reveals hepatic stellate cells as dominant contributors to liver fibrosis independent of its aetiology. Nat Commun *4*, 2823.
54. Mochizuki, H., Scherer, S.W., Xi, T., Nickle, D.C., Majer, M., Huizenga, J.J., Tsui, L.C., and Prochazka, M. (1998). Human *PON2* gene at 7q21.3: cloning, multiple mRNA forms, and missense polymorphisms in the coding sequence. Gene *213*, 149-157.
55. Moustafa, T., Fickert, P., Magnes, C., Guelly, C., Thueringer, A., Frank, S., Kratky, D., Sattler, W., Reicher, H., Sinner, F.*, et al.* (2012). Alterations in lipid metabolism mediate inflammation, fibrosis, and proliferation in a mouse model of chronic cholestatic liver injury. Gastroenterology *142*, 140-151 e112.
56. Müllenbach, R., Linton, K.J., Wiltshire, S., Weerasekera, N., Chambers, J., Elias, E., Higgins, C.F., Johnston, D.G., McCarthy, M.I., and Williamson, C. (2003). *ABCB4* gene sequence variation in women with intrahepatic cholestasis of pregnancy. J Med Genet *40*, e70.
57. Murphy, F.R., Issa, R., Zhou, X., Ratnarajah, S., Nagase, H., Arthur, M.J., Benyon, C., and Iredale, J.P. (2002). Inhibition of apoptosis of activated hepatic stellate cells by tissue inhibitor of metalloproteinase-1 is mediated via effects on matrix metalloproteinase inhibition: implications for reversibility of liver fibrosis. J Biol Chem *277*, 11069-11076.
58. Nakano, T., Cheng, Y.F., Lai, C.Y., Hsu, L.W., Chang, Y.C., Deng, J.Y., Huang, Y.Z., Honda, H., Chen, K.D., Wang, C.C.*, et al.* (2011). Impact of artificial sunlight therapy on the progress of non-alcoholic fatty liver disease in rats. J Hepatol *55*, 415-425.

59. Nakchbandi, I.A., and van der Merwe, S.W. (2009). Current understanding of osteoporosis associated with liver disease. Nature reviews Gastroenterology & hepatology *6*, 660-670.
60. Navasa, M., Forns, X., Sanchez, V., Andreu, H., Marcos, V., Borras, J.M., Rimola, A., Grande, L., Garcia-Valdecasas, J.C., Granados, A.*, et al.* (1996). Quality of life, major medical complications and hospital service utilization in patients with primary biliary cirrhosis after liver transplantation. J Hepatol *25*, 129-134.
61. Neve, A., Corrado, A., and Cantatore, F.P. (2012). Osteocalcin: Skeletal and extra-skeletal effects. J Cell Physiol *228*, 1149-1153.
62. Ntambi, J.M., Miyazaki, M., Stoehr, J.P., Lan, H., Kendziorski, C.M., Yandell, B.S., Song, Y., Cohen, P., Friedman, J.M., and Attie, A.D. (2002). Loss of stearoyl-CoA desaturase-1 function protects mice against adiposity. Proc Natl Acad Sci U S A *99*, 11482-11486.
63. Ntambi, J.M., and Miyazaki, M. (2004). Regulation of stearoyl-CoA desaturases and role in metabolism. Prog Lipid Res *43*, 91-104.
64. Nüssler, A.K., Wildemann, B., Freude, T., Litzka, C., Soldo, P., Friess, H., Hammad, S., Hengstler, J.G., Braun, K.F., Trak-Smayra, V.*, et al.* (2014). Chronic CCl_4 intoxication causes liver and bone damage similar to the human pathology of hepatic osteodystrophy: a mouse model to analyse the liver-bone axis. Arch Toxicol *88*, 997-1006.
65. Oosterveer, M.H., Mataki, C., Yamamoto, H., Harach, T., Moullan, N., van Dijk, T.H., Ayuso, E., Bosch, F., Postic, C., Groen, A.K.*, et al.* (2012). LRH-1-dependent glucose sensing determines intermediary metabolism in liver. J Clin Invest *122*, 2817-2826.
66. Ortlund, E.A., Lee, Y., Solomon, I.H., Hager, J.M., Safi, R., Choi, Y., Guan, Z., Tripathy, A., Raetz, C.R., McDonnell, D.P.*, et al.* (2005). Modulation of human nuclear receptor LRH-1 activity by phospholipids and SHP. Nat Struct Mol Biol *12*, 357-363.
67. Petta, S., Camma, C., Scazzone, C., Tripodo, C., Di Marco, V., Bono, A., Cabibi, D., Licata, G., Porcasi, R., Marchesini, G.*, et al.* (2010). Low vitamin D serum level is related to severe fibrosis and low responsiveness to interferon-based therapy in genotype 1 chronic hepatitis C. Hepatology *51*, 1158-1167.
68. Pfeilschifter, J., Bonewald, L., and Mundy, G.R. (1990). Characterization of the latent transforming growth factor beta complex in bone. J Bone Miner Res *5*, 49-58.
69. Poudyal, H., and Brown, L. (2011). Stearoyl-CoA desaturase: a vital checkpoint in the development and progression of obesity. Endocr Metab Immune Disord Drug Targets *11*, 217-231.
70. Poupon, R., Rosmorduc, O., Boelle, P.Y., Chretien, Y., Corpechot, C., Chazouilleres, O., Housset, C., and Barbu, V. (2013). Genotype-phenotype relationships in the low-phospholipid-associated cholelithiasis syndrome: a study of 156 consecutive patients. Hepatology *58*, 1105-1110.
71. Prochazka, M., Mochizuki, H., Baier, L.J., Cohen, P.T., and Bogardus, C. (1995). Molecular and linkage analysis of type-1 protein phosphatase catalytic beta-subunit gene: lack of evidence for its major role in insulin resistance in Pima Indians. Diabetologia *38*, 461-466.
72. Pusl, T., and Beuers, U. (2005). Extrahepatic manifestations of cholestatic liver diseases: pathogenesis and therapy. Clin Rev Allergy Immunol *28*, 147-157.
73. Putz-Bankuti, C., Pilz, S., Stojakovic, T., Scharnagl, H., Pieber, T.R., Trauner, M., Obermayer-Pietsch, B., and Stauber, R.E. (2012). Association of 25-hydroxyvitamin D levels with liver dysfunction and mortality in chronic liver disease. Liver Int *32*, 845-851.
74. Rosmorduc, O., Hermelin, B., and Poupon, R. (2001). MDR3 gene defect in adults with symptomatic intrahepatic and gallbladder cholesterol cholelithiasis. Gastroenterology *120*, 1459-1467.
75. Rosmorduc, O., Hermelin, B., Boelle, P.Y., Parc, R., Taboury, J., and Poupon, R. (2003). ABCB4 gene mutation-associated cholelithiasis in adults. Gastroenterology *125*, 452-459.
76. Ruetz, S., and Gros, P. (1994). Phosphatidylcholine translocase: a physiological role for the mdr2 gene. Cell *77*, 1071-1081.

77. Ruiz-Gaspà, S., Guañabens, N., Enjuanes, A., Peris, P., Martinez-Ferrer, A., de Osaba, M.J., Gonzalez, B., Alvarez, L., Monegal, A., Combalia, A.*, et al.* (2010). Lithocholic acid downregulates vitamin D effects in human osteoblasts. Eur J Clin Invest *40*, 25-34.
78. Small, D.M. (2003). Role of ABC transporters in secretion of cholesterol from liver into bile. Proc Natl Acad Sci U S A *100*, 4-6.
79. Smit, J.J., Schinkel, A.H., Oude Elferink, R.P., Groen, A.K., Wagenaar, E., van Deemter, L., Mol, C.A., Ottenhoff, R., van der Lugt, N.M., van Roon, M.A.*, et al.* (1993). Homozygous disruption of the murine mdr2 P-glycoprotein gene leads to a complete absence of phospholipid from bile and to liver disease. Cell *75*, 451-462.
80. Smith, A.J., Timmermans-Hereijgers, J.L., Roelofsen, B., Wirtz, K.W., van Blitterswijk, W.J., Smit, J.J., Schinkel, A.H., and Borst, P. (1994). The human MDR3 P-glycoprotein promotes translocation of phosphatidylcholine through the plasma membrane of fibroblasts from transgenic mice. FEBS Lett *354*, 263-266.
81. Song, B.J., and Rockey, D.C. (2013). Status of research on vitamin D supplementation in treating or preventing liver fibrosis. Liver Int *33*, 653-655.
82. Stokes, C.S., Volmer, D.A., Grünhage, F., and Lammert, F. (2013). Vitamin D in chronic liver disease. Liver Int *33*, 338-352.
83. Trauner, M., Meier, P.J., and Boyer, J.L. (1998). Molecular pathogenesis of cholestasis. The New England journal of medicine *339*, 1217-1227.
84. Troeger, J.S., Mederacke, I., Gwak, G.Y., Dapito, D.H., Mu, X., Hsu, C.C., Pradere, J.P., Friedman, R.A., and Schwabe, R.F. (2012). Deactivation of hepatic stellate cells during liver fibrosis resolution in mice. Gastroenterology *143*, 1073-1083 e1022.
85. van Nieuwerk, C.M., Groen, A.K., Ottenhoff, R., van Wijland, M., van den Bergh Weerman, M.A., Tytgat, G.N., Offerhaus, J.J., and Oude Elferink, R.P. (1997). The role of bile salt composition in liver pathology of *mdr2* (-/-) mice: differences between males and females. J Hepatol *26*, 138-145.
86. Wallace, K., Burt, A.D., and Wright, M.C. (2008). Liver fibrosis. The Biochemical journal *411*, 1-18.
87. Wang, Y.D., Chen, W.D., Moore, D.D., and Huang, W. (2008). FXR: a metabolic regulator and cell protector. Cell Res *18*, 1087-1095.
88. Wasmuth, H.E., Glantz, A., Keppeler, H., Simon, E., Bartz, C., Rath, W., Mattsson, L.A., Marschall, H.U., and Lammert, F. (2007). Intrahepatic cholestasis of pregnancy: the severe form is associated with common variants of the hepatobiliary phospholipid transporter ABCB4 gene. Gut *56*, 265-270.
89. Watanabe, M., Houten, S.M., Mataki, C., Christoffolete, M.A., Kim, B.W., Sato, H., Messaddeq, N., Harney, J.W., Ezaki, O., Kodama, T.*, et al.* (2006). Bile acids induce energy expenditure by promoting intracellular thyroid hormone activation. Nature *439*, 484-489.
90. Wehrli, F.W. (2007). Structural and functional assessment of trabecular and cortical bone by micro magnetic resonance imaging. J Magn Reson Imaging *25*, 390-409.
91. Wong, B.X., Kyle, R.A., Myhill, P.C., Croft, K.D., Quinn, C.M., Jessup, W., and Yeap, B.B. (2011). Dyslipidemic diabetic serum increases lipid accumulation and expression of stearoyl-CoA desaturase in human macrophages. Lipids *46*, 931-941.
92. Yang, S., Smith, C., Prahl, J.M., Luo, X., and DeLuca, H.F. (1993). Vitamin D deficiency suppresses cell-mediated immunity in vivo. Arch Biochem Biophys *303*, 98-106.
93. Yasui, T., Kadono, Y., Nakamura, M., Oshima, Y., Matsumoto, T., Masuda, H., Hirose, J., Omata, Y., Yasuda, H., Imamura, T.*, et al.* (2011). Regulation of RANKL-induced osteoclastogenesis by TGF-β through molecular interaction between Smad3 and Traf6. J Bone Miner Res *26*, 1447-1456.
94. Zhang, Y., Lee, F.Y., Barrera, G., Lee, H., Vales, C., Gonzalez, F.J., Willson, T.M., and Edwards, P.A. (2006). Activation of the nuclear receptor FXR improves hyperglycemia and hyperlipidemia in diabetic mice. Proc Natl Acad Sci U S A *103*, 1006-1011.
95. Zittermann, A. (2010). The estimated benefits of vitamin D for Germany. Mol Nutr Food Res 54, 1164-1171.

ZUSAMMENFASSUNG

Das *ABCB4*-Gen kodiert das gleichnamige Transportprotein, das selektiv in der Leber exprimiert wird und Phosphatidylcholin über die kanalikuläre Membran in die Galle transloziert. Die *Abcb4* (*ATP-binding cassette transporter B4*) knockout (*Abcb4*$^{-/-}$) Maus ist ein etabliertes präklinisches Modell für chronische cholestatische Lebererkrankungen wie die sklerosierende Cholangitis und biliäre Fibrose. Die Konsequenz dieser Erkrankungen auf den Gesamtorganismus und die Wechselwirkungen mit dem extrahepatischen Organsystem sind bisher nur in Teilen bekannt. Mit dem Ziel, die pathobiologischen Mechanismen besser zu verstehen und Einflussgrößen der Fibrogenese in cholestatischen Lebererkrankungen identifizieren zu können, wurden in dieser Arbeit systemische Auswirkungen der *Abcb4*-Defizienz charakterisiert. Aufbauend auf einer umfangreichen standardisierten Phänotypisierung des *Abcb4*$^{-/-}$-Mausmodells erfolgten detaillierte Studien zur Glukose- und Lipidhomöostase sowie des Knochen- und Vitamin D-Stoffwechsels. Des Weiteren wurde in einer Interventionsstudie der Einfluss des Vitamin D-Hormons auf die Knochenmorphologie und die Leberfibrogenese in *Abcb4*$^{-/-}$-Tieren untersucht.

Die Charakterisierung des Glukosestoffwechsels ergab, dass die *Abcb4*-Defizienz mit einer höheren Glukosetoleranz und einer veränderten Genexpression von Enzymen des Glukosestoffwechsels in der Leber einhergeht. Gleichzeitig findet sich bei *Abcb4*$^{-/-}$-Tieren eine erhöhte hepatische Expression des anti-diabetischen nukleären Rezeptors LRH-1, dessen spezifische Phosphatidylcholin-Liganden in der Leber nachgewiesen werden konnten. In zwei unabhängigen europäischen Kohorten konnte eine Assoziation des Glukosespiegels mit der häufig vorkommenden procholestatischen Variante c.711A>T des humanen *ABCB4*-Gens nachgewiesen werden. Diese Studien belegen damit erstmals Wechselwirkungen des ABCB4-Transporters mit der Glukosehomöostase bei Maus und Mensch.

Analysen der Morphologie und des Stoffwechsels der Knochen weisen nach, dass *Abcb4*$^{-/-}$-Mäuse eine Osteodystrophie entwickeln. So finden sich in den

Knochen von Knockout-Tieren mit einer fortgeschrittenen Fibrose eine Abnahme des Mineralgehalts, Veränderungen der trabekulären Architektur und eine verminderte kortikale Dichte. Dysregulationen von Genen des Knochenumbaus und des Vitamin D-Stoffwechsels konnten ebenfalls gemessen werden. Die Supplementation mit Vitamin D beeinflusst die Knochenphänotypen, kann die Knochenqualität aber nicht sicherstellen, so dass ein Einfluss weiterer Faktoren auf die Knochenmorphologie anzunehmen ist.

Weiterhin verdeutlicht die Interventionsstudie, dass Vitamin D die Leberfibrogenese in *Abcb4*$^{-/-}$-Mäusen moduliert. Während ABCB4-defiziente Mäuse unter einer Vitamin D-Mangeldiät eine gesteigerte Kollagenablagerung und eine fortgeschrittenere Fibrose entwickeln, vermindert eine ausreichende Vitamin D-Versorgung die Leberschädigung. Die hochdosierte Vitamingabe verringert indessen lediglich die Transaminasenaktivitäten im Serum. Diese Studie lässt vermuten, dass der Ausgleich eines Vitamin D-Mangels bei Patienten mit cholestatischen Leberkrankheiten anti-fibrotische Effekte haben könnte, dass eine exzessive Vitamin D-Gabe jedoch keine zusätzlichen therapeutischen Wirkungen entfaltet. In ihrer Gesamtheit belegen diese Studien die umfangreichen systemischen Auswirkungen eines leberspezifischen Transporterdefekts und weisen auf die Wechselwirkungen hepatischer und extrahepatischer Symptome bei Patienten mit chronischer Cholestase hin.

SUMMARY

The ABCB4 gene encodes the hepatocanalicular phospholipid floppase, which translocates phosphatidylcholine from liver into bile. Abcb4 (ATP-binding cassette transporter B4 knockout (*Abcb4*$^{-/-}$) mice develop chronic liver injury and fibrosis similar to primary sclerosing cholangitis in humans. Mutations of the orthologous human gene cause progressive familial intrahepatic cholestasis. To date, the extrahepatic consequences of this disease have not been fully defined. The aim of this work was to characterize the systemic effects of *Abcb4*-deficiency. Standardized phenotyping of *Abcb4*$^{-/-}$ mice revealed multiple changes of the systemic metabolism. Subsequently, we performed detailed analyses of glucose and lipid homoeostasis as well as bone and vitamin D metabolism. Furthermore, a vitamin D intervention study was carried out in *Abcb4*$^{-/-}$ mice to examine the effect of vitamin D on bone morphology and liver fibrosis.

Mice lacking the ABCB4 protein demonstrate improved glucose tolerance and altered hepatic expression of glucose metabolism enzymes as compared to wild-type controls. In line with this phenotype, the hepatic expression of the anti-diabetic nuclear receptor 5A2 (LRH-1) is induced in *Abcb4*$^{-/-}$ mice, and its specific rare phosphatidylcholine ligands (diundecanoyl- and dilauroyl-phosphatidylcholine) were detected in liver. Genetic case-control association studies in two independent European cohorts showed that individuals carrying the common ABCB4 pro-cholestatic risk variant c.711A>T display decreased serum glucose levels. These results provide evidence for an association between the ABCB4 transporter and systemic glucose homeostasis in both mice and humans.

The comprehensive study of bone metabolism demonstrated that *Abcb4*$^{-/-}$ mice develop osteodystrophy with altered bone metabolism, structure and density. *Abcb4*$^{-/-}$ mice with severe liver fibrosis show reduced bone mineral contents as well as changes in trabecular bone architecture and decreased cortical bone densities; dysregulated expression of genes involved in bone remodeling and vitamin D metabolism is also observed. Vitamin D supplementation did not fully restore the bone phenotypes of *Abcb4*$^{-/-}$ animals, pointing to the pathobiological

role of additional factors during the development of hepatic osteodystrophy in this model.

Dietary vitamin D supplementation modulates biliary fibrosis in vivo: *Abcb4*$^{-/-}$ mice on the low vitamin D diet demonstrate most advanced liver fibrosis and highest hepatic collagen contents. Feeding *Abcb4*$^{-/-}$ mice a high vitamin D-diet decreased serum liver enzyme activities and ameliorated, in part, liver injury. Therefore, we speculate that an adequate vitamin D intake improves liver damage and induces anti-fibrotic effects in chronic cholestasis in humans, but excessive vitamin D supplementation may not result in further therapeutic effects. Overall, these studies illustrate the complex systemic interactions of the liver-specific ABCB4 defect with multiple links between hepatic phenotypes and extrahepatic symptoms in chronic cholestasis.

PUBLIKATIONSLISTE

„Vitamin D modulates biliary fibrosis in ABCB4 deficient mice"

K. Hochrath, CS Stokes, J. Geisel, MJ Pollheimer, P. Fickert, S. Dooley and F. Lammert; *Hepatol Int*. 2014; 1-10

„System genetics of liver fibrosis: identification of fibrogenic and expression quantitative trait loci in the BXD murine reference population"

RA Hall, R. Liebe, K. Hochrath, A. Kazakov, R. Alberts, U. Laufs, M. Böhm, HP Fischer, RW Williams, K. Schughart, SN Weber, F. Lammert; *PLOS ONE* 2014; 9(2): e89279.

„Modelling hepatic osteodystrophy in *Abcb4*-deficient mice"

K. Hochrath*, S. Ehnert*, CL Ackert-Bicknell, Y. Lau, A. Schmid, M. Krawczyk, JG Hengstler, J. Dunn, K. Hittatiya, B. Rathkolb, K. Micklich, W. Hans, H. Fuchs, V. Gailus-Durner, E. Wolf, M. Hrabě de Angelis, S. Dooley, B. Paigen, B. Wildemann, F. Lammert and AK Nüssler; *BONE* 2013; 55: 501-11.

„The hepatic phosphatidylcholine transporter ABCB4 as modulator of glucose homeostasis"

K. Hochrath*, M. Krawczyk*, R. Goebel, M. Langhirt, B. Rathkolb, K. Micklich, J. Rozman, M. Horsch, J. Beckers, M. Klingenspor, H. Fuchs, V. Gailus-Durner, E. Wolf, M. Acalovschi, DA Volmer, M. Hrabě de Angelis, F. Lammert; *FASEB J.* 2012; 26: 5081-91.

„Identification of RARRES1 as core regulator in liver fibrosis"

A. Teufel, D. Becker, SN Weber, S. Dooley, K. Breitkopf-Heinlein, T. Maass, K. Hochrath, M. Krupp, JU Marquardt, M. Kolb, B. Korn, C Niehrs, T. Zimmermann, P. Godoy, PR Galle, F. Lammert; *J Mol Med.* 2012; 90: 1439-47.

„Common genetic variation in vitamin D metabolism is associated with liver stiffness"

F. Grünhage*, K. Hochrath*, M. Krawczyk, A. Höblinger, B. Obermayer-Pietsch, J. Geisel, M. Trauner, T. Sauerbruch, F. Lammert; *Hepatology* 2012; 56: 1883-91.

„Expression of the megalin C-terminal fragment by macrophages during liver fibrogenesis in mice"

U. Pieper-Fürst, RA Hall, S. Huss, K. Hochrath, HP Fischer, F. Tacke, R. Weiskirchen, F. Lammert; *Biochim Biophys Acta.* 2011; 1812: 1640-48.

*Authors contributed equally

DANKSAGUNG

An dieser Stelle einen ganz herzlichen Dank an all die Menschen die zu dem Gelingen dieser Arbeit beigetragen haben.

Herrn Prof. Dr. Lammert möchte ich für die Überlassung des Themas danken, das mich auch heute noch fasziniert, für den Freiraum und die Gestaltungsmöglichkeiten bei der Umsetzung, sowie die gute Vorbereitung auf diverse Vorträge und die kritische Durchsicht von gefühlten 1000 Abstracts, Postern und Manuskriptentwürfen. Danken möchte ich auch für das vorgelebte Engagement und die Begeisterung für die Wissenschaft.

Frau Prof. Dr. Meier möchte ich danken, dass sie die Aufgabe der Erstgutachterin übernimmt.

Ein großer Dank geht auch an meine Co-Autoren, die erst eine kumulative Dissertation ermöglicht haben. Insbesondere Dr. Caroline Stokes und Dr. Marcin Krawczyk, mit ihrer Freude und dem Feingefühl für die Englische Sprache seien hier genannt.

Für die praktische Arbeit im Labor standen mir mit Rat und Tatkraft Annika Bohner, Miriam Langhirt, Rabea Hall und Reinhild Goebel zur Seite. Danke, dass ihr ausgeholfen habt, wenn es zeitlich eng war.

Besonders bedanken möchte ich mich bei meiner Familie und meinen Freunden, die auf ganz unterschiedliche Art und Weise die Rahmenbedingungen für diese Arbeit geschaffen und mir den Rücken frei gehalten haben. Ich danke Euch von Herzen, dass Ihr nie einen Zweifel erkennen lassen habt.